

DESORPTION OF LITHIUM 7 ISOTOPE FROM A DEGRADED
AMBERLITE LITHIATED MIXED-BED RESIN

MOSES BASITERE

CAPE PENINSULA
UNIVERSITY OF TECHNOLOGY
Library and Information Services
Dewey No. ARC 669.0381 BAS

377 532

CAPE PENINSULA
UNIVERSITY OF TECHNOLOGY



20114674

CPT ARC 661.0381 BAS

(green)

**DESORPTION OF LITHIUM 7 ISOTOPE FROM A DEGRADED
AMBERLITE LITHIATED MIXED-BED RESIN**

Moses Basitere

Thesis submitted in fulfilment of the requirements for the degree

MTECH: ENGINEERING: CHEMICAL

In the

FACULTY OF ENGINEERING

at the

CAPE PENINSULA UNIVERSITY OF TECHNOLOGY

SUPERVISOR: DR. SETENO KARABO NTWAMPE

CO-SUPERVISOR: PROF. MARSHALL SHEERENE SHELDON

CAPE TOWN

2011

CPUT Copyright Information

The dissertation/thesis may not be published either in part (in scholarly, scientific or technical journals), or as a whole (as a monograph), unless permission has been obtained from the university

“Courage is not the absence of fear, but is inspiring others to move beyond it”

– NR Mandela

‘Maña a mutukana asi vhumatshelo hawe’- Venda proverb

DECLARATION

I, **Moses Basitere**, hereby declare that the contents of this thesis represent my own work and that this thesis has not previously been submitted for academic examination for any other qualification. Furthermore, it represents my own opinions and not necessarily those of the Cape Peninsula University of Technology.

Signature:

A handwritten signature in black ink, appearing to read 'M Basitere', written over a horizontal line.

Date:

12/09/2011

ABSTRACT

Lithium 7 (${}^7\text{Li}^+$) is an isotope, which is used in the nuclear industry as lithium hydroxide (${}^7\text{LiOH}$) for the chemical control (pH control) of the high purity reactor coolant water process in order to prevent corrosion in the Pressurised Water Reactor (PWR). Furthermore, the ${}^7\text{Li}^+$ isotope is used in an ionic form in the nuclear grade cation ion-exchange resin. This resin is used to purify the nuclear reactor coolant water by reducing cationic corrosion by-products such as Cesium and Cobalt, which are generated from nuclear fission reactions. In view of the fact that an inorganic salt of the isotope is used as an alkalisng agent in the PWR, the use of lithiated resin prevents the removal of the ${}^7\text{Li}^+$ isotope in the coolant water. As most users of the nuclear grade resin purchase their resin in bulk, it follows that the resin has to be evaluated in order to determine its usability. In certain cases, the resin may be considered unusable as a result of the degradation caused by unsuitable transportation and storage conditions. These, in turn, perpetuate the release of leachates, which may further contribute to corrosion in the PWR. This necessitated the undertaking of this study, which was to evaluate whether it is possible to recover the high value ${}^7\text{Li}^+$ isotope from a degraded nuclear grade resin in such a way that the isotope may be used in the PWR.

The desorption of the ${}^7\text{Li}^+$ isotope was investigated using commercial grade acids, such as hydrochloric acid (HCl), a sulphuric acid (H_2SO_4) and biologically produced H_2SO_4 , on a laboratory scale using an ion-exchange column. The biological production of H_2SO_4 involved the oxidation of elemental sulphur using *Acidithiobacillus caldus* (*A. caldus*) in order to produce titres of H_2SO_4 with the required optimal acid concentration. This was investigated as an alternative process. Thereafter, the desorption rate of the ${}^7\text{Li}^+$ isotope using both the commercial grade acids and the biologically produced acid was compared. A decontamination process was designed in order to reduce unwanted leachates from the resin so as to enable the use of the ${}^7\text{Li}^+$ containing effluent in the PWR. Furthermore, a mathematical model was developed in order to simulate and predict the desorption rate of the ${}^7\text{Li}^+$ isotope from the degraded mixed-bed resin. An Ordinary Differential Equation (ODE) solver was used to model the desorption rate of ${}^7\text{Li}^+$ while taking into consideration design parameters such as eluent flow rate, bed porosity and reactor dimensions. The correlation between the modelled and the experimental data was also evaluated.

The concentration of leachates in the recovered effluent, which contained ${}^7\text{Li}^+$, was quantified by passing Milli-Q water, 1M commercial grade HCl, H_2SO_4 and biological H_2SO_4 through a bed of degraded Amberlite IRN 217 lithiated mixed-bed resin. The leachates' concentration was found to be high in the degraded resin in comparison to the level of leachates obtained from a new batch of Amberlite mixed-bed resin, thus confirming the degradation of the mixed-bed resin. Furthermore, broken pieces of the degraded resin were found in the effluent which had been recovered when rinsing the resin bed with Milli-Q water. The favourable eluent concentration for both commercial grade HCl and H_2SO_4 acid was determined to be 1M. This necessitated the development of a sustainable and environmentally friendly biological process in which it was possible to produce an acid concentration of 1M. In an aerated batch bioreactor the H_2SO_4 production achieved by oxidising elemental sulphur was 0.4M over a period of 16 days. The titres were concentrated in such a way that acid concentration of 1M was achieved by evaporating 80% (v/v) of the water. The concentrated biological H_2SO_4 showed a similar desorption rate ($> 90\%$) of ${}^7\text{Li}^+$ isotope as the commercial grade H_2SO_4 after 18 bed volumes (BVs). However, a high desorption rate ($> 80\%$) was observed for the biological acid during the initial stages (≤ 2 BVs) compared to the commercial grade H_2SO_4 for which a desorption rate of 61% had been achieved at the same stage.

The desorption rates' kinetics were determined to be described by first order reaction kinetics for all the experiments conducted. The mathematical model developed showed a sufficient correlation between the experimental data and the simulated data with a correlation coefficient (R^2) of 0.99 and 0.99 for commercial grade HCl and H_2SO_4 , respectively, while a correlation coefficient of 0.98 was achieved for the biological sulphuric acid experiments. From the research, it was determined that, for 30 ml of the degraded resin, it was possible to recover > 2000 mg/L of the ${}^7\text{Li}^+$ using 540 ml of the acidic eluents. Thus, this research has contributed to the recovery of a high value isotope from a degraded nuclear grade resin.

DEDICATION

To my parents

Chiawelo Basitere and Elelwani Basitere

and

my grandmother (the late)

Thinavhuyo Basitere,

with love

LIST OF OUTPUTS

The following outputs comprise the candidate's contribution to scientific development and knowledge during his master's candidacy (2009 - 2010).

Accepted manuscripts for publication:

Basitere, M., Ntwampe, S.K.O. and Sheldon, M.S. 2010. Lithium 7 isotope ($^7\text{Li}^+$) desorption from a degraded Amberlite IRN 217 lithiated mixed-bed resin (accepted for publication with minor revisions, *Journal of Solvent Extraction and Ion-Exchange*, February 2011; Manuscript No: M10-37).

Submitted manuscript for publication under review:

Basitere, M., Ntwampe, S.K.O. and Sheldon, M.S. 2010. Desorption of lithium isotope from a degraded lithiated mixed bed ion-exchange resin using *Acidithiobacillus caldus*. (submitted for publication, *Biochemical Engineering Journal*, June 2011; manuscript No: BEJ-D-11-00454).

Local/international conference(s): poster presentation(s):

Poster title: Basitere, M., Ntwampe, S.K.O., and Sheldon, M.S. Elution of lithium 7 ($^7\text{Li}^+$) isotope from Amberlite IRN 217 lithiated mixed-bed resin. CPUT Research Day, 20 November 2009. Cape Peninsula University of Technology, Cape Town, South Africa.

Poster title: Basitere, M., Ntwampe, S.K.O., and Sheldon, M.S. Bio-desorption of lithium isotope ($^7\text{Li}^+$) from a degraded lithiated mixed-bed ion-exchange resin using *Acidithiobacillus caldus*. Accepted for presentation at the 5th International Symposium on Bio- & Hydrometallurgy, 8 - 9 November 2010, Cape Town, South Africa.

ACKNOWLEDGEMENTS

I would like to express my sincere appreciation and gratitude to the following persons and institutions for their support during my postgraduate studies at the Cape Peninsula University of Technology:

- To my supervisors, Dr. Seteno Karabo Ntwampe and Prof. Marshall Sheldon, for their guidance, patience and motivation throughout my postgraduate studies and also for believing in this research. You helped me to realise my own potential.
- To Dr. Gift Muchatibaya for his assistance with mathematical modelling and for giving me the confidence to understand and illustrate the mathematical concepts involved.
- To the technical officer, Mrs Hannelene Small and Mr Alwyn Bester, for their assistance and input during this study.
- To Mr Buntu Godongwana, Ms Debbie de Jager, Mr Petrus Zeelie, Mr Moreetsi Ratshefola, Mr Conrad Maluleke, Mr Phakamani Dani and my other biotechnology laboratory colleagues for their assistance and for providing an environment conducive to learning and research.
- To my family, my adoptive parents, Mr Shaun and Mrs Nicky Brown, and all my close friends for their support, love and patience.
- To the National Research Foundation and Cape Peninsula University of Technology Research Funding for the financial support which enabled the completion of this research.
- To the Eskom Koeberg Nuclear Power Station for donating the degraded Amberlite IRN 217 lithiated mixed-bed lithiated resin.
- To Rohm and Haas for donating a new batch of Amberlite IRN 217 lithiated resin, Amberlite IRN 78 anion resin and for their guidance in respect of ion-exchange resin processes.

- To Glasschem (Stellenbosch, RSA) for the manufacturing columns used in the study and to the Stellenbosch University geology laboratory as well as BEMLAB (Pty) Ltd for the analysis of the samples.

TABLE OF CONTENTS

DECLARATION	iii
ABSTRACT	iv
DEDICATION	vi
LIST OF OUTPUTS	vii
ACKNOWLEDGEMENTS	viii
LIST OF FIGURES	xiv
LIST OF TABLES	xvi
LIST OF ABBREVIATIONS	xix
CHAPTER 1: INTRODUCTION	1
1.1 Background	1
1.2 Problem statement	2
1.3 Research questions	2
1.4 Research objectives	3
1.5 Significance of the study	3
1.6 Delineation of the study	4
1.7 Layout of the thesis	4
CHAPTER 2: LITERATURE REVIEW	6
2.1 Introduction	6
2.2 Pressurised water reactor systems	6
2.3 Nuclear grade resin	8
2.3.1 Chemical and physical properties	8
2.3.2 The manufacturing of nuclear grade resin	9
2.3.3 Activation of the cation-exchanger	12
2.3.4 Activation of the anion-exchanger	13

2.3.5	Ion-exchange process mechanism	15
2.3.6	Storage conditions for unused ion-exchange resin	18
2.4	The chemistry of lithium 7 Isotope (${}^7\text{Li}^+$) in the PWR	18
2.5	Recovery of lithium from different sources	20
2.6	Desorption of metal ions adsorbed on resin	20
2.7	Biological production of sulphuric acid and its application	21
2.7.1	Micro-organisms involved in sulphur oxidation to produce sulphuric acid	22
2.7.2	Properties and applications of <i>Acidithiobacillus</i> bacteria	25
2.7.3	<i>Acidithiobacillus caldus</i>	26
2.7.4	Biological sulphuric acid production in small scale aerated batch bioreactors	27
2.7.5	Recovery of sulphuric acid from biological titres	27
2.8	Summary	27
CHAPTER 3: MODELLING DESORPTION KINETICS FOR A POROUS REACTIVE BED		29
3.1	Introduction	29
3.2	Theory: characteristic method for solving partial differential equations	29
3.3	Modelling the desorption kinetics for a porous reactive bed from basic mass transfer principles	31
3.4	Developing a solution for a partial differential equation describing the desorption kinetics for a reactive bed	35
3.5	Summary	37
CHAPTER 4: MATERIALS AND METHODS		39
4.1	Introduction	39
4.2	Experimental materials and methodology	39
4.2.1	Characteristics of the Amberlite IRN 217 lithiated mixed-bed resin	39
4.2.2	Determination of favourable eluent concentration: Batch reactor elution	40
4.2.3	Packed-bed column desorption process	41
4.2.4	Biological production of sulphuric acids	44

4.2.5	Ordinary differential equation solver	47
CHAPTER 5: RESULTS		49
5.1	Introduction	49
5.2	Materials and Method	52
5.2.1	Experimental procedure	52
5.2.2	Analytical method	52
5.2.3	Mathematical model: desorption kinetics	52
5.3	Results and discussion	53
5.3.1	Resin degradation	53
5.3.2	Determination of favourable eluent concentration in a batch reactor	56
5.3.3	Packed-bed column desorption process	59
5.4	Conclusion	66
5.5	Summary	67
CHAPTER 6: RESULTS		70
6.1	Introduction	70
6.2.1	Experimental procedure	71
6.2.2	Analytical methods	71
6.3	Results and discussion	71
6.3.1	Sulphuric acid production	71
6.3.2	Bio-desorption of the $^7\text{Li}^+$ isotope from degraded mixed-bed resin	74
6.4	Conclusion	80
6.5	Summary	80
CHAPTER 7: OVERALL DISCUSSION AND CONCLUSIONS		81
7.1	Overall discussion	81
7.1.1	Capability of eluents in respect of desorpting the $^7\text{Li}^+$ isotope from degraded lithiated mixed-bed resin	81
7.1.2	Suitability of the mathematical model	81

7.1.3 Overview of the results achieved	82
7.2 Overall conclusions	83
7.3 Recommendations: future research	84
CHAPTER 8: REFERENCES	85
APPENDIX A: DATA SHEET FOR AMBERLITE IRN 217 LITHIATED MIXED-BED RESIN AND AMBERLITE IRN 78 ANION RESIN	93
APPENDIX B: SUMMARY AND RECOMMENDATION OF AMBERLITE IRN 217 LITHIATED MIXED-BED STOCK INVESTIGATION-ESKOM NUCLEAR POWER STATION	94
APPENDIX C: ROHM AND HAAS REPORT ON THE AMBERLITE DEGRADED RESIN	95
APPENDIX D: PREPARATION OF THE NUTRIENT MEDIUM FOR <i>ACIDITHIOBACILLUS CALDUS</i>	96
APPENDIX E: EXPERIMENTAL RESULTS AND SIMULATED RESULTS	97
APPENDIX F: DETERMINATION OF REACTION ORDER KINETICS	99

LIST OF FIGURES

Figure 2.1: The Reactor Chemical and Volume Control (RCV) System of the pressurised water reactor (PWR).	7
Figure 2.2: Polymer chains, cross-links, water of hydration, fixed ion-exchange sites and mobile exchangeable ions.	10
Figure 2.3: The cation resin manufacturing process:	11
Figure 2.4: Cation-exchange resin reaction illustrating an exchange reaction of lithiated resin with dilute solutions of HCl	12
Figure 2.5: Anion resin manufacturing flow process	14
Figure 2.6: Anion-exchange reaction indicating the exchange of ${}^7\text{Li}^+\text{Cl}^-$	15
Figure 2.7: A photograph of bioleaching bacteria, A) mesophiles, B) moderate thermophile and C) extreme thermophiles.	23
Figure 3.1: A schematic diagram illustrating the process used to model the desorption kinetics of ionic species from a porous reactive bed.	32
Figure 4.1: Schematic illustration of the batch extraction of lithium (${}^7\text{Li}^+$) isotope from Amberlite IRN 217 lithiated mixed bed resin.	41
Figure 4.2: A schematic illustration of the column used for the elution of lithium isotope (${}^7\text{Li}^+$) from 30 ml degraded Amberlite 217 lithiated mixed-bed resin and [B]the anion decontamination process.	42
Figure 4.3: The recovery of H_2SO_4 from the batch bioreactor.	45
Figure 4.4: bioreactor in operation and (B+C) samples recovered from the bioreactor before and after ultra-filtration	46
Figure 5.1: Degraded Amberlite IRN 217 lithiated mixed-bed resin.	50
Figure 5.2: (A) Lithium isotope (${}^7\text{Li}^+$) eluted using HCl and H_2SO_4 in batch reactors sampled at 24 and 48 hr. (B) The achievable elution percentage for HCl and H_2SO_4 (1M = 86 and 84.42%, 3M = 89.63 and 84.42%, 5M = 97.88 and 84.66%, respectively)	58

Figure 5.3: Relationship between the eluting volume and the lithium isotope ($^7\text{Li}^+$) concentration eluted from Amberlite IRN 217 lithiated mixed-bed resin using 1M HCl and H_2SO_4 , respectively.	60
Figure 5.4: Percentage elution of lithium isotope ($^7\text{Li}^+$) from Amberlite IRN 217 lithiated mixed-bed resin in a continuous ion-exchange column	61
Figure 5.5: Simulated and experimental desorption curve for lithium isotope at 1M HCl and H_2SO_4 and the correlation between experimental and simulated data	63
Figure 5.6: Concentration of cation leachates in the recovered effluent	66
Figure 6.1: [A] pH evolution during the oxidation of elemental sulphur; [B] cumulative production of H_2SO_4 in an aerated batch bioreactor with <i>A. caldus</i> immobilised on elemental sulphur; [C] graph showing the acid concentration increase with the percentage of moisture loss.	73
Figure 6.2: Lithium 7 isotope desorption using biologically produced sulphuric acid by <i>A. caldus</i> cells compared with mineral H_2SO_4 .	75
Figure 6.3: Cations in the biological and commercial grade H_2SO_4 influent	76
Figure 6.4: Simulated and experimental desorption curve for lithium isotope at 1M biological H_2SO_4 and the correlation between experimental and simulated data.	77
Figure 6.5: [A] Cations and [B] anions leachates in the $^7\text{Li}^+$ isotope effluent from the desorption process	78

LIST OF TABLES

Table 2.1: Chemolithotrophic bacteria with bio-hydrometallurgical potential	24
Table 4.1: Properties of the Amberlite IRN 217 lithiated mixed-bed resin	40
Table 5.1: Analysis of leachates from the degraded Amberlite IRN 217 lithiated mixed-bed resin compared to a new batch of Amberlite IRN217 lithiated mixed-bed resin	55
Table 5.2: Statistical analysis of $^7\text{Li}^+$ desorption in batch reactors	57
Table 5.3: Averaged anion removal from the $^7\text{Li}^+$ effluent using Amberlite IRN 78 anion resin	65
Table 6.1: Averaged anion removal from the $^7\text{Li}^+$ effluent using Amberlite IRN 78 anion resin	79

LIST OF SYMBOLS

Nomenclature	Definition	Units
A_1, A_2	Constants	-
a, b, c	Coefficients of the ODE	-
C	Parametric curve	-
d	Time	day
D	Diffusive coefficient	m^2/min
i, j, k	Unit dimensional vector	-
\bar{k}	Desorption rate constant	min^{-1}
L	Length	m
n	Normal vector	-
p	Vector	-
Q	The parameter of a curve	-
r	Particle radius	-
S_l	Three dimensional surface	-
S_e	Amount of lithium in the resin at exit port	mg/L
S	Concentration of lithium in the resin	mg/L
S_o	Total amount of ${}^7Li^+$ isotope adsorbed on Amberlite IRN Resin	mg/L
u	Eluent flow rate	L/min
u_o	Eluent flow rate at the point of entry	L/min
r	Position vector	-
r_i	Rate of desorption from reactive bed	mg/L.min
t	Time	min
x, y, z	Cartesian plane coordinates	-
Z	Axial position in the column	-

Subscripts

u_x, u_y, u_z Convective transport in three dimensions, x, y, z L/min

Greek symbol(s)

ϵ Resin bed porosity -

LIST OF ABBREVIATIONS

<i>A. caldus</i>	<i>Acidithiobacillus caldus</i>
<i>A. thioxidans</i>	<i>Acidithiobacillus thioxidans</i>
<i>A. ferroxidans</i>	<i>Acidithiobacillus ferroxidans</i>
BV	Bed volume
DVB	Divinylbenzene
$^7\text{Li}^+$	Lithium 7 Isotope
ODE	Ordinary differential equation
PDE	Partial differential equation
PWR	Pressurised water reactor
PZR	Pressuriser
RCV	Reactor chemical and volume control
S/G	Steam generator

CHAPTER 1

INTRODUCTION

1.1 Background

In view of their high treatment capacity, high ion removal efficiency and fast kinetics, ion-exchange processes have been widely used in the nuclear industry in order to remove anionic and cationic contaminants from process water (Helfferich, 1995; Cheremisinoff, 1995; Reynolds & Richards, 1996). The resin used in the nuclear industry in South Africa is either Amberlite or Duolite nuclear grade resin. These resins may be classified as nuclear grade resins and have been designed to meet the stringent requirements of the nuclear industry with regard to purity, special ionic form and size (Rohm & Haas, 2003). A degraded resin, classified as the Amberlite IRN 217 lithiated mixed-bed resin, is the main focus of this thesis.

Amberlite IRN 217 lithiated mixed-bed resin is a mixture of uniform particle sized gelular polystyrene divinylbenzene, which contains both cation and anion-exchange resin. This mixed-bed resin has been designed for use in the Reactor Chemical and Volume Control System (RCV) for the purification of the reactor coolant water in the Pressurised Water Reactor (PWR), which is used in the nuclear industry (Rohm & Haas, 2003; Caratin *et al.*, 2008). The cation part of the mixed-bed resin operates in lithium 7 (${}^7\text{Li}^+$) form, while the anion part of the resin operates in Borate (BO_3^{2-}) form. The latter prevents the removal of ${}^7\text{Li}^+$ isotope and boron in the reactor coolant water. The reactor coolant water is used to remove heat from the nuclear reactor core and is essentially demineralised water containing boron and ${}^7\text{Li}^+$, and includes a small amount of dissolved hydrogen (Otte & Liebman, 1987). A portion of the reactor coolant water is purified on a continuous basis by the lithiated mixed-bed demineraliser system in order to reduce the radioactive isotopes such as cesium 137 (Cs-137), cobalt 58 (Co-58) and other impurities such as sulphates, as well as the chlorides formed during the fission reaction (Otte & Liebman, 1987; Minato & Ohsumi, 1989; Meintker, Boltz, Enkler & Ruhle, 2003).

Currently at a South African nuclear power station there are batches of degraded resin which have been reported to be unsuitable for use in the RCV system as a result of anion

degradation. The replacement value of the degraded Amberlite IRN 217 lithiated resin was determined as approximately ZAR 8.5 million during 2009. A sample of this resin was sent to the manufacturers of the resin, Rohm and Haas (France), in order to determine whether the resin was suitable for use in the RCV. The chemical, physical and usability characteristics of the resin included the following: ion-exchange capacity, moisture content, strong base capacity and the optical aspect of the resin, which refers to the determination of the percentage of unbroken resin and broken resin beads. The feedback from Rohm and Haas pointed to the fact that the anion part of the resin had lost its strong base capacity (this should be 100%) and was, in fact, degraded as confirmed by the optical aspects analysis (see Appendix B). However, the cation resin with the valuable $^7\text{Li}^+$ isotope was reported to be in excellent condition with good physical appearance (see Figure 5.1). As a result, it was imperative to evaluate the possibility of recovering the valuable $^7\text{Li}^+$ isotope on the cation resin for re-use in the PWR as the cation resin was still in good condition. Accordingly, the work presented in this thesis demonstrates the method which may be used to recover the $^7\text{Li}^+$ isotope in lithiated degraded mixed-bed resin batches, which do not meet the nuclear industry specifications as a result of the degradation.

1.2 Problem statement

The Amberlite IRN 217 lithiated mixed-bed resin stock, which had been stored at a nuclear power station for a long period of time, was reported to be unsuitable for use in the RCV of the PWR as a result of the degradation of the anion part of the resin. The anion part of the resin had lost its strong base capacity, while the cation resin with valuable $^7\text{Li}^+$ isotope was still in excellent condition.

1.3 Research questions

- Will dilute solutions of the commercial grade acids (HCl and H_2SO_4) be able to elute $^7\text{Li}^+$ isotope from the degraded Amberlite resin?
- Will the biologically produced acid be capable of effectively eluting the $^7\text{Li}^+$ isotope from the resin in a way that is similar to the process used for commercial grade acids after it has been concentrated by an evaporation process?

- What type of anion/cation leachates will be found in the $^7\text{Li}^+$ isotope effluent?
- Will the mathematical model developed be suitable to model the desorption rates of the $^7\text{Li}^+$ from the degraded Amberlite IRN 217 lithiated mixed-bed resin for processes involving both the commercial grade acids and the biologically produced acid?

1.4 Research objectives

The study focused on the desorption of valuable $^7\text{Li}^+$ from the cation part of a degraded Amberlite IRN 217 lithiated mixed-bed resin, which had been determined to be unsuitable for use in the PWR of a local nuclear power plant. The recovered $^7\text{Li}^+$ isotope may be reused in the PWR as lithium hydroxide ($^7\text{LiOH}$) in order to raise the pH of the coolant water or it may be adsorbed onto a suitable resin in such a way that it may be re-used in the RCV of the PWR. The specific objectives of the study included the following:

- Elute the $^7\text{Li}^+$ using (1) freely available reagents such as commercial grade mineral acids and (2) biologically produced sulphuric acid (H_2SO_4).
- Identify a suitable micro-organism that is capable of producing acidic titres in a more environmentally friendly process. This acid, which was produced by the selected micro-organism, was evaluated for its ability to elute the $^7\text{Li}^+$ isotope from the degraded lithiated mixed-bed resin in an effective way.
- Compare the desorption kinetics of $^7\text{Li}^+$ from degraded resin using the biologically produced acid and commercial grade mineral acids.
- Develop a mathematical model taking into account the design parameters such as the eluent flow rate, bed porosity and reactor dimensions for the desorption of the $^7\text{Li}^+$ isotope from the degraded Amberlite IRN 217 lithiated resin.

1.5 Significance of the study

This study provided insight into the mechanism of desorbing the valuable $^7\text{Li}^+$ isotope from a degraded polystyrene-based resin, which has not been done before. Furthermore, the study also evaluated the possibility of desorbing the $^7\text{Li}^+$ isotope using biologically produced



H₂SO₄ using a process that is more environmentally friendly. Biological H₂SO₄ was produced by the oxidation of sulphur using the *Acidithiobacillus caldus* (*A. caldus*) bacteria. The bacteria utilise the sulphur as a source of energy in the presence of oxygen in order to produce acid titres (Semenza, Viera, Curutchet & Donati, 2002). The biological technique explored in this project may also be used by hydro-metallurgists to recover other metal ions adsorbed on ion-exchange in order to replace the commonly used commercial grade acid and, thus, to promote a biological production of H₂SO₄, which is more environmentally friendly. The desorption techniques investigated in this thesis can be used for degraded resin or resin stored past the shelf-life for the recovery of valuable elements.

1.6 Delineation of the study

- Building a commercial sized pilot plant unit.
- Separation of the mixed-bed resin and the accommodation of other types of degraded lithiated resin.
- The use of sulphur waste to produce H₂SO₄.
- The evaluation and re-use of the ⁷Li⁺ recovered from degraded mixed-bed lithiated resin in the PWR of a nuclear power station.
- Cost analysis, as this will be carried out as part of a future study.

1.7 Layout of the thesis

Chapter 2 contains the literature review as well as a discussion of the theory on the application of ion-exchange resin in the PWR. Sections 2.2 to 2.6 describe: 1) the chemical properties of the nuclear grade divinylbenzene ion-exchange resin; 2) the process of manufacturing both polystyrene cross-linked cation and anion resin; 3) the degradation mechanism and the storage conditions resulting in the degradation of the ion-exchange resin, 4) the chemistry of the ⁷Li⁺ in the PWR and 5) the recovery of lithium using different processes and the desorption of metallic ions from resin. The biological production of H₂SO₄ is discussed in section 2.8. Chapter 3 describes the methodology used to develop the mathematical model utilised to simulate the desorption kinetics of the ⁷Li⁺ isotope from the

degraded Amberlite IRN 217 lithiated resin. Chapter 4 presents the materials and methods used to attain the objectives of the study while Chapters 5 and 6 contain the results of the study. The overall discussion and conclusions, including recommendations for future studies, are discussed in Chapter 7. It was essential to repeat some of the methods in Chapter 4 in chapter 5 and 6 in order to elucidate presentation of the overall results.

CHAPTER 2

LITERATURE REVIEW

2.1 Introduction

The literature review consists of: 1) the application of Amberlite IRN 217 lithiated mixed-bed resin in the PWR in the nuclear industry; 2) the characteristics and properties of the Amberlite resin; 3) the chemical desorption of metal ions using commercial grade acids from different sources and 4) the biological production of H₂SO₄ and its function in metal recovery processes.

2.2 Pressurised water reactor systems

PWR systems constitute an integral aspect of the generation of electrical energy in the nuclear industry, where nuclear fission reactions are used. Fission reactions involve the splitting of heavy atoms such as Uranium 235 (²³⁵U) by neutron collision. Energy in the form of heat is released from this process (Rowlands, 1991; Nordmann, 2002). The heat generated from the reactor core is removed by coolant water and transferred to the steam generator at a high temperature (Otte & Liebman, 1987). The steam thus generated is fed to the turbine generator for the production of electrical power.

The coolant water used to remove the heat from the reactor core is demineralised water, which contains boron, ⁷Li⁺ and a small amount of dissolved hydrogen (Otte & Liebman, 1987). The boron serves as an absorbent for any neutrons generated during the fission reactions, while the ⁷Li⁺ in a form of alkaline lithium hydroxide (LiOH) controls the pH of the coolant water in order to prevent corrosion within the nuclear reactor (Nordmann, 2002; Meintker *et al.*, 2003). The reactor coolant water is kept under pressure to prevent it from boiling. A portion of this reactor coolant water is continuously passed through a heat exchanger and is further processed in the RCV system for purification purposes. The RCV system is illustrated in Figure 2.1.

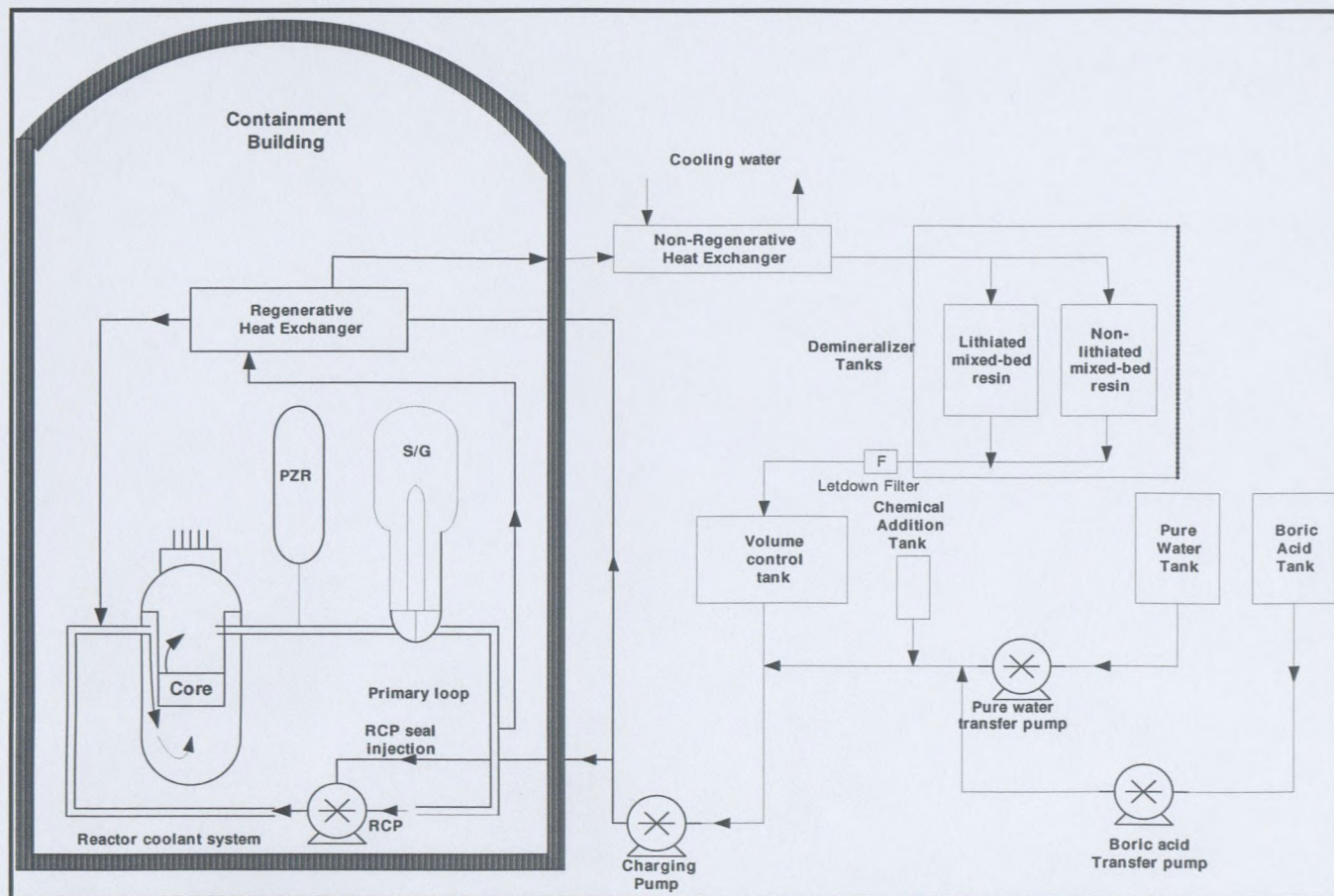


Figure 2.1: The Reactor Chemical and Volume Control (RCV) system of the pressurised water reactor (PWR).

The RCV constitutes a major support system in the purification process of the reactor coolant water system. The function of the RCV system is: 1) to purify the reactor coolant system using filters and a demineraliser (resin); 2) to add and remove boron from the coolant water when necessary; and 3) to maintain the level of the pressuriser at the desired set-point (Dorner & Kleiter, 1977; Corpora *et al.*, 1996). The coolant water is purified in order to reduce corrosion by-products such as cesium, cobalt and impurities such as sulphates and chlorides produced by the anion and cation mixed-bed resin (Otte & Liebman, 1987). Corrosion by-products are generated from the reactor core and are transported to the demineraliser tanks by the coolant water (McGlure & Copora, 1992). The ionic form of the cation resin used in the demineraliser tanks is in ${}^7\text{Li}^+$ form in order to prevent the removal of the ${}^7\text{Li}^+$ from the coolant water. The ${}^7\text{LiOH}$ is, in turn, used as an additive for pH control in the coolant water (Hartly, Gore & Young, 1978; Otte & Liebman, 1987; Ohashi *et al.*, 1989). In addition, the anion resin is conditioned to operate in borate form to prevent the removal of

boron from the coolant water. The cation resin in the mixed-bed resin removes all the cationic radioisotopes and impurities, while the anion resin removes the anionic impurities.

2.3 Nuclear grade resin

2.3.1 Chemical and physical properties

Nuclear grade resin, made of organic material is one of the most significant classes of resin used in the nuclear industry. The structural matrix of this resin consists of a macromolecular three dimensional network of hydrocarbon chains (Helfferrich, 1995; Owens, 1999). This matrix carries anion or cation groups. Divinylbenzene is introduced as a cross-linking agent to render the resin insoluble in water solvents. The structure of the resin determines its chemical, thermal and mechanical stability. Additionally, this depends on the nature and degree of cross-linking in the resin matrix and the number of fixed ionic groups (Helfferrich, 1995; Owens, 1999). The mesh width of the matrix is dependent on the degree of cross-linking and determines both the swelling ability of the resin and the overall mobility of counter ions in the resin. When stored under suitable conditions, highly cross-linked resins are more resistant to mechanical breakdown and attrition (Helfferrich, 1995; Owens, 1999). The chemical and thermal degradation of the resin matrix, by means of oxidation and the loss of the ionic group, causes the resin to deteriorate, thus affecting the ion-exchange capacity and rendering the resin unusable. Commercially, resins are stable in industrial solvents, except when in contact with strong oxidising and reducing agents, such as nitric acid, which lead to resin degradation and explosion as a result of violent exothermic reactions (Miers & Palmer, 1992; Helfferrich, 1995; Rohm & Haas, 2003). With the exception of strong base anion resins that deteriorate at temperatures above 60°C, these resins are normally stable at temperatures of up to 100°C (Helfferrich, 1995). The deterioration of an anion resin is as a result of Hoffmann degradation and involves the loss of the strong base functional group, which in turn, leads to the liberation of amines (Harland, 1994).

Nuclear grade resins are specially manufactured to a high purity standard in order to minimise leachates' leakages and to keep the nuclear reactor circuits free of contaminants (Helfferrich, 1995; Rohm & Haas, 2003). This also prevents an increase in the radioactivity that may be caused by the activation of leachates in the nuclear reactor core. This resin

undergoes special treatment after polymerisation, both to remove any traces of unsuitable soluble organic compounds and to keep inorganic impurities at low levels in order to minimise the presence of chlorides and sulphates (Helfferich, 1995; Rohm & Haas, 2003).

Cation resins are either in hydrogen (H^+) or Li^+ form. Effective regeneration processes of the cationic resin are carried out using a solution of either H_2SO_4 or $LiOH$ in order to ensure that the cation-exchanger resin is in the appropriate ionic form (H^+ or Li^+) with high conversion levels and minimum metallic impurities (Helfferich, 1995; Rohm & Haas, 2003). The strong base anion-exchange resin is supplied in a regenerated hydroxide (OH^-) form with special treatment being applied to minimise the chlorides and sulphates impurities in the resin. Precautions are taken to minimise carbonation as the resin contains moisture and it is recommended that the resin be stored in an airtight container during transportation and storage (Helfferich, 1995; Rohm & Haas, 2003).

2.3.2 The manufacturing of nuclear grade resin

Nuclear grade ion-exchange resins consist of both a polymer matrix and functional groups that interact with ions in a liquid (Helfferich, 1995; Owens, 1999). The functional groups attached to the polymer matrix are hydrophobic and draw moisture to the inner polymer matrix. This, in turn, leads to swelling of the polymer strands (Miers & Palmer, 1992; Helfferich, 1995; Rideaux, 1999). The moisture inside the polymer matrix is known as the chemical moisture of the resin, while the quantity of moisture that may be held by an ion-exchange resin is known as the moisture holding capacity. The latter is dependent on the size of the resin bead (Helfferich, 1995; Rideaux, 1999). Figure 2.2 illustrates the polymer chains, cross-linkage, water of hydration and fixed sites with mobile exchangeable ions for an ion-exchange resin (Helfferich, 1995; Rideaux, 1999).

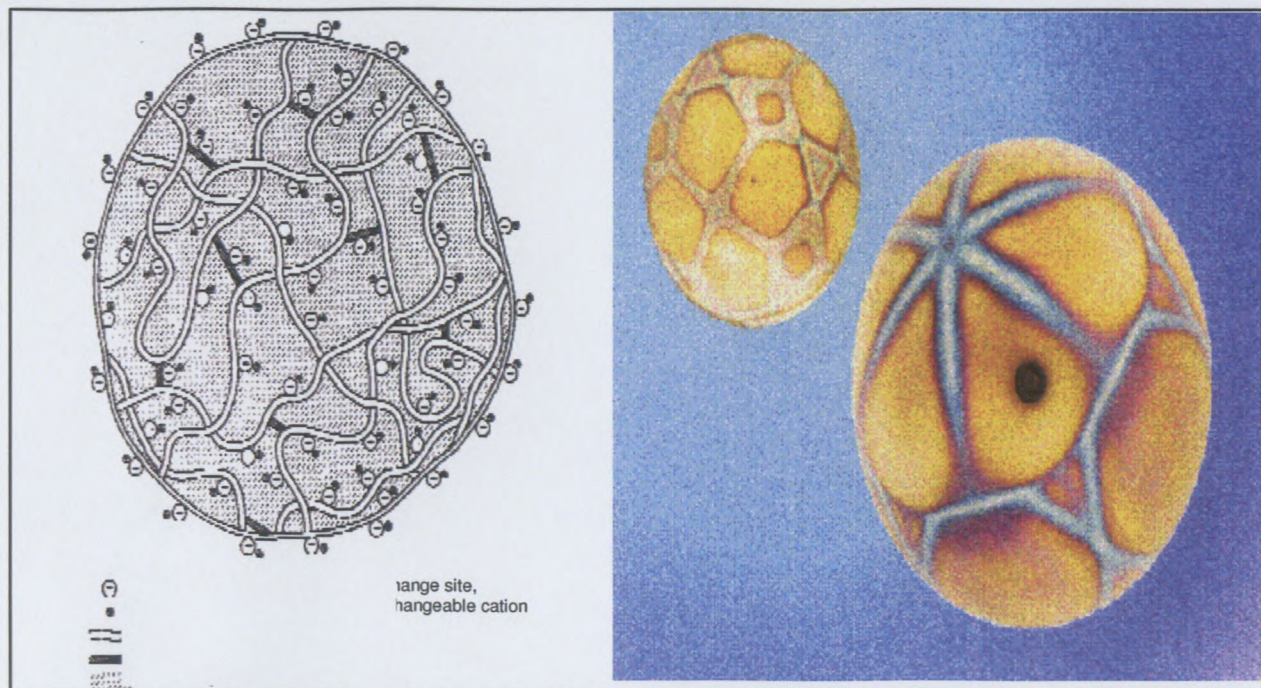


Figure 2.2: Polymer chains, cross-links, water of hydration, fixed ion-exchange sites and mobile exchangeable ions (Helfferich, 1995; Rideaux, 1999)

The Amberlite IRN 217 lithiated mixed-bed resin used during this study was made up of polystyrene divinylbenzene as a polymer matrix with a combination of sulphonic and trimethylammonium functional groups on the cation and anion resins, respectively. Polystyrene divinylbenzene is a polymer, which is made from two different monomers, namely, styrene and divinylbenzene. The carbon-carbon double bonds on the styrene monomers open up to single bonds, while the outside bonds are joined with the other monomer that has double bonds. In terms of this process – termed polymerisation – heat and a catalyst are required to form a long-chain polymer known as a polystyrene (Helfferich, 1995; Owens, 1999). In order to obtain a cross-linked polymer, divinylbenzene (DVB) is added to the styrene’s monomer and they are polymerised in the presence of a benzoyl peroxide catalyst (Harland, 1994). The divinylbenzene has reactive groups on both ends of the benzene ring and is, therefore, capable of attaching to the benzene on both ends, thus linking the two chains together, as illustrated in Figure 2.3 (Owens, 1999).

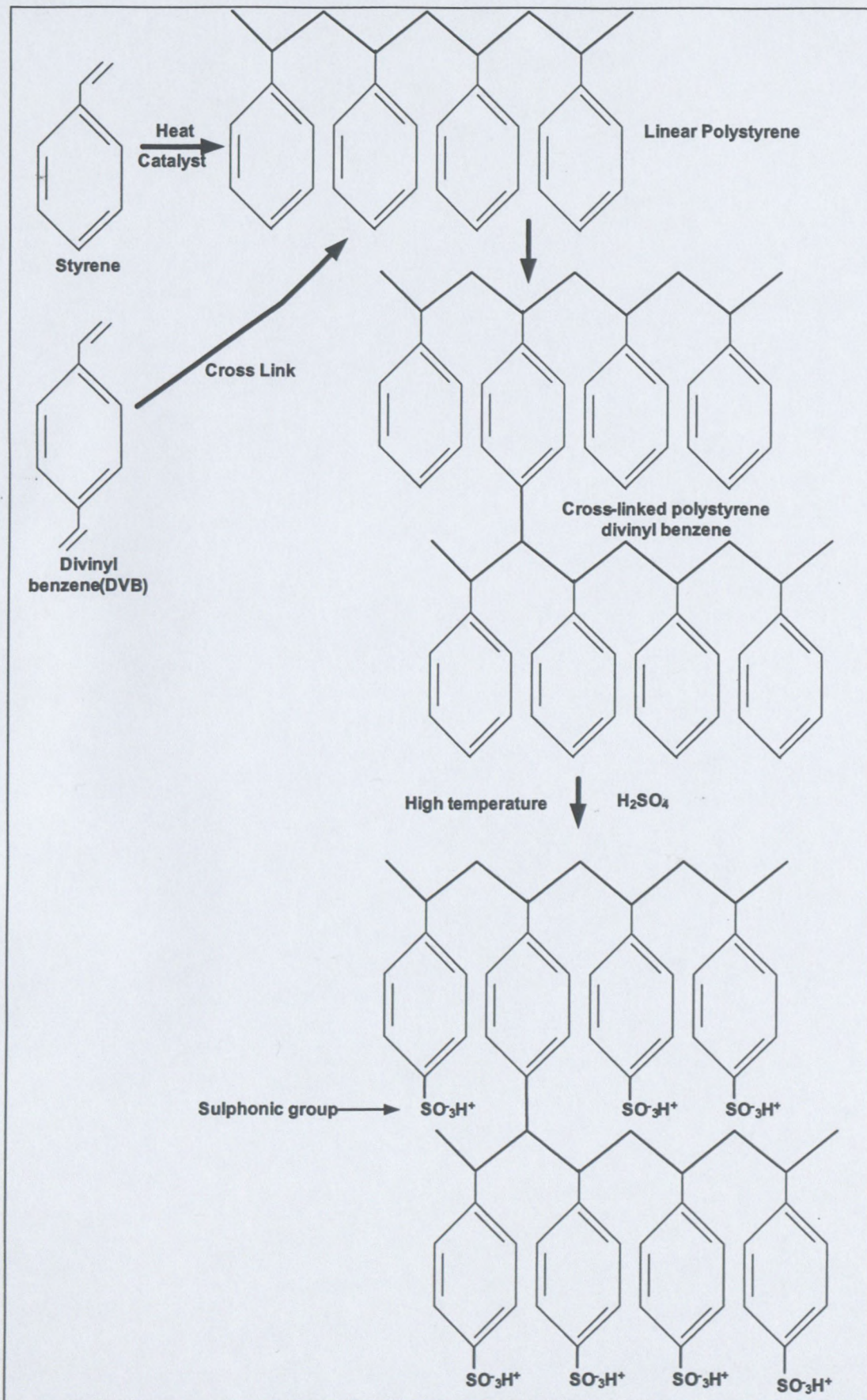


Figure 2.3: The cation resin manufacturing process (Owens, 1999)

This cross-linking process provides the polymer structure with its strength, insolubility and resistance to melting or distortion over a wide temperature range. The cross-links determine the tightness and porosity of the structure (Owens, 1999). The cross-linked polymer structure is further treated with suitable reagents in order to add the required ion-exchange functional group to the resin (Owens, 1999).

2.3.3 Activation of the cation-exchanger

The activation of the cross-linked non-reactive polystyrene divinylbenzene co-polymer used for cation resin production is carried out by the sulphonation of the resin matrix with hot H_2SO_4 . This process introduces the sulphonic acid functional group, thus giving the resin a strongly acidic cation-exchange group. The process of manufacturing the cation resin is illustrated in Figure 2.3 (Helfferich, 1995; Owens, 1999).

2.3.3.1 The cation ion-exchanger mechanism

Positively charged ions penetrate the structure of the resin and interchange with other positively charged ions which are available on the fixed ionic group. Cation resins may be categorised in two groups (Helfferich, 1995):

- strong acid exchange resin
- weak acid exchange resin

The functional groups of strong acid exchange resins usually derive from H_2SO_4 (Helfferich, 1995; Owens, 1999). The cation-exchange resin reaction may be represented by Figure 2.4, which illustrates an exchange reaction of lithiated resin with dilute solutions of HCl.



Figure 2.4: Cation-exchange resin reaction illustrating an exchange reaction of lithiated resin with dilute solutions of HCl

If the H^+ concentration is increased then the reaction will shift to the right and Li^+ will be eluted. This resin are designed so as to have different affinities for different cations, as shown in Eq 2.1 (Helfferich, 1995; Owens, 1999).



The functional groups of weak acid exchange resins originate from the use of weak acids during the manufacturing process of the resin. During this manufacturing process carboxylic or phenolic acids are commonly used. These resins are useful only within a narrow pH range (Helfferich, 1995; Owens, 1999).

2.3.4 Activation of the anion-exchanger

The process of producing a strong basic anion-exchange resin is subject to a two step activation process. The first step is via the Friedal-Crafts reaction in terms of which the chloromethylation of the styrene-divinylbenzene is applied. This is then followed by an amination process (Harland, 1994). The chloromethylation process introduces the chloromethyl groups- (CH_2Cl) into the presence of aluminium chloride, which acts as the catalyst. The chloromethylation temperature will be in the range of 20 to 60°C for a period of 2 to 20 hours (Song & Lee, 2003). The final stage is the purification of the chloromethylated styrene-divinylbenzene co-polymer. This involves the substitution of the functional group by reaction with trimethylamine $(CH_3)_3N$ which, in turn, culminates in a quaternary benzyl trimethyl ammonium chloride functional group $R-(CH_2N)-(CH_3)_3^+Cl^-$ (Harland, 1994; Song *et al.*, 1996). This process of manufacturing the anion resin is illustrated in Figure 2.4.

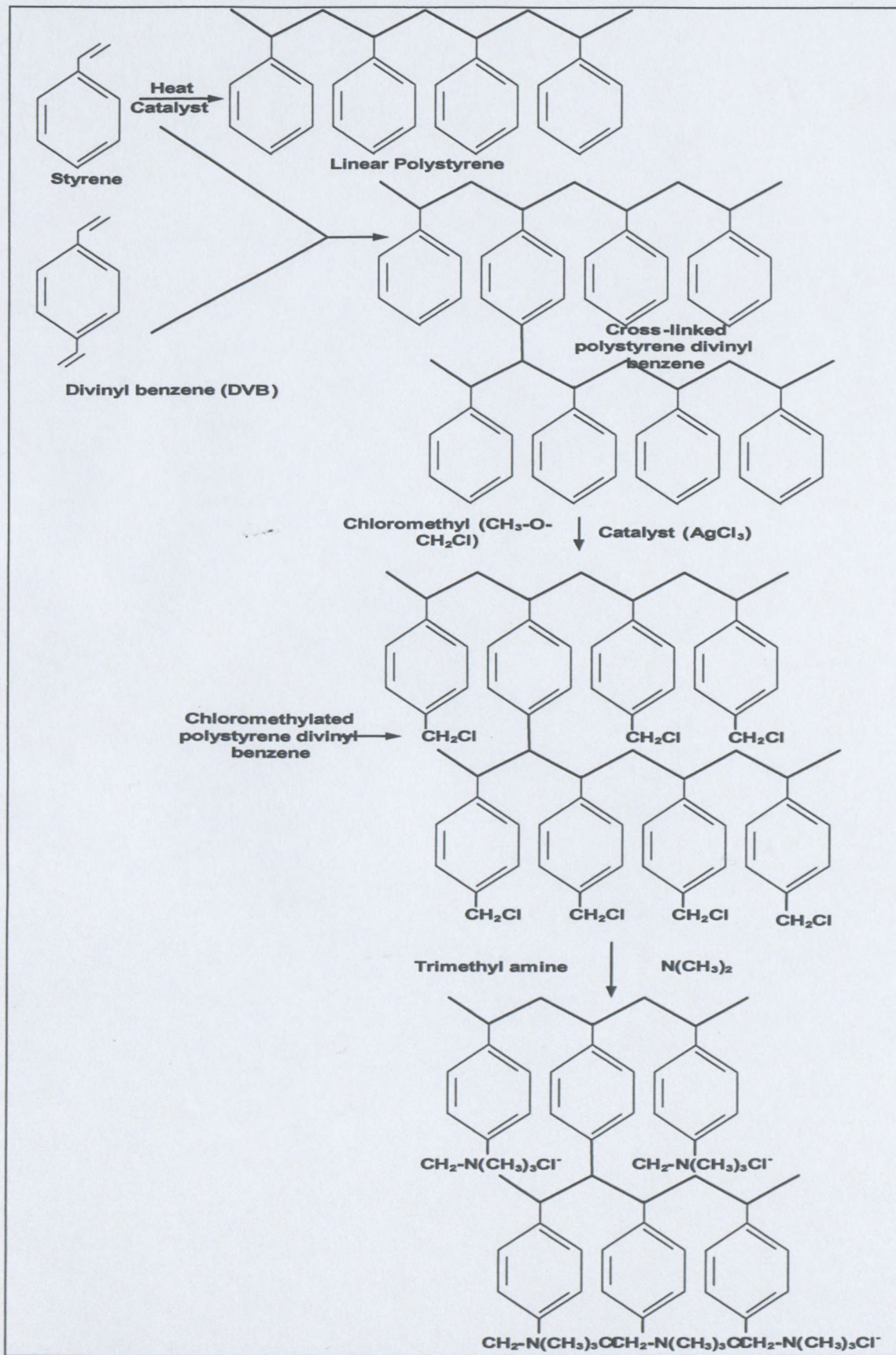


Figure 2.5: Anion resin manufacturing flow process (Owens, 1999)

2.3.4.1 The anion-exchanger mechanism

The functional group of the strong base resin usually comprises an ammonium group (NH_4^+) with a permanent positive charge (Helfferich, 1995; Owens, 1999). The anion-exchange reaction is represented by Figure 2.6 and it indicates the exchange of ${}^7\text{Li}^+\text{Cl}^-$ when in contact with anion resin.

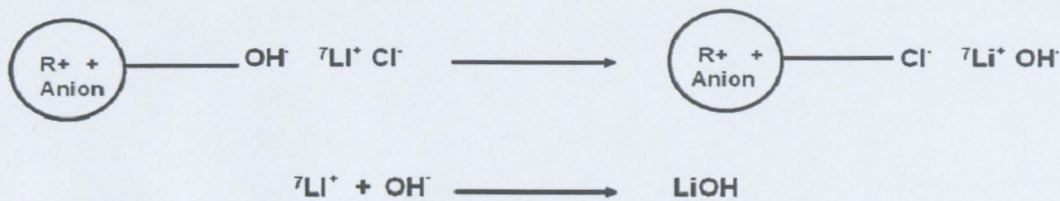


Figure 2.6: Anion-exchange reaction indicating the exchange of ${}^7\text{Li}^+\text{Cl}^-$

Similar to Eq. 2.1, a corresponding list of the affinity of anions for amine bases anion exchangers is as given in Eq. 2.2 (Helfferich, 1995; Owens, 1999):



2.3.5 Ion-exchange process mechanism

Ion-exchange is purely a diffusion phenomenon. This phenomenon may be categorised by the following steps (Helfferich, 1995):

- Diffusion of ions from the bulk liquid to the external surface of the resin.
- Diffusion of ions inward through the resin to the exchange site.
- Exchange of the ions at active sites.
- Outward diffusion of released ions to the surface of the resin.
- Diffusion of the released ions from the surface of the resin to the bulk liquid.

The models illustrated in Figures 2.4 and 2.6 represent and describe ion exchange kinetics. The rate depends on the mobility of counter ions. The rate of exchange can be predicted using a rough estimate (Helfferich, 1962).

2.3.5.1 Ion-exchange rate kinetics, their evaluation and experimental parameters used

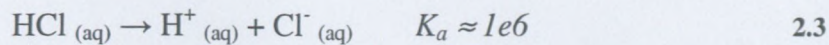
The mechanism of ion-exchange involves the movement of ions from the resin into the solution, while ions from the eluent replace those in the resin, i.e., any ions that leave the resin are replaced by an equivalent quantity of other ions in the eluent depending on the affinity of the exchange ions. The ion-exchange kinetics is determined and influenced by two rate determining steps which are: 1) The movement of counter ions within the resin and 2) the movement of counter ions in the adherent films. Additionally, the rate of ions' exchange can be simulated by applying a well known mass transfer equation, taking into consideration the operational parameters of the process used. Thus, in general cases, a differential equation and well described boundary conditions, can be used to estimate the rate at which ions are exchanged in the resin. Furthermore, a limiting case of ion exchange is that the exchange of trace components can be described as the uptake or release of traces of one counter ion in the presence of a large excess counter ion in both the ion-exchange matrix and eluent (Helfferich, 1962). Due to the nature of the resin used in this study, i.e. degraded resin, it is hypothesised that trace ions will be present in the resin bed.

Furthermore, ion-exchange rates, i.e., the rate at which ions exchange in the resin bed can be estimated by applying appropriate rate laws, which involves the counter ions in the exchanger and the eluent used. Other factors influencing the rate of ion-exchange are; 1) the selectivity of the ion exchanger; 2) its size; and 3) the eluents' concentration. Ion-exchange rates can be measured in batch experiments, in which there is a known amount of an ion-exchanger with a known concentration and volume of the eluant. Agitation can be provided by stirring or shaking. For a convectonal column operation, an ion exchange operation is set-up such that a liquid feed is passed through the column at a specific flow rate with the intention of replacing the counter ion by counter specie (Helfferich, 1962). In engineering design theory, it is required that the mass transfer model of laboratory scale operations takes into consideration parameters that influences the process at a pilot and large scale (Sinnott, 1994). Helfferich

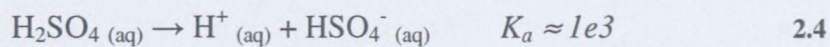
(1962) states that, the quantitative or mathematical treatment of column processes can be based on simplifying assumptions to yield approximate results, which will have to be validated by practical evaluation. Furthermore, as the applicable mathematical theories are generic, they can be applied with modification for sorption, ion-exchange and desorption.

2.3.5.2 Eluent selection, concentration and dissociation in water

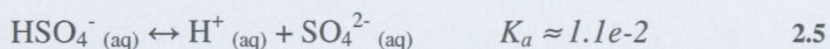
Eluent selection and concentration in ion-exchange processes plays a vital role. HCl and H₂SO₄ are common Eluents used in ion-exchange for this purpose. For strong acid cation exchangers, with a DVB cross-linked matrix, regenerants' or eluents' concentration vary from 0.7 to 3M for HCl and 0.2 to 1.1M for H₂SO₄, respectively, using a service flow rate of 5 to 20 Bed Volume per hour. However, lower concentrations of HCl or H₂SO₄ can be used for weakly acidic resins. Furthermore, the capacity of the resin must be taken into consideration when the eluent of a particular resin is prepared (Rohm & Haas, 2003). These eluents are used as dilute solutions. Eluents are prepared by diluting strong acids with water to produce a hydronium ion (H⁺). A strong acid such as HCl dissociates completely in water, as shown in Eq. 2.3 (Ebbing, 1993):



Furthermore, H₂SO₄ can lose two protons in water with the first H⁺ being lost completely as shown in Eq 2.4 (Ebbing, 1993):



While the resultant hydrogen sulphate ion HSO₄⁻, which is considered a weak acid, will dissociate further in which event equilibrium exists as illustrated in Eq. 2.5 (Ebbing, 1993):



By using acid-dissociation equilibrium quantitative techniques and dissociation constants in Eq. 2.3 to 2.5, when 1M of HCl and H₂SO₄ is used, 1M H⁺ and 1.1M H⁺ will be achieved, respectively. In terms of desorption kinetics, 1M HCl should compare favourably with 1M H₂SO₄ (Ebbing, 1993).

2.3.6 Storage conditions for unused ion-exchange resin

Unused ion-exchange resin may be stored under proper conditions for longer than its recommended shelf-life without experiencing a decline in physical properties (Miers, 1992). The minimum shelf-life of an anion resin under proper conditions is two years with five years being the minimum shelf-life for the cation resin (Miers, 1992; Rideaux, 1999). In addition, storage temperatures should be kept between 0 and 30°C (32 to 86°F) in order to avoid resin degradation (Rideaux, 1999). Storage temperatures of above 30°C may result in a premature loss of the hydroxyl anion resin capacity, while storage temperatures below 0°C may result in the ion-exchange resin freezing (Shiao & Tsai, 1990; Rideaux, 1999; Mamo, Ginting, Renken & Eghball, 2004). When resin is subject to temperatures below 0°C, the moisture content inside the resin expands as the resin becomes a solid. This, in turn, leads to the stretching of the resin polymer (Rideaux, 1999; Mamo *et al.*, 2004). Repeated cycles of freezing and thawing (expansion and contraction) may result in resin bead damage because of broken polymer bonds and the loss of the functional group (Miers, 1992; Rideaux, 1999; Mamo *et al.*, 2004).

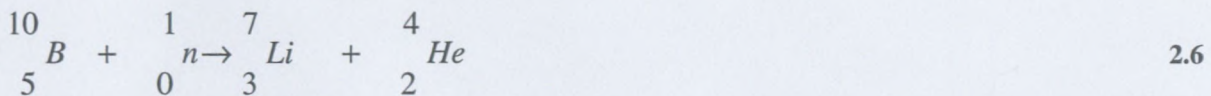
In view of the fact that most users of resin purchase their supply of resin from the manufacturers in bulk, the transportation and storage conditions of the resin are largely unmonitored. This may result in the resin being stored in unsuitable storage facilities for extended periods of time, thus rendering the resin susceptible to numerous degradation promoting conditions and mechanisms.

2.4 The chemistry of lithium 7 Isotope (⁷Li⁺) in the PWR

In a PWR, boron, in the form of boric acid (H₃BO₃), is added to the reactor coolant water for the purpose of absorbing neutrons that have been generated. This serves to protect the reactor

components from radiation (Nordmann, 2002; Meintker *et al.*, 2003). However, H_3BO_3 may have an adverse effect in that it lowers the pH of the cooling water. This effect is not desirable in the light of the necessity of protecting the reactor components against acid-based corrosion. This acidification of the coolant water may be reduced by the addition of a suitable alkalisng agent, which may raise the pH of the coolant water to an acceptable level.

In view of the fact that the isotopically pure lithium 7 (${}^7Li^+$), possesses the desired nuclear reaction properties with the neutrons present in the core of the reactor, this isotopically pure ${}^7Li^+$ in form 7LiOH is normally used as an alkalisng agent. Furthermore, the ${}^7Li^+$ isotope is formed continuously in the reactor when the boron absorbs a neutron (Nordmann, 2002; Meintker *et al.*, 2003). Natural lithium is not used in the nuclear reactor since it contains a high proportion of lithium 6 (${}^6Li^+$) and lithium 6 may be highly activated to undesirable tritium, which has a potential of increasing radioactive contamination (Nordmann, 2002). Eq 2.6 illustrates the formation of ${}^7Li^+$ from a neutronic reaction with boron.



The ${}^7Li^+$ is added to the primary coolant water in the form of 7LiOH as an alkalisng agent with it being present as a monovalent cation ${}^7Li^+$ as a consequence of the dissociation of 7LiOH in solution. However, it is essential that the ${}^7Li^+$ concentration in the PWR be limited to 2.2 ppm (2.2 mg/L) to avoid fuel cladding corrosion in the reactor core (Nordmann, 2002). The production of the isotopically pure ${}^7Li^+$ is costly making it extremely valuable, having an economic importance in the context of an operational plant for which it contributes a large capital (Meintker *et al.*, 2003).

When a nuclear reaction occurs cationic impurities such as cesium (Cs) and cobalt (Co) nuclides, as well as ${}^7Li^+$, which is formed from the boron, are formed continuously in the nuclear reactor. The formation of these nuclides results in the contamination of the coolant water. In order to prevent the removal of the ${}^7Li^+$ isotope when removing the cationic impurities the cationic radioactive waste in the coolant water is transferred to a cation-

exchanger resin such as Amberlite IRN 217 or a membrane, which is saturated with ${}^7\text{Li}^+$ cations (Meintker *et al.*, 2003). The cationic impurities exchange with the monovalent ${}^7\text{Li}^+$ on the resin. The ${}^7\text{Li}^+$ in the form of LiOH present in the coolant water passes through the resin and circulates through the PWR circuit as an alkalising agent (Meintker *et al.*, 2003).

2.5 Recovery of lithium from different sources

The recovery of lithium has been investigated by other researchers who used a solvent extraction from ores and brines (Dang & Steinberg, 1978; Averil & Olson, 1978) in sea water (Koyanaka & Yasunda, 1977), co-precipitation of lithium as lithium alluminate (Kitamura & Wada, 1978) and also various micro-organisms (Tsuruta, 2005). These studies focused on the recovery of the abundant Li^+ , which is commonly found in various sources in nature. However, it became obvious from the literature reviewed that there was no information available on the recovery of the enriched ${}^7\text{Li}^+$ isotope, specifically from a degraded nuclear grade resin.

Since degraded resin was used in this research, leachates from the degraded resin can have a limiting effect on the rate kinetics. The effect can be overcome by using higher concentrations of eluents for ion-exchange studies. According to Helfferich (1962), a particular limiting case of ion exchange is the presence and exchange of trace components. In a case where there are trace counter ions and other counter ions, which are in excess, the exchange of the trace ion, as the minority component, is always rate controlling.

2.6 Desorption of metal ions adsorbed on resin

The recovery of metal ions from organic extractants, such as ion-exchange resin, has been practised commercially by hydrometallurgists for a number of years (Cupertino & Tasker, 1994). This technique, which is known as an elution process, involves the contact of the organic solid phase (resin) which contains adsorbed metals with aqueous solutions of mineral acids such as HCl, H_2SO_4 (Kataoka & Matsunda, 1988) and carbonic acid (H_2CO_3) (Silva & Brunner, 2006). The hydrogen ions (H^+) from the acid exchange with the ions from the ion-exchange resin on which metals ions are adsorbed. The metal ions are eluted from the resin

continuously in the effluent stream from the process. For example; metals such as antimony, which were adsorbed on chelating ion-exchange resins, were eluted using 4 to 6M HCl (Motoba & Narita, 1998). The acid was allowed to react with the chelating resin and the H⁺ ions exchanged with the antimony adsorbed on the resin. Antimony in this case was eluted as an aqueous solution of antimony chloride (SbCl₃). Other metal ions such as indium and zinc were eluted using H₂SO₄ (Fortes *et al.*, 2007).

In view of the fact that the manufacture of technical commercial grade HCl and H₂SO₄ requires high capital investment costs and the manufacturing process involves both an environmentally unfriendly process, due to green house SO₂ gas produced, and a cost intensive process; the use of this manufacturing process was considered unfavourable. Consequently, the logical step was to investigate the production of an acid from a readily available feedstock. There is limited information on the production of HCl from readily available resources using a more environmentally friendly process. Therefore, the production of H₂SO₄, using a biological process, was investigated.

2.7 Biological production of sulphuric acid and its application

In view of its desirable properties and its wide range of industrial applications, H₂SO₄ is the most universally produced and used mineral acid. Its industrial applications include its use in phosphorous and nitrogen fertiliser production, petroleum refining, mineral leaching, that is, copper, zinc, nickel and titanium extraction; paint manufacturing and in the non-ferrous metallurgical industries (Young, Green, Rice, Karlage, Premeau & Cassells, 2004).

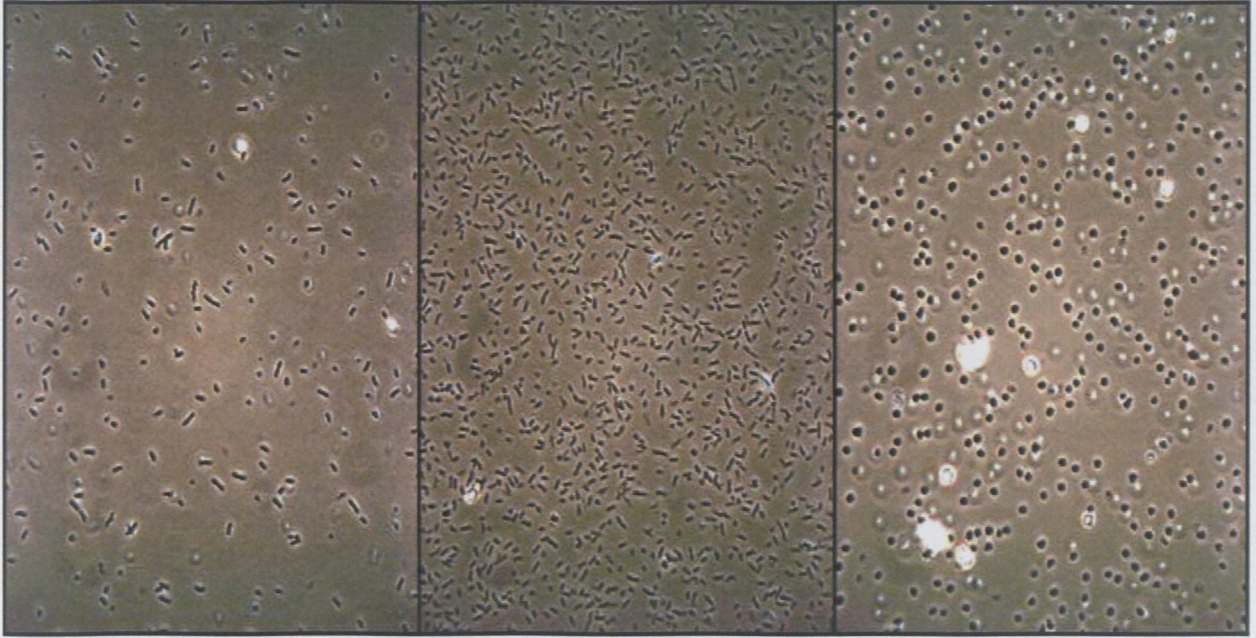
Traditionally, H₂SO₄ was produced by a catalysed transformation of sulphur dioxide (SO₂) to sulphur trioxide (SO₃) followed by reaction with water to produce H₂SO₄. However, this process has been considered to be environmentally unfriendly in view of the release of hazardous emissions when burning elemental sulphur in order to produce SO₂. The advantage of producing H₂SO₄ biologically is the reduction of hazardous compounds being released into the environment, as is the case currently associated with various, current industrial processes. The production of H₂SO₄ in a biological process is more cost efficient, sustainable and environmentally friendly, as it eliminates environmental hazards (Young *et al.*, 2004).

The biological production of H_2SO_4 involves the use of bacteria such as *Acidithiobacillus*. These bacteria are used because of their ability to oxidise either elemental sulphur or pyrites to form H_2SO_4 (Semenza *et al.*, 2002). The elemental sulphur is biologically transformed with acidophilic microbes in the presence of oxygen, water and essential micro-nutrients in order to maintain desired cell growth and a sufficient level of H_2SO_4 production (Cerruti, Curutchet & Donati., 1998; Young *et al.*, 2004; Liu, Lan & Cheng, 2004).

2.7.1 Micro-organisms involved in sulphur oxidation to produce sulphuric acid

There are several commonly known families of micro-organisms that are involved in the bio-leaching and bio-hydrometallurgy of sulphur containing ores. The first family is known as the *Acidithiobacillaceae* and it is to this family that species such as *Acidithiobacillus thiooxidans* (*A. thiooxidans*), *Acidithiobacillus caldus* (*A. caldus*) and *Acidithiobacillus ferrooxidans* (*A. ferrooxidans*), belong. The other families are known as *Trichocomaceae* and *Bacillaceae* and they include bacteria and fungi such as *Bacillus mucilaginosus* and *Asperigillus niger*. This thesis will focus on the *Acidithiobacillus* bacteria as these bacteria have been shown to produce the highest concentration of H_2SO_4 by oxidising sulphide ores or elemental sulphur as a source of energy in order to produce H_2SO_4 .

The acidophilic bacteria that grow at a pH of 1.5 to 4, have the ability to oxidise sulphide ores or elemental sulphur as a source of energy. These micro-organisms are divided into the following three main groups: A) mesophiles, B) moderate thermophiles and C) hyperthermophiles, as shown in Figure 2.7. Mesophile bacteria, shown in Figure 2.7(A), are rod shaped with a dimension of about $0.5 \times 2.0 \mu m$ and operate optimally between 30 and $42^\circ C$. These micro-organisms belong to the genera *Acidithiobacillus* and *Leptospirillum*. Moderate thermophile micro-organisms, Figure 2.7(B), have a morphology similar to mesophiles, and grow optimally at temperatures between 45 to $55^\circ C$. These micro-organisms generally belong to the genus *Sulphobacillus*. Hyperthermophiles are spherical and have a diameter of 1 to $2 \mu m$ as shown in Figure 2.7(C). They grow at elevated temperatures between 60 and $90^\circ C$ and belong to the genera *Sulfolobus*, *Acidanus*, *Metallosphaera* and *Sulfurococcus* (Neale, 2006).



A

B

C

Figure 2.7: A photograph of bio-leaching bacteria and archaea; A) mesophiles, B) moderate thermophiles and C) extremophiles (Neale, 2006)

Table 2.1: Chemolithotrophic bacteria with bio-hydrometallurgical potential (Jonglertjunya, 2003)

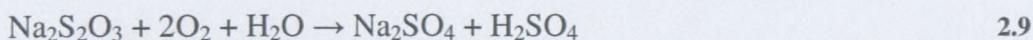
Micro-organism	Ore mineral	Reference
<i>Acidithiobacillus ferrooxidans</i>	Chalcopyrite concentrate	(Nakazawa, Fujisawa & Sato, 1998)
	ZnS concentrate	(Blancarte-Zurita, Branion, & Lawrence, 1986)
	Pyrite concentrate	(Fowler, Branion, & Lawrence, 2001)
	Covellite concentrate (CuS)	(Curutchet & Donati, 2000)
	Chalcopyrite low grade	(Bhattacharya, 1990)
	Heazlewoodite (Ni ₃ S ₂)	(Giaveno & Donati, 2001)
	Sphalerite concentrate	(Bállester, 1990)
<i>Acidithiobacillus thiooxidans</i>	Pyrrhotite	(Veglió, 2000)
<i>Acidithiobacillus caldus</i>	Arsenopyrite	(Valdes, Quatrini, Hallberg, Dopson, Valenzuela & Holmes, 2009)
<i>Leptospirillum ferrooxidans</i>	Pyrite concentrate	(Boon, 1999)
<i>Arthrobacter spp.</i>	Pyrolusite (MnO ₂) concentrate	(Cardone, Ercole, Breccia, Lepidi., 1999)
<i>Acidianus brierleyi</i>	Chalcopyrite concentrate	(Konishi, Asai & Tokushige, 1999)
	Pyrite concentrate	(Konishi, Kogasaki & Asai, 1997)
<i>Sulfobacillus thermosulfidooxidans</i>	Pyrite and Arsenopyrite concentrate	(Clark & Norris, 1996)
<i>Sulfolobus rivotincti</i>	Chalcopyrite concentrate	(Gómez, Blázquez, Ballester, 1999)
<i>Sulfolobus metallicus</i>	Pyrite concentrate	(Nemati, Harrison, Hansford & Webb, 1998)
<i>Metallosphaera sedula</i>	Pyrite concentrate	(Han & Kelly, 1998)

The use of chemolithotrophic, specifically mesophilic and moderately thermophilic acidophilic bacteria, is deemed appropriate because of the low energy requirements for a process designed for these bacteria in the biological production of H₂SO₄ as they are known to produce higher titres of the acid (Tichý, Janssen, Grotenhuis, Letting & Rulkens, 1994).

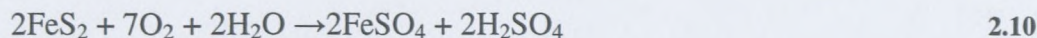
2.7.2 Properties and applications of *Acidithiobacillus* bacteria

Acidithiobacillus bacteria are colourless, rod shaped, gram negative proteobacteria with polar flagella (Semenza *et al.*, 2002). They are strictly proteobacteria as they are essentially aerobic and chemoautotrophic organisms requiring inorganic molecules as electron donors (Neale, 2006). These micro-organisms are known mainly for their ability to oxidise elemental sulphur and sulphur containing compounds. The growth conditions for these micro-organisms, i.e., pH and temperature, are extremely dependent on the physiological properties of the micro-organism to be used. These micro-organisms grow in a nutrient medium with a pH of 0.5 to 10 with some of the micro-organisms being acidophiles, while others grow under neutral condition. Most mesophiles have an optimum growth temperature of approximately 30°C. However, it is possible for these micro-organisms to grow and to oxidise inorganic substrates within a wide temperature range of between 2°C and 37°C (Barrett, Hughes, Karavaiko & Spencer, 1993). Certain *Acidithiobacillus* bacteria, such as the sulphur oxidiser, *A. caldus*, are moderately thermophilic. They oxidise sulphur at a temperature range of between 40 and 50°C and have been used in the bioleaching of pyrite and arsenopyrite (Semenza *et al.*, 2002). The *Acidithiobacillus* species, such as *A. ferroxidans*, *A. thioxidans* and *A. caldus*, have played an important role in the bio-leaching of metal sulphides from ores. They obtain their nutrients by oxidising iron to ferric iron and elemental sulphur to H₂SO₄ in the presence of dissolved oxygen.

The three commonly used sulphur oxidising acidophilic bacteria i.e. *A. caldus*, *A. ferroxidans* and *A. thioxidans* of the genus *Acidithiobacillus* are known for their ability to oxidise a wide range of sulphur compounds (i.e. S²⁻, S⁰, S₂O₄, S₂O₃²⁻). The oxidation of various sulphur-based compounds is illustrated in Eq. 2.7 to 2.9 (Suzuki, 2001);



Acidithiobacillus such as *A. ferrooxidans* derive their energy from iron oxidation as shown in Eq 2.10:



Sulphur oxidising bacteria such as *A. caldus*, which grow under acidic conditions and which are able to oxidise elemental sulphur to produce H_2SO_4 , were considered the most relevant for this study and are discussed in detail in the subsequent section. The reason for this is because the recovered H_2SO_4 titres need to have a low metallic ion content in order to be suitable for use in ion-exchange processes.

2.7.3 *Acidithiobacillus caldus*

2.7.3.1 Characteristics and physiology

A. caldus with an optimum growth temperature of between 40 and 50°C has been reported to dominate sulphur-oxidising bacterial population in commercial bio-leaching and biooxidation plants (Hallberg & Lindstrom, 1994; Semenza *et al.*, 2002). *A. caldus* is moderately thermophilic, it is unable to oxidise IRON(II) and its characteristics closely resemble those of the mesophilic bacteria *A. thiooxidans* (Hallberg & Lindstrom, 1994; Hallberg *et al.*, 1996; Rawlings *et al.*, 1997). *A. caldus* is an aerobic, gram negative and chemoautotrophic micro-organism that grows on elemental sulphur as an energy source in order to produce H_2SO_4 as the end-product. The elemental sulphur is biologically transformed by *A. caldus* in the presence of air, water and essential micro-nutrients so as to maintain the desired cell growth and H_2SO_4 production (Cerruti *et al.*, 1998; Young *et al.*, 2004; Liu *et al.*, 2004). *A. caldus* has five main characteristics (Nemati *et al.*, 1998) :

- Gram-negative and chemolithotrophic - grow using energy obtained from the oxidation of sulphur to produce H_2SO_4 .
- Autotrophic - carbon dioxide may be used as a cellular carbon source, while nitrogen, phosphorus and trace minerals such as K, Mg, Na, Ca and Co are essential for optimal cellular growth.
- Aerobic - dissolved oxygen is essential as an electron acceptor. An oxygen supply may be achieved by using ambient air to provide the required oxygen and carbon dioxide.

- Acidophilic-optimum bacterial growth is at a pH range of between 1.5 to 4.
- Moderately thermophilic - growth temperature range is between 40 and 50°C.

2.7.4 Biological sulphuric acid production in small scale aerated batch bioreactors

The concept of the biological production of H₂SO₄ in small scale submerged reactors has been reported in literature whereby the bio-dissolution of spent nickel-cadmium batteries using *A. ferroxidans* (Cerruti *et al.*, 1998) was utilised, while the combined degradation of covellite by *A. thioxidans* and *A. ferroxidans* and the oxidation of biologically produced sulphur in continuous mixed-suspension reactors was investigated (Tichýa *et al.*, 1994). In a study by Tichýa *et al.* (1994), elemental sulphur was used in powder, flour and crystalline form for a laboratory scale operation. However, Tichýa *et al.* (1994) indicated that the production rates using elemental flour were too low and industrial application was thus doubtful.

2.7.5 Recovery of sulphuric acid from biological titres

During the production of H₂SO₄ using a biological process a product stream of acid may either be removed directly for acidification or else acid may be concentrated using various processes. Commercial methods used to concentrate the acid include reverse osmosis, membrane separation, filtration, distillation and a cryogenesis methodology (Young *et al.*, 2004). In this study a combination of membrane filtration and evaporation was used. The acid recovered may be used to elute ⁷Li⁺ from a degraded nuclear grade ion-exchange resin in which the isotope is mobilised.

2.8 Summary

Commonly used commercial grade mineral acids such as H₂SO₄ and HCl were identified as suitable eluents for the desorption of ⁷Li⁺ isotope from degraded lithiated mixed-bed resin as these mineral acids have been shown to have sufficient efficiency to elute other metals such as antimony from ion-exchange resin. However, although mineral acids have been used to recover metals from different resins, the use of these acids in a degraded nuclear grade resin has not previously been investigated. In addition, there is no information on the recovery of the ⁷Li⁺ isotope from a degraded cross-linked polystyrene resin. Furthermore, despite the fact

that the production of biological H_2SO_4 was widely reported in the literature reviewed, the compatibility of such an acid with a degraded polystyrene resin has never been investigated. In ion-exchange research the quantification of leachates due to resin degradation has also been sparsely reported. Since this study investigates the possibility of recovering the high value $^7\text{Li}^+$ isotope it was clearly essential also to monitor the leachates in the effluent recovered, and to evaluate whether it was possible to reduce these leachates in such a way that the solution containing $^7\text{Li}^+$ isotope could be used in the PWR of a nuclear power plant.

The production of H_2SO_4 from the oxidation of elemental sulphur and its related compounds has been extensively researched. However, the production of high strength H_2SO_4 titres exceeding 0.38M in a biological process in terms of which *A. caldus* is immobilised on elemental sulphur in an aerated batch bioreactor has not previously been reported. Nevertheless, there is extensive literature on the production of H_2SO_4 using *A. thiooxidans*. There is general consensus that *A. thiooxidans* is able to produce H_2SO_4 with different sulphurous sources. In addition, this research also explored the possibility of concentrating biologically produced H_2SO_4 by evaporation. The development of the mathematical model for the design process to simulate ion-exchange process design parameters is discussed in Chapter 3. The following questions emanated from the literature review and have been addressed in the chapters presenting the findings of the study:

- Will dilute solutions of the mineral acids identified (HCl and H_2SO_4) be able to elute significant amounts of $^7\text{Li}^+$ isotope from the degraded Amberlite resin? (Chapter 5)
- Will the biologically produced acid be capable of effectively eluting the $^7\text{Li}^+$ isotope from the resin in a process similar to the process used for mineral acids? (Chapter 6)
- What type of leachates will be found in the $^7\text{Li}^+$ isotope effluent when commercial grade mineral acid and biological acid are used? (Chapters 5 and 6)
- Will the mathematical model developed be suitable to model the desorption rates of $^7\text{Li}^+$ from the degraded Amberlite IRN 217 lithiated mixed-bed resin for processes involving both the mineral acids and the biologically produced acids? (The development of the mathematical model is described in Chapter 3 and evaluated in Chapters 5 and 6).

CHAPTER 3

MODELLING DESORPTION KINETICS FOR A POROUS REACTIVE BED

3.1 Introduction

The development of the desorption model was based on the mass conservation of an ionic species desorption using a packed-bed column. Conventional ion-exchange adsorption-desorption isotherms are generally used for modelling desorption of metals from resin. However, these isotherms do not take into consideration design parameters such as eluent flow rate, bed porosity, ion exchange rates and length of the column reactor (Silva and Brunner, 2006). The model developed in this study will consider all these parameters. This model was based on the mass balance equation from Treybal (1980) and similar to that used by Tan and Liou (1988). The model developed took into consideration the conditions and assumptions for this system. The model developed in this study was verified using experimental data obtained in order to evaluate the suitability of the model for the desorption process. Process design parameter such as equipment dimensions, eluent flow rate and bed porosity were used in this model in order to simulate the desorption process on a laboratory scale.

3.2 Theory: characteristic method for solving partial differential equations

The characteristic method is a technique that is used to solve first order partial differential equations (PDE). This method reduces a PDE to a family of first order ordinary differential equations (ODE) and its solution may be integrated from given initial boundary conditions and then transformed into a solution pertaining to the original PDE. The method of characteristics may be illustrated by a first order PDE of the form:

$$a(x,t,u)\frac{\partial u}{\partial x} + b(x,t,u)\frac{\partial u}{\partial z} = c(x,t,u) \quad 3.1$$

Where a , b and c are general functions of x , t and $u(x, t)$. Equation 3.1 is said to be quasilinear as it is linear in the derivative terms but it may contain non-linear expressions of the form $u \partial u / \partial t$ or u^2 . If a solution to the equation above is found then the tuple $\{x, t, u(x, t)\}$ defines a surface, S_1 , in the Cartesian co-ordinate system, where the position vector, \mathbf{r} , to any point on the surface will be given by:

$$\mathbf{r}(x, t) = xi + ti + u(x, t, u)k \quad 3.2$$

The normal vector to the surface is given by the formula below:

$$\mathbf{n} = \frac{\partial \mathbf{r}}{\partial x} \times \frac{\partial \mathbf{r}}{\partial t} / \left[\frac{\partial \mathbf{r}}{\partial x} \times \frac{\partial \mathbf{r}}{\partial t} \right] \quad 3.3$$

The vector $\partial \mathbf{r} / \partial x \cdot \partial \mathbf{r} / \partial t$ may be represented as follows:

$$\frac{\partial \mathbf{r}}{\partial x} \times \frac{\partial \mathbf{r}}{\partial t} = \left(\mathbf{i} + \frac{\partial u}{\partial x} \mathbf{k} \right) \times \left(\mathbf{j} + \frac{\partial u}{\partial t} \mathbf{k} \right) = \pm \left(\frac{\partial u}{\partial x} \mathbf{i} + \frac{\partial u}{\partial t} \mathbf{j} \pm \mathbf{k} \right) \quad 3.4$$

Thus, if $u(x, t)$ is a solution to Eq.3.1, then the vector $\mathbf{p} = (a \mathbf{i} + b \mathbf{j} + c \mathbf{k})$ must be orthogonal to the surface normal as shown in Eq 3.5:

$$\mathbf{p} \cdot \mathbf{n} \equiv \mathbf{p} \cdot \frac{\left(\frac{\partial u}{\partial x} \mathbf{i} + \frac{\partial u}{\partial t} \mathbf{j} \pm \mathbf{k} \right)}{\left| \frac{\partial \mathbf{r}}{\partial x} \cdot \frac{\partial \mathbf{r}}{\partial t} \right|} = a \frac{\partial u}{\partial x} + b \frac{\partial u}{\partial t} - c = 0 \quad 3.5$$

Accordingly, it may be concluded that the vector, \mathbf{p} , must lie on the tangent of the plane of the solution surface, S_1 . Eq. 3.1 may be solved by finding a surface, S_1 , such that every point on the surface, \mathbf{p} , lies tangent to the plane.

If a curve, C , that lies on the surface, S_1 , such that its position vector, $\mathbf{r}(x, t)$, may be defined as in Eq.3.2, then the parametric curve in terms of Q may be represented as follows:

$$\mathbf{r} = (x(Q), y(Q)) = x(Q)\mathbf{i} + t(Q)\mathbf{j} + u[x(Q), t(Q)]\mathbf{k} \quad 3.6$$

The tangent vector local to the curve C is given by:

$$\frac{\partial \mathbf{r}}{\partial Q} = \frac{\partial x}{\partial Q}\mathbf{i} + \frac{\partial t}{\partial Q}\mathbf{j} + \frac{\partial u}{\partial Q}\mathbf{k} \quad 3.7$$

If the vector equation $\mathbf{p} = (a\mathbf{i} + b\mathbf{j} + c\mathbf{k})$ is in a tangent plane then it must also be tangential to curve C . Thus, the parametric equation (Eq.3.8) will hold:

$$\frac{\partial r}{\partial Q} = a[x(Q), t(Q)]; \quad \frac{\partial t}{\partial Q} = b[x(Q), t(Q)]; \quad \frac{\partial u}{\partial Q} = c[x(Q), t(Q)] \quad 3.8$$

The solving of this system of PDEs provides assurance that \mathbf{p} is a tangent to the curve, C , which, in turn, lies in the solution surface, S_1 . The curve C is termed an integral curve of the vector field of Eq. 3.1. Integral curves are also known as characteristic curves of PDE.

3.3 Modelling the desorption kinetics for a porous reactive bed from basic mass transfer principles

The mathematical model that describes the desorption kinetics of an ionic species from a porous reactive bed was developed from a mass balance equation (Treybal, 1980) for an

infinitesimal section of a solid packed-bed ion-exchange resin in terms of which the column (length and inner diameter) may be divided into finite difference volume elements (Δz) (see Figure 3.1). The acidic fluid flows along the packed-bed with organic material (solid phase) containing the adsorbed metallic species from a region of high concentration zone to that of lower concentration zones. The cationic or anionic ion species in the acidic fluid react with the solid packed-bed, thus exchanging with the other cationic or anionic ions species adsorbed in the packed-bed resin. This technique is known as an elution or a desorption process. Figure 3.1 illustrates a schematic diagram that may be used to develop the model.

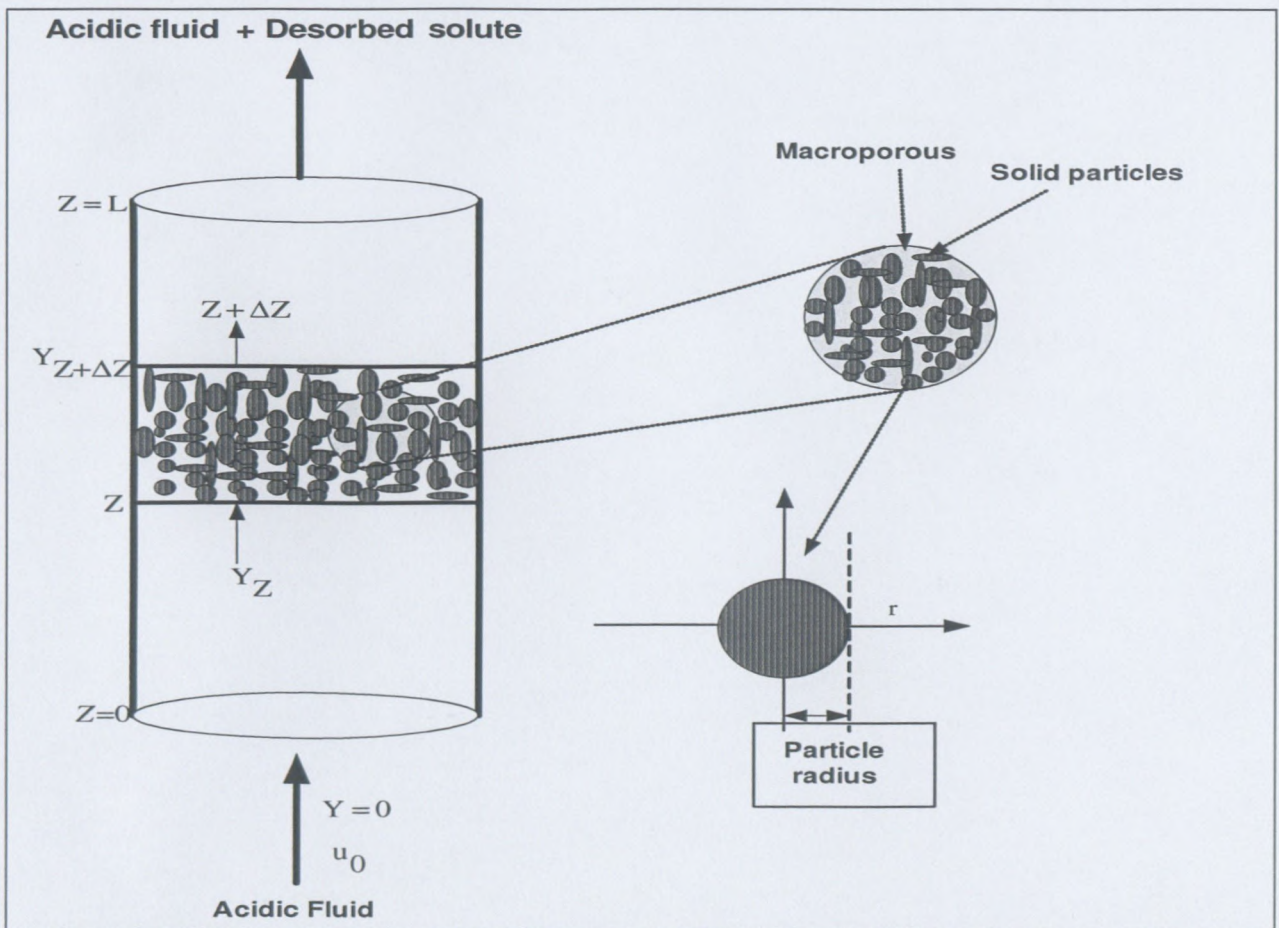


Figure 3.1: The schematic diagram illustrating the process used to model the desorption kinetics of ionic species from a porous reactive bed

The mass transport of species in an elemental volume occurs through convection, diffusion, rate of consumption and accumulation. This process may be represented by a mass balance equation in three dimensions in rectangular coordinates as depicted in Eq. 3.9 (Treybal, 1980):

$$\begin{aligned} \varepsilon \frac{\partial S}{\partial t} (1) + \left(u_x \frac{\partial S}{\partial x} + u_y \frac{\partial S}{\partial y} + u_z \frac{\partial S}{\partial z} \right) (2) + \frac{\partial S}{\partial \theta} (3) \\ = D \left(\frac{\partial^2 S}{\partial x^2} + \frac{\partial^2 S}{\partial y^2} + \frac{\partial^2 S}{\partial z^2} \right) (4) + (1 - \varepsilon) r_i (5) \end{aligned} \quad 3.9$$

Where the numbers represent:

- (1) The concentration of the ionic species desorbed from the reactive bed with respect to time.
- (2) Convective transport in three dimensions through the reactive bed (x, y, z).
- (3) Accumulation of the ionic species within the packed-bed ion-exchange column.
- (4) Diffusive transport of the ionic species from the porous bed in three dimensions (x, y, z).
- (5) Desorption or adsorption rate of the ionic species from the packed-bed column.
- ε - Porosity of the bed in the packed ion-exchange column.

In order to simplify Eq 3.9 the following assumptions were made:

- In view of the convective movement of the eluent in the axial direction the transport in the ion-exchange packed-bed column was in the axial (z) direction only. Accordingly, radial distribution and movement of the ionic species in the bed were considered to be negligible.
- Axial eluent velocity (u_z) was assumed to be constant as a result of the pumping effect of the eluent at a predetermined flow rate. In addition, the diffusive transport of the ionic species from the resin bed was assumed to be negligible when compared to the convective transport.
- Minimal bed expansion occurs due to the use of a controlled flow rate through the bed in order to minimise ion-exchange bed fluidisation.
- There is limited accumulation of the ionic species in the packed-bed column as a result of the continuous extraction of the eluent from the column.
- The ionic species desorbs from the reactive bed and minimal re-adsorption occurs.

Considering these assumptions, Eq 3.9 becomes:

$$\varepsilon \frac{\partial S}{\partial t} + u_z \frac{\partial S}{\partial z} = (1 - \varepsilon)r_i \quad 3.10$$

The rate of desorption from the reactive bed may be expressed in terms of linear first order desorption kinetics such that the desorption term on the R.H.S. of Eq. 3.10 becomes:

$$r_i = \frac{\partial S}{\partial t} = -\bar{k}S \quad 3.11$$

Eq. 3.11 represents the desorbed ionic species leaving the packed-bed column. Furthermore, Eq. 3.11 may be solved by using integration and by applying the following boundary conditions:

$$\text{at } t = 0; S = S_0. \quad 3.12$$

The solution is as follows:

$$S = S_0 e^{-\bar{k}t} \quad 3.13$$

Eq. 3.10 and Eq. 3.11 were combined to provide a solution of the mass balance for the ionic species desorbed from the packed-bed such that;

$$\varepsilon \frac{\partial S}{\partial t} + u_z \frac{\partial S}{\partial z} = -(1 - \varepsilon)\bar{k}S \quad 3.14$$

By substituting Eq 3.13, Eq 3.14 may be rewritten as:

$$\varepsilon \frac{\partial S}{\partial t} + u_z \frac{\partial S}{\partial z} = -(1 - \varepsilon)\bar{k}S_0 e^{-\bar{k}t} \quad 3.15$$

Eq 3.15 is a first order PDE, which may be used to simulate the desorption kinetics of an ionic species from a reactive porous bed.

3.4 Developing a solution for a partial differential equation describing the desorption kinetics for a reactive bed

This section describes the procedure used to quantify the solution for Eq. 3.7 by utilising the method of characteristics used to solve a first order PDE. In order to solve Eq. 3.15 by the characteristics method of first order PDE, a parameter, Q , is introduced along the curve such that the origin of the curve satisfies the boundary conditions in Eq. 3.16:

$$\text{at the inlet port } z = 0; S = 0; t = 0 \quad 3.16$$

$$\frac{\partial t}{\partial Q} = \varepsilon; \quad \frac{\partial z}{\partial Q} = u_z; \quad \frac{\partial S}{\partial Q} = -(1 - \varepsilon)\bar{k}S_0 e^{-t} \quad 3.17$$

Eq. 3.17 may be represented in a similar way to the parametric Eq. 3.8:

$$\frac{\partial t}{\varepsilon} = \frac{\partial z}{u_z} = \frac{\partial S}{-(1 - \varepsilon)\bar{k}S_0 e^{-kt}} \quad 3.18$$

This means that:

$$\frac{\partial t}{\varepsilon} = \frac{\partial z}{u_z} \quad 3.19 \quad \text{and} \quad \frac{\partial t}{\varepsilon} = \frac{\partial S}{-(1 - \varepsilon)\bar{k}S_0 e^{-kt}} \quad 3.20$$

By integrating Eq. 3.19 and Eq. 3.20 the solution becomes:

$$t = \frac{\varepsilon z}{u_z} + A_1 \quad 3.21 \quad \text{and} \quad -\frac{(1 - \varepsilon)}{\varepsilon} S_0 e^{-kt} = S + A_2 \quad 3.22$$

The generalised equation may be expressed by Eq. 3.23 and Eq. 3.25 in terms of which F is an arbitrary function that depends on the solution of the elution curve such that:

$$F(A_1; A_2) = 0 \quad 3.23$$

And

$$A_1 = F(A_2) \quad 3.24 \quad \text{or} \quad A_2 = F(A_1) \quad 3.25$$

By making S the subject of the formula, Eq. 3.14 may be expressed as:

$$S = -A_2 - \frac{(1-\varepsilon)}{\varepsilon} S_0 e^{-\bar{k}t} \quad 3.26$$

By substituting Eq. 3.25 into Eq. 3.26 the solution becomes:

$$S = -F(A_1) - \frac{(1-\varepsilon)}{\varepsilon} S_0 e^{-\bar{k}t} \quad 3.27$$

By substituting the solution to A_1 in Eq. 3.21 directly into Eq. 3.27, the following equation will emerge:

$$S = -F\left(t - \frac{\varepsilon z}{u_z}\right) - \frac{(1-\varepsilon)}{\varepsilon} S_0 e^{-\bar{k}t} \quad 3.28$$

When the boundary conditions in Eq. 3.16 are applied to Eq. 3.28 the equation is transformed to:

$$F(t) = -\frac{(1-\varepsilon)}{\varepsilon} S_0 e^{-\bar{k}t} \quad 3.29$$

This means that:

$$F\left(t - \frac{\varepsilon z}{u_z}\right) = -\frac{(1-\varepsilon)}{\varepsilon} S_0 e^{-\bar{k}\left(t - \frac{\varepsilon z}{u_z}\right)} \quad 3.30$$

By substituting Eq. 3.30 into Eq. 3.28 the following equation will be achieved:

$$S = \frac{(1-\varepsilon)}{\varepsilon} S_0 e^{-\bar{k}\left(t - \frac{\varepsilon z}{u_z}\right)} - \frac{(1-\varepsilon)}{\varepsilon} S_0 e^{-\bar{k}t} \quad 3.31$$

In order to determine the exit concentration (S_e) of the ionic species leaving the packed-bed column the following conditions may be applied:

$$\text{at the exit port } S = S_e \quad \text{and} \quad z = L \quad 3.32$$

Where L is the length of the ion-exchange column.

Eq. 3.31 then becomes:

$$S_e = \frac{(1-\varepsilon)}{\varepsilon} S_0 e^{-\bar{k}\left(t - \frac{\varepsilon L}{u_z}\right)} - \frac{(1-\varepsilon)}{\varepsilon} S_0 e^{-\bar{k}t} = \frac{(1-\varepsilon)}{\varepsilon} S_0 \left[e^{-\bar{k}\left(t - \frac{\varepsilon L}{u_z}\right)} - e^{-\bar{k}t} \right] \quad 3.33$$

Since Eq. 3.33 will be used for simulation purposes using an ODE solver (Polymath), the first order differential format of Eq. 3.25 is:

$$\frac{dS_e}{dt} = -\frac{(1-\varepsilon)}{\varepsilon} \bar{k} S_0 \left[e^{-\bar{k}\left(t - \frac{\varepsilon L}{u_z}\right)} - e^{-\bar{k}t} \right] \quad 3.34$$

3.5 Summary

The mathematical model developed in this section was similar to that which was previously used to model the desorption of ethyl acetate from activated carbon (Tan & Liou, 1988). However, the model in this study was applied in a desorption-based process to model the

recovery of high value ionic species from a degraded polymeric material such as polystyrene divinylbenzene ion-exchange resin.

The following question arose from this chapter and will be addressed in Chapters 5 and 6:

- Will the mathematical model which was developed be suitable to model the desorption rates of ${}^7\text{Li}^+$ from the degraded Amberlite IRN 217 lithiated mixed-bed resin for processes involving both the mineral acids and the biologically produced acids?

The question above is linked to the following objective which will be addressed Chapter 5:

- To develop a mathematical model for the desorption of ${}^7\text{Li}^+$ isotope from degraded Amberlite IRN 217 lithiated resin. The mathematical model was used to predict the desorption rate of the isotope from the resin for design purposes.

CHAPTER 4

MATERIALS AND METHODS

4.1 Introduction

This chapter describes the materials as well as all the analytical techniques that were used to obtain the requisite data needed to realise the objectives of the study. The criteria used to validate the data are discussed in the chapter together with evidence of the validity from other related studies.

4.2 Experimental materials and methodology

4.2.1 Characteristics of the Amberlite IRN 217 lithiated mixed-bed resin

The experiments in the study were carried out using a degraded nuclear grade Amberlite IRN 217 lithiated mixed-bed resin with both strong acid cation and strong base anion resins obtained from Koeberg nuclear power station (South Africa). A new batch of Amberlite IRN 217 lithiated resin obtained from Rohm and Haas (manufacturer) was used as a control. The resin was made of polystyrene and cross-linked with divinylbenzene gel matrix. The anion and the cation resin in the mixed-bed were matched to ensure that they were inseparable on loading (Rohm & Haas, 2003). The physical and chemical properties of the resins are presented in Table 4.1 and Appendix A. The anion part of the mixed-bed resin was confirmed by Rohm and Haas to be degraded (See Appendix B).

Table 4.1: Properties of the Amberlite IRN 217 lithiated mixed-bed resin

Physical characteristics	Cation resin	Anion resin
Physical form	Uniform particle size spherical beads	Uniform particle size spherical beads
Shipping weight	690 g/L	690 g/L
Harmonic mean size	650 ± 50 µm	630 ± 50 µm
Uniformity coefficient	≤ 1.2	≤ 1.2
Particle size	< 0.3 mm : 0.2 % max	< 0.3 mm : 0.2 % max
Whole beads	98 % min	98 % min
Chemical characteristics	Cation resin	Anion resin
Matrix	Polystyrene DVB gel	Polystyrene DVB gel
Functional groups	Sulphonic acid	Trimethylammonium
Ionic form as shipped	⁷ Li ⁺	OH ⁻
Total exchange capacity	≥ 1.75 eq/L (⁷ Li ⁺ form)*	≥ 1.2 eq/L (OH ⁻ form)
Strong base capacity	-	≥ 90 %
Moisture holding capacity	49 - 55% (H ⁺ form)	54 - 60 % (OH ⁻ form)
Ionic conversion	99% min ⁷ Li ⁺	95% min OH ⁻
CO ³⁻	-	5% max
Cl ⁻	-	0.1% max
SO ₄ ²⁻	-	0.1% max

*Batch dependent, i.e. varies depending on individual manufactured batches

4.2.2 Determination of favourable eluent concentration: Batch reactor elution

Solutions with an acid concentration of 1, 3 and 5M HCl and H₂SO₄, respectively were prepared. Milli-Q water (distilled, with pH of 7.0) was used as the control for the experiment, i.e. water without acid. The acid solutions were prepared by diluting 32% HCl and 98% H₂SO₄ with distilled water. The acid eluents were prepared in 250 ml Schott bottles and 30 ml of the degraded mixed-bed resin was added. The experiments were performed in triplicate for each acid concentration in order to validate the results obtained. The reactors containing the different acid solutions were placed on a roller at a speed of 50 rpm for a period of 48 hours at room temperature (25°C). Samples were taken after 24 hours to determine the concentration of the ⁷Li⁺ isotope in the solution. These batch experiments were part of a preliminary study to determine the favourable desorption acid concentration to be used in the continuous elution column. From the three acid concentration tested, the results obtained for

the batch experiment showed that 1M HCl and H₂SO₄, respectively, were the most favourable to be used in the continuous column. The results will be discussed in Chapter 5.

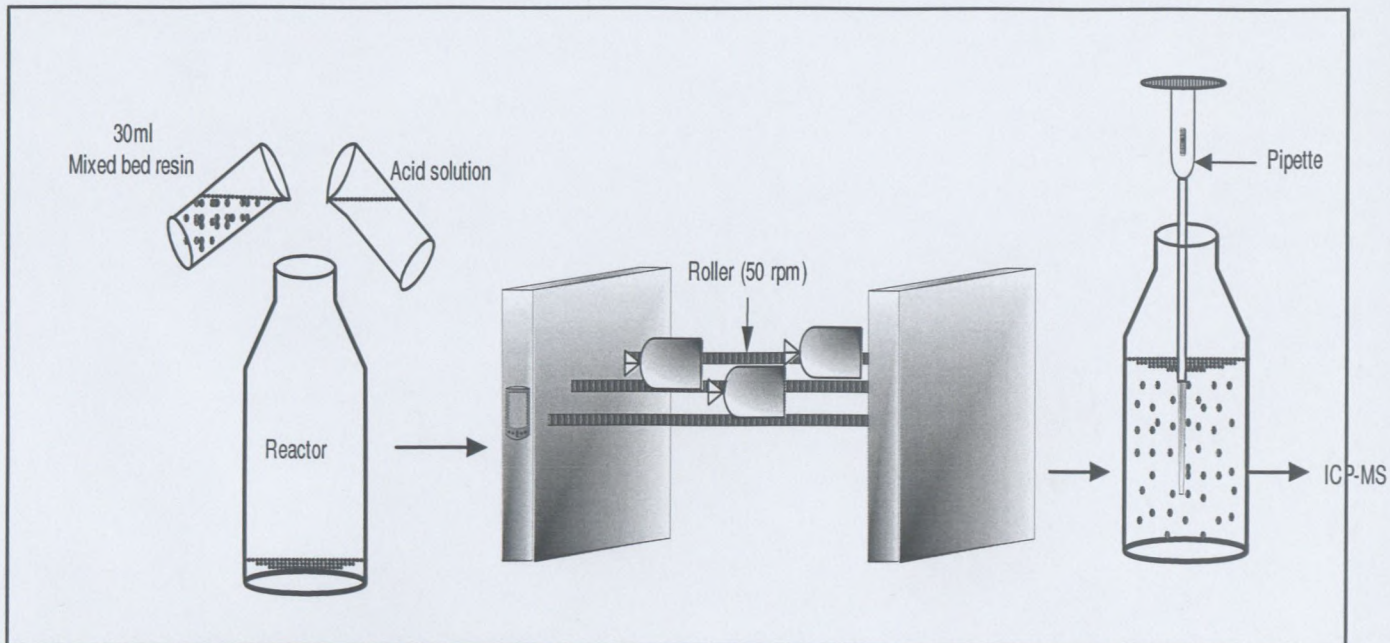


Figure 4.1: Schematic illustration of the batch extraction of lithium (⁷Li⁺) isotope from Amberlite IRN 217 lithiated mixed bed resin

4.2.3 Packed-bed column desorption process

4.2.3.1 Desorption stage

The continuous desorption experiments were carried out in a glass ion-exchange column with an internal diameter of 25 mm and a length of 300 mm; as shown in Figure 4.2(A). All the piping and connections used were made of silicone tubing. The column was filled with 30 ml of degraded Amberlite IRN 217 lithiated mixed-bed resin. Acid solutions containing 1M HCl and H₂SO₄, respectively, were passed axially through the mixed-bed column at a constant flow rate of 6.65 ml/min using a Gilson Minipuls evolution peristaltic pump. This flow rate corresponded to 13 bed volumes per hour (BV/hr). One bed volume (1BV) was defined as the volume of the elution solution that is equivalent to the volume of the resin in the column. The flow rate used enabled adequate sampling of the eluent for the profiling of ⁷Li⁺ isotope desorption from the resin but without fluidising the resin bed. This flow rate was slightly higher than the flow rate used by Lukey and van Deventer (2000) who studied the elution of copper and iron cyanide complexes from ion-exchange resins. Eighteen bed volumes (18 BV)

of the eluents were passed through the column for each experiment. The experiments were performed in triplicate and the results presented are the average of the three experimental results obtained. Effluent samples were taken at each 2 BV (60 ml) for a period of 9 minutes. The effluent was analysed for the ${}^7\text{Li}^+$ isotope as well as anion and cation leachates, explained in section 4.2.4.3.

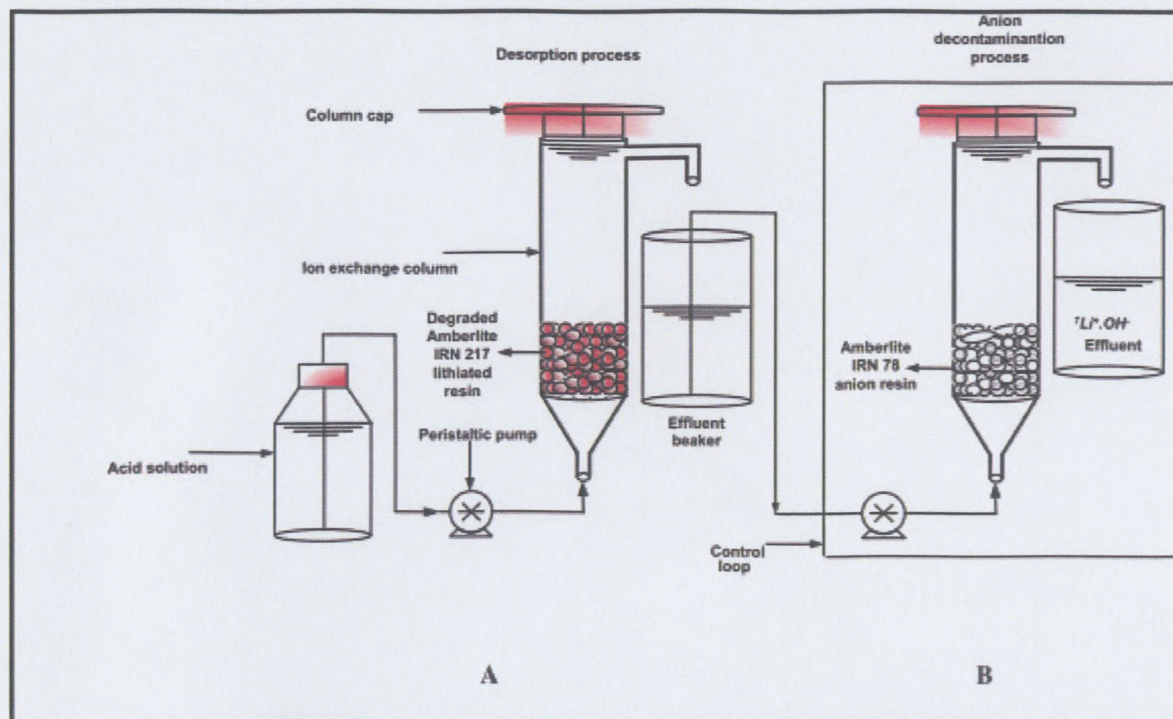


Figure 4.2: [A] A schematic illustration of the column used for the elution of lithium isotope (${}^7\text{Li}^+$) from 30 ml degraded Amberlite 217 lithiated mixed-bed resin and [B] the anion decontamination process

4.2.3.2 The reduction of anion leachates (Anion decontamination process)

The anion contaminants, that is, the leachates from the resin, were reduced in a process that was carried out under similar conditions to those used during the desorption stage (as shown in Figure 4.2B). The leachates' reduction column was filled with 90 ml of Amberlite IRN 78 anion resin (Rohm & Haas, 2003). The effluent from the elution stage was passed through the Amberlite IRN 78 anion resin so as to remove the anion leachates. This was done in order to evaluate whether it was possible to reduce the anion leachates using the Amberlite IRN 78 resin. The levels of the cation contaminants in the effluent recovered from the decontamination process were also quantified. This was only to evaluate the process and the aim was not to bring the concentration to below the specified requirements of $50 \mu\text{g/L}$. The optimization of this process will be done in a subsequent study. The experiments were

performed in triplicate and the results presented are the average of the three experimental results obtained.

4.2.3.3 Lithium isotope (${}^7\text{Li}^+$) eluting ratio

The desorption degree of the lithium isotope (${}^7\text{Li}^+$) from the Amberlite 217 lithiated mixed-bed resin may be expressed by the following eluting ratio:

$$\text{The eluting ratio} = (S_e / S_o) \times 100 (\%) \quad 4.1$$

- S_e is the amount of lithium isotope (${}^7\text{Li}^+$) from the Amberlite IRN 217 lithiated mixed-bed resin (mg/L) at the exit of the column.
- S_o is the total amount of lithium isotope (${}^7\text{Li}^+$) adsorbed on the Amberlite IRN 217 lithiated mixed-bed resin based on a cation capacity = 2.19 eq/L.

4.2.3.4 Development of the parameters used in the ODE model

The porosity of the Amberlite IRN 217 lithiated mixed-bed resin was determined by weighing 30 ml of the mixed-bed resin in a measuring cylinder. The density of the resin was then determined using a Pycnometer (ACCUPYC 1330). The mass of the 30 ml resin was divided by the resin density measured to give the actual volume which the resin beads occupied. The pore volume was determined as the difference between the apparent resin volume (30 ml) and the volume obtained from the density calculation (actual resin volume). Thereafter, the fraction of the resin pore volume, ϵ , was determined as a ratio between the pore volume and the apparent resin volume. The amount of ${}^7\text{Li}^+$ on the 30 ml Amberlite IRN 217 lithiated resin, S_o , was determined to be equivalent to 15330 mg/L. This was based on the anion/cation ratio (1:1.4) and the quantified concentration of ${}^7\text{Li}^+$ on the resin (2.19 eq/L ${}^7\text{Li}^+$) as indicated on the certificate of analysis from the manufacturer (Rohm and Haas, France). The desorption rate constant (\bar{k}); parameter was determined from experimental data using Microsoft Excel 2000 Solver[®] to solve non-linear regression problems. The (\bar{k}) was solved to find values that minimised the absolute error between the experimental and the calculated data for both HCl and H₂SO₄. The fit of the model was discussed based on the minimum sum

of square differences (SSD) and the regression coefficient (R^2) between the experimental and calculated data.

4.2.4 Biological production of sulphuric acids

The biological production of H_2SO_4 was evaluated as an alternative to the commonly used commercial grade minerals acids. This was done in order to evaluate its capability in terms of recovering the $^7Li^+$ isotope on the degraded Amberlite IRN 217 lithiated mixed-bed resin. Biological methods are both cost efficient and environmentally friendly as they reduce environmental hazards.

4.2.4.1 Micro-organism and media

A. caldus (DSM 8584), which was isolated from mine water taken from continuous flow bio-oxidation tanks, was chosen as the base strain for this study because it has been found to dominate other sulphur oxidising bacterial populations in commercial bio-leaching, thus rendering it suitable for large scale processes (Semenza *et al.*, 2002). The culture strain, DSM 8584, used in this study was obtained from the Department of Chemical Engineering, University of Cape Town (South Africa).

An iron free medium DSMZ 150 (without a yeast extract) mixed with a filter sterilised (0.22 μm filter) DSMZ 150a (trace element) solution was used to culture the micro-organism. The DSMZ 150 used contained (g) $(NH_4)_2SO_4$ (3.0); $K_2HPO_4 \cdot 3H_2O$ (0.50); $MgSO_4 \cdot 7H_2O$ (0.50); KCl (0.10); $Ca(NO_3)_2$ (0.01) and 1000 ml of distilled water. The pH of the DSMZ 150 was adjusted to 2.5 using 6M sulphuric acid. The trace element solution contained (mg) $FeCl_3 \cdot 6H_2O$ (11.0); $CuSO_4 \cdot 5H_2O$ (0.5); H_3BO_3 (2.0); $MnSO_4 \cdot H_2O$ (2.0); $Na_2MoO_4 \cdot 2H_2O$ (0.8); $CoCl_2 \cdot 6H_2O$ (0.6); $ZnSO_4 \cdot 7H_2O$ (0.9) and 10.0 ml of distilled water. For every 1000 ml of the DSMZ 150 medium 10 ml of the DSMZ 150a and 27.78 g of sulphur was added.

4.2.4.2 Inoculum preparation, bioreactor operation and acid recovery

The bacterial strain was grown in the medium as described in section 4.2.4.1 for a period of 7 d (until the pH <1). After this period 50 ml of the culture was used as an inoculum in a 2000 ml Erlenmeyer flask, which contained 1800 ml nutrient medium. Five flasks (total volume = 9000 ml) were incubated at a temperature of 40°C in a rotary shaker at 200 rpm. The flasks were aerated continuously at 0.7 L/min. The pH and the H₂SO₄ were monitored every 8 d over a period of 16 d. The H₂SO₄ was recovered by means of vacuum filtration using pure aluminium oxide ceramic membranes (OD = 0.010 m; ID = 0.007 m; L = 0.25 m, average pore size across wall thickness = 3 μm, operating pH = 0 - 14, burst pressure = 10 bar) and a vacuum pump operating at -10 bars. The H₂SO₄ was further processed by filtering the acid, which had been recovered using a 0.22 μm filter to remove some of the cells and sulphur colloids. The H₂SO₄ was concentrated by evaporation 80% (v/v) of moisture at a temperature of 80°C. The process is illustrated schematically in Figure 4.3 and Figure 4.4 illustrates the bioreactor in operation and samples before and after ultra-filtration.

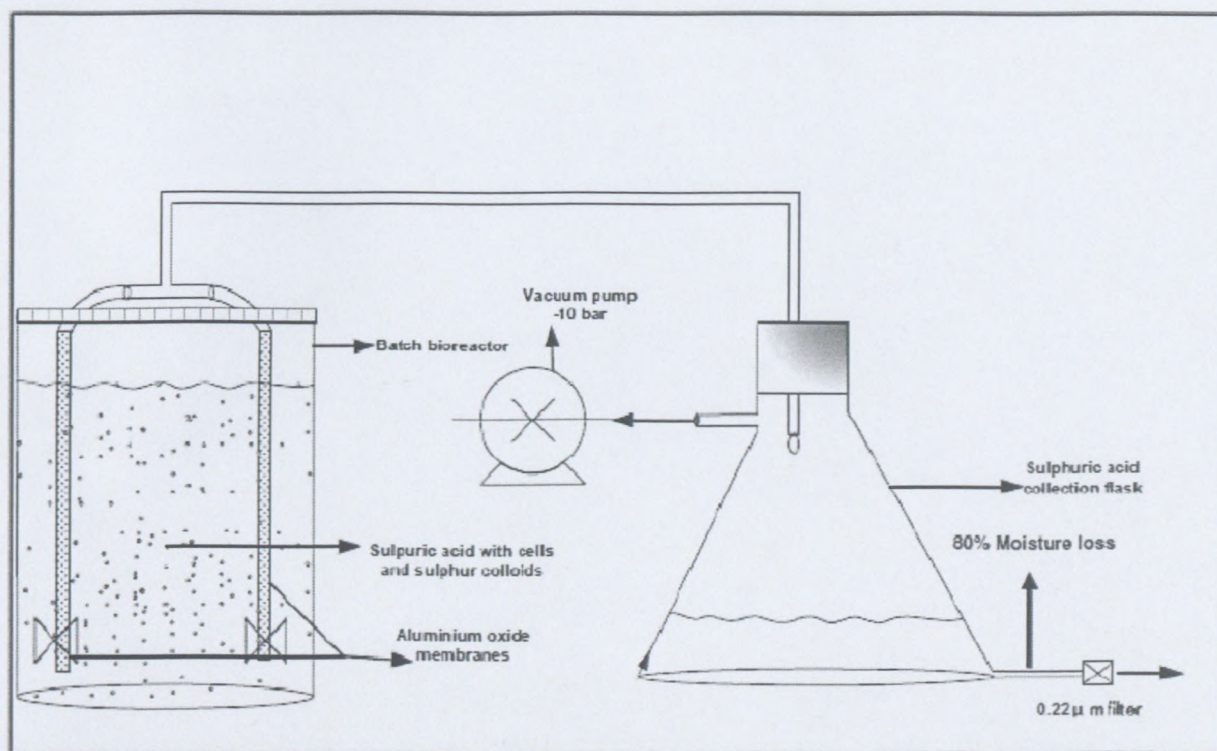


Figure 4.3: The recovery of H₂SO₄ from the batch bioreactor

(A) Bioreactors in operation



(B) Samples recovered from the bioreactor before ultra-filtration.



(C) Samples recovered from the bioreactor after ultra-filtration.



Figure 4.4: A) bioreactor in operation and (B+C) samples recovered from the bioreactor before and after ultra-filtration.

4.2.4.3 Analysis of pH, sulphuric acid, $^7\text{Li}^+$ and anion and cation leachates

The pH level was monitored using a Metrohm 744 pH meter. The H_2SO_4 concentration was determined by titration with 0.175M of sodium hydroxide (NaOH) solution with phenolphthalein as the acid base indicator (Cerruti *et al.*, 1998). The concentration of $^7\text{Li}^+$ and cation leachates recovered in the effluent solution was determined using a Varian Liberty II Radial ICP-AES instrument (Geology Department at Stellenbosch University, South Africa). HCl samples were diluted – 10x and H_2SO_4 samples 20x – before analysis. Matrix matched calibration standards were prepared for both the HCl and H_2SO_4 samples, and the accuracy of calibration was verified using a quality control standard before conducting the analysis.

Nitrates ($\text{NO}_3\text{-N}$) were analysed using an auto-analyser by means of the Cadmium reduction method (Mitsch *et al.*, 2005), while the chlorides (Cl^-) were analysed by titrating standardised silver nitrates solutions to the first potentiometric end-point which corresponded to the micromoles of chloride ions present in the eluent (Tang & Gordon, 1980). Furthermore, fluorides (F^-) were determined using a Colometric Spectrometer (Tokalioglu, Sahin & Kartal, 2001). The sulphates (SO_4^{2-}) and phosphates (PO_4^{2-}) were both determined using an Inductively Coupled Plasma Spectrometer (ICP-MS) while the carbonates (CO_3^{2-}) were determined by titration with HCl acid (BEMLAB (Pty) Ltd, Stellenbosch, South Africa).

4.2.4.4 Desorption of lithium isotope by biologically produced sulphuric acid

The desorption of lithium isotope with biologically produced H_2SO_4 was performed in a process similar to the experiment depicted in Figure 4.2, Section 4.2.3.1.

4.2.5 Ordinary differential equation solver

In this study a general purpose and user friendly ordinary differential equation (ODE) solver software package known as Polymath 5.1 was used to generate the data that was used to simulate the experimental results obtained.

CHAPTER 5

RESULTS

Lithium 7 isotope ($^7\text{Li}^+$) desorption from a degraded Amberlite IRN 217 lithiated mixed-bed resin

Prepared for publication in the *Solvent Extraction and Ion-exchange Journal*

(Accepted for publication)

CHAPTER 5: RESULTS

Lithium 7 isotope ($^7\text{Li}^+$) desorption from a degraded Amberlite IRN 217 lithiated mixed-bed ion-exchange resin

5.1 Introduction

Amberlite IRN 217 lithiated mixed-bed resin is a mixture of uniform particle size gelular polystyrene divinylbenzene (DVB) cation and anion-exchange resin. The mixed-bed resin is designed for use in the Reactor Chemical and Volume Control System (RCV) used in the purification of reactor coolant water in a pressurised water reactor (PWR) that is employed in the nuclear industry (Rohm & Haas, 2003; Caratin *et al.*, 2008). The reactor coolant that is used to remove heat from the reactor core is, essentially, demineralised water that contains boron, lithium 7 isotope ($^7\text{Li}^+$) and a small amount of dissolved hydrogen (Otte & Liebman, 1987). A portion of the reactor coolant water is purified continuously by a mixed-bed demineraliser in order to reduce the radioactive isotopes such as cesium 137, cobalt 58 and other impurities such as sulphates and chlorides that are formed during the fission reaction (Otte & Liebman, 1987; Ohashi *et al.*, 1989; Meintker *et al.*, 2003). The cation part of the resin operates in $^7\text{Li}^+$ form with the anion resin operating in borate form. This, in turn, prevents the removal of the $^7\text{Li}^+$ isotope and boron in the reactor coolant water (Hartly *et al.*, 1978; Otte & Liebman, 1987; Corpora *et al.*, 1996; Nordmann, 2002; Meintker *et al.*, 2003; Barois *et al.*, 2009). The $^7\text{Li}^+$ isotope in the form of lithium hydroxide ($^7\text{LiOH}$) is used to control the pH of the coolant water. Boron in the form of boric acid (H_3BO_3) is added to the reactor coolant water for the purpose of absorbing neutrons, while it also serves to protect reactor components from radiation (Nordmann, 2002; Meintker *et al.*, 2003).

Amberlite IRN 217 lithiated mixed-bed resin stored in unsuitable storage conditions often results in the degradation of the anion part of the mixed-bed resin, thus resulting in an inefficient ion-exchange process. Resin degradation may be caused by fluctuating storage temperature conditions which, in turn, affects the shelf-life of the ion-exchange resin (Harland, 1994; Rideaux, 1999). If resin is stored over a long period of time under varying temperature conditions, this will result in the moisture content inside the resin expanding as it

becomes solid in sub-zero temperatures. This, in turn, leads to the resin polymer stretching as a result of freezing (Rideaux, 1999; Mamo *et al.*, 2004). A repeated freezing-thawing cycle causes resin breakdown and the release of organically bound impurities due to broken polymer bonds (Mamo *et al.*, 2004). The minimum shelf-life of the anion and cation parts of the Amberlite IRN 217 lithiated mixed-bed resin is 2 years and 5 years, respectively (Rideaux, 1999). However, the resin may be stored for a time period longer than the recommended shelf-life under good storage temperature conditions and it may be analysed for potential leachates before use (Harland, 1994; Helfferich, 1995; Rideaux, 1999; Rohm & Haas, 2003).

Figure 5.1 illustrates the degraded Amberlite IRN 217 lithiated mixed-bed resin used in this study with the cation beads having a clear and smooth external surface, while the degraded anion beads (brown) indicates the compromised external surface of the resin.

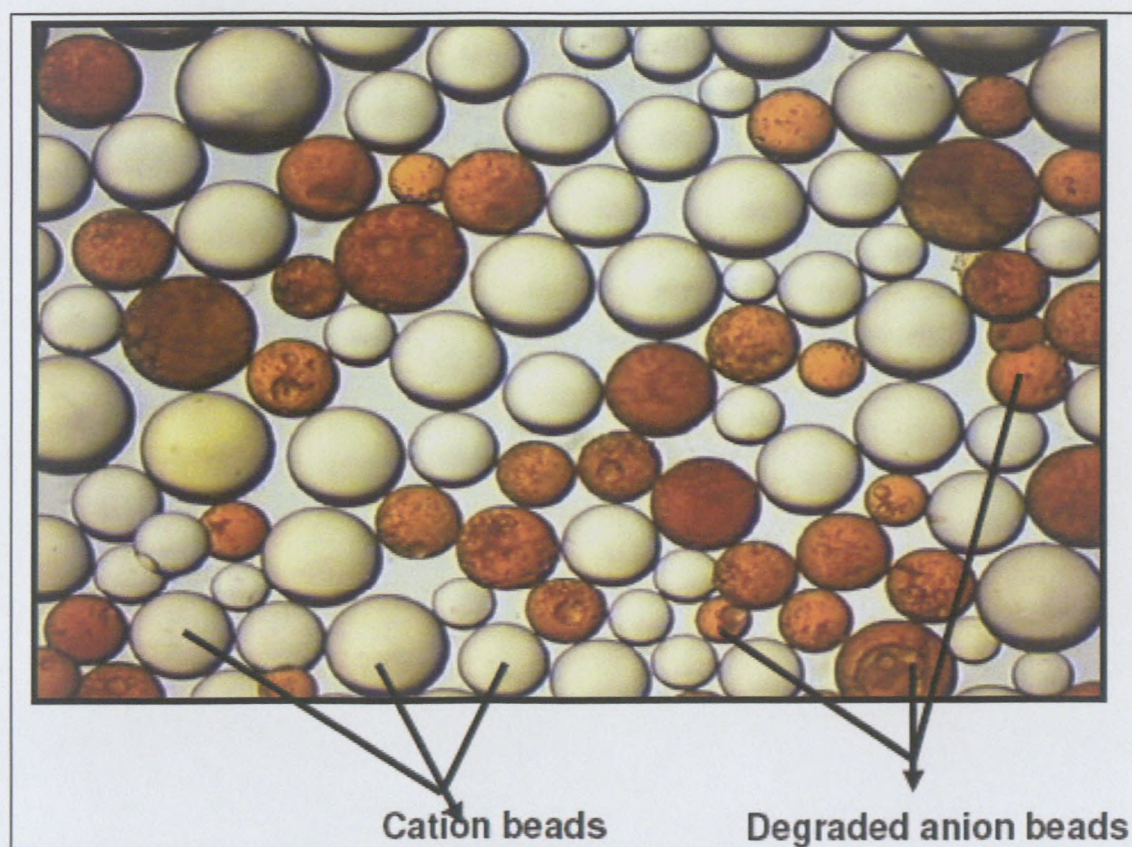


Figure 5.1: Scanning electron microscope (SEM) view of degraded Amberlite IRN 217 lithiated mixed-bed resin (Rohm and Haas, 2003)

Degradation of the hydroxide form (OH^-) of a strong base anion resin may be explained in terms of the Hoffman degradation mechanisms (Harland, 1994; Helfferich, 1995). The predominant route of degradation is the loss of the functional group on the resin, thus resulting in the liberation of leachates and free amine. After evaluation of the Rohm and Haas evaluation report, (see Appendix C), the anion resin was reported to have lost its strong base capacity and it had degraded. The cation part of the resin with the valuable $^7\text{Li}^+$ isotope was reported to be in a desirable condition with a good physical appearance and excellent chemical properties. The isotopically pure $^7\text{Li}^+$ immobilised on the cation part of the mixed-bed resin is expensive (Meintker *et al.*, 2003), as compared to the cation resin in hydrogen (H^+) form in other Amberlite resin or Duolite. As a result of the value of the $^7\text{Li}^+$ isotope, an investigation was conducted to evaluate methods to recover the isotopically pure $^7\text{Li}^+$ isotope from the cation resin and to profile the anion and cation leachates in the recovered $^7\text{Li}^+$ isotope effluent. The decrease of these leachates in the recovered effluent was also evaluated. The recovered $^7\text{Li}^+$ isotope may be used in a form of lithium hydroxide ($^7\text{LiOH}$) in the PWR as an alkalising agent to raise the pH of the reactor coolant water (Meintker *et al.*, 2003).

The recovery of lithium isotopes has been investigated by other researchers using solvent extraction processes from ores and brines (Dang & Steinberg, 1978; Averil & Olson, 1978); from sea water (Koyanaka & Yasunda, 1977); by the co-precipitation of lithium as lithium alluminate (Kitamura & Wada, 1978) and also by using various micro-organisms (Tsuruta, 2005). The recovery of metal ions from an organic extractant such as an ion-exchange resin has been practised commercially by hydrometallurgists for a number of years (Cupertino & Tasker, 1994). This is done by bringing the ion-exchange resin with the adsorbed metal ions into contact with an aqueous solution of mineral acids such as hydrochloric (HCl) and sulphuric acids (H_2SO_4) (Kataoka & Matsunda, 1988). Metals such as antimony, which was adsorbed on a chelating resin, was eluted using 4 to 6M HCl solutions (Motoba & Narita, 1999). The HCl solution was allowed to react with the chelating resin in which the antimony had been adsorbed in an ion-exchange packed-bed column. The antimony was then eluted as a solution of antimony chloride (SbCl_3) (Motoba & Narita, 1999). Other metals, such as zinc (Lukey & Van Deventer, 2000) and indium (Fortes *et al.*, 2007) which had adsorbed on polymeric ion-exchange resin were eluted using H_2SO_4 . However, despite the fact that several studies have investigated the elution of metals from ion-exchange resin there is

limited information on the elution of the ${}^7\text{Li}^+$ isotope adsorbed on polystyrene divinylbenzene ion-exchange resin. This study provides an insight into the mechanism of desorbing the ${}^7\text{Li}^+$ isotope from a degraded polystyrene divinylbenzene-based mixed-bed ion-exchange resin known commercially as Amberlite IRN 217 lithiated mixed-bed resin using aqueous solutions of HCl and H_2SO_4 .

5.2 Materials and Method

5.2.1 Experimental procedure

Experimental procedure for this part of the study was previously explained in Chapter 4, section 4.2.1 to 4.2.3.1.

5.2.2 Analytical method

The analytical method used for this part of the study was previously explained in section 4.2.4.3.

5.2.3 Mathematical model: desorption kinetics

The development of the desorption model was explained previously in Chapter 3. The model developed was compared with the experimental data in order to evaluate the suitability of the model. The mass balance equation for the movement of ionic species in the bulk phase within a column in an axial direction was developed in Chapter 3 and the following equations were extracted:

$$\varepsilon \frac{\partial S}{\partial t} + u_z \frac{\partial S}{\partial z} = -(1 - \varepsilon)r_i \quad 3.10$$

Where, r_i is the desorption rate from a porous packed-bed column represented by first-order desorption kinetics such that:

$$r_i = \frac{\partial S}{\partial t} = -\bar{k}S \quad 3.11$$

Where \bar{k} is the desorption rate constant, while taking into consideration the following initial boundary conditions:

$$t = 0; S = S_0 \quad 3.12$$

In order to determine the exit concentration of the ionic species leaving the packed-bed column, S_e , the following conditions were also applied:

$$\text{At the entry port: } z=0; S=0; t=0 \quad 3.16$$

$$\text{At the exit port: } S = S_e; z = L \quad 3.32$$

Where L is the length of the ion-exchange column.

The solution for Eq. 3.10 was developed using the characteristic method used to solve partial differential equations while taking into consideration Eq.3.11 and the overall operating conditions (Eq. 3.12 to 3.32) in order to obtain the following first-order differential equation (ODE):

$$\frac{dS_e}{dt} = -\frac{(1-\varepsilon)\bar{k}S_0}{\varepsilon} \left[e^{-\bar{k}\left(t-\frac{\varepsilon L}{u_z}\right)} - e^{-\bar{k}t} \right] \quad 3.34$$

5.3 Results and discussion

5.3.1 Resin degradation

When comparing a new batch of Amberlite IRN 217 lithiated mixed-bed resin (obtained from Rohm and Hass), the anion resin on the degraded Amberlite mixed-bed resin (obtained from Eskom), the degraded resin was confirmed to have been subjected to Hoffman degradation. The level of the anions found after passing Milli-Q water, 1M HCl and 1M H₂SO₄ through the new batch of Amberlite resin was significantly lower compared to the degraded

Amberlite IRN 217 lithiated resin, as shown in Table 5.1. This was also confirmed by the level of cationic leachates in the recovered effluent as the level was lower for the new batch when compared to the degraded mixed-bed resin. The anion part of the new batch mixed-bed resin showed a reduction of the anions from the HCl and H₂SO₄ eluents.

Table 5.1: Analysis of leachates from the degraded Amberlite IRN 217 lithiated mixed-bed resin compared to the new batch of Amberlite IRN217 lithiated mixed-bed resin

Sample description	Cl⁻ (mg/L)	SO₄²⁻ (mg/L)	CO₃²⁻ (mg/L)	NO₃⁻ (mg/L)	F⁻ (mg/L)	PO₄²⁻ (mg/L)
Milli-Q-Water (after passing through degraded resin)	44.06	31.3	0.06	0.3	0	0.05
Milli-Q-Water (after passing through new resin)	35.3	23.9	0.04	0	0	0.01
1M HCl (after passing through degraded resin)	84165.2	48.5	0	26.92	nd	0.24
1M H ₂ SO ₄ (after passing through degraded resin)	36460.9	48277.3	nd	27.98	nd	nd
1M HCl (after passing through the new resin)	40249.8	5.7	0	0.33	0	0.25
1M H ₂ SO ₄ (after passing through the new resin)	8767.2	41443.4	0	17.5	0	0.55

nd- not detected

However, this phenomenon was not observed on the new batch of the mixed-bed resin. In addition, the degraded resin was observed to be drier compared to the new batch and this was attributed to the loss of moisture during the continuous freeze-thawing cycle. The higher level of anions and cations from the degraded mixed-bed resin showed that the anion resin had degraded and lost its capacity, thus reducing its ability to remove trace ions from acid eluents (Rideaux, 1999; Mamo *et al.*, 2004). Furthermore, it was observed that the degraded resin used in this study had broken pieces, which were released during the rinsing of the bed using the eluents and the Milli-Q water.

5.3.2 Determination of favourable eluent concentration in a batch reactor

Figure 5.2 depicts the desorption curve of the $^7\text{Li}^+$ isotope eluted from the 30 ml Amberlite IRN 217 lithiated mixed-bed resin using 1, 3 and 5M of HCl and H_2SO_4 , respectively, in a batch reactor. The desorption profiles represent the combined average results obtained at intervals of 24 and 48 hr for individual acid concentrations. Standard error bars were generated using Sigma Plot 8.0 to indicate the deviation during the sampling periods identified.

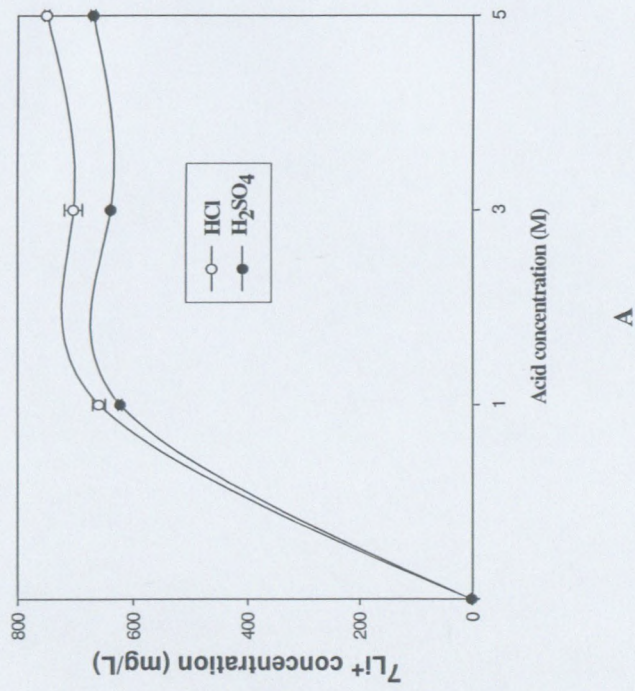
Table 5.2: Statistical analysis of $^7\text{Li}^+$ desorption in batch reactors

Concentration (M)	
HCl	P-values
0M vs. 1M	0.00
1M vs. 3M	0.06
3M vs. 5M	0.035
H_2SO_4	
	P-values
0M vs. 1M	0.00
1M vs. 3M	0.105
3M vs. 5M	0.008

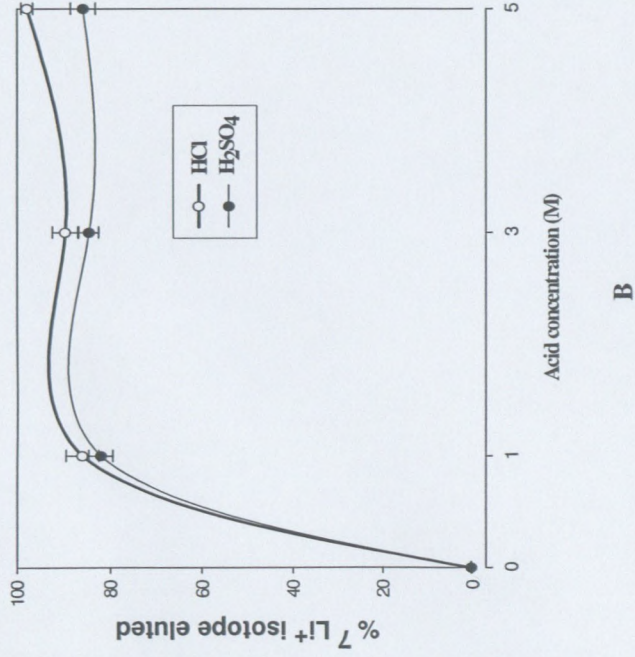
If the $p \leq 0.05$, there is a statistically significant difference between the two groups

A comparative study was performed using a t-test to evaluate the effect of the sampling periods (24 and 48 hr) on the $^7\text{Li}^+$ isotope desorption rate for both HCl and H_2SO_4 . The p-values obtained for the HCl concentrations were 0.847 (0M), 0.596 (1M), 0.684 (3M) and 0.486 (5M), thus indicating no significant difference between the $^7\text{Li}^+$ isotope concentrations obtained at sampling periods of 24 hr and 48 hr. The p-values obtained for H_2SO_4 acid were 0.847 (0M), 0.703 (1M), 0.460 (3M) and 0.268 (5M), also indicating a negligible difference between the samples obtained at 24 and 48 hr. These results were similar to the HCl experiments. It was concluded that the sampling period has a negligible effect on the $^7\text{Li}^+$ concentration in the effluent recovered from the batch reactors. Accordingly, the results for the sampling periods 24 and 48 hr were averaged in Figure 5.2 and compared for HCl and H_2SO_4 .

The results showed an increase in the $^7\text{Li}^+$ isotope desorption with an increase in the acid solution concentration for both HCl and H_2SO_4 . Desorption percentages of 86% and 84.4% at 1M; 89.63% and 84.4% at 3M; with 97.8% and 84.6% being achieved using 5M HCl and H_2SO_4 solutions, respectively. When comparing the two eluents the results showed that the HCl had a slightly higher recovery of $^7\text{Li}^+$ isotope from the resin than the H_2SO_4 . This was confirmed by a t-test using SPSS 16.0, which showed p-values of less than 0.05 for the $^7\text{Li}^+$ isotope recovered by HCl and H_2SO_4 at various acid concentrations. A repeated measure Anova method, which was determined using SPSS 16.0 software was used to evaluate the difference in the desorption efficiency of $^7\text{Li}^+$ isotope at the different acid concentrations (Table 5.2). A p-value of 0.0 was obtained for the comparison of the control experiment (0M) and 1M of HCl and H_2SO_4 , respectively, thus indicating a significant difference in the $^7\text{Li}^+$ isotope desorption rate.



A



B

Figure 5.2: (A) Lithium isotope (${}^7\text{Li}^+$) concentration eluted using HCl and H₂SO₄ in batch reactors. (B) Percent ${}^7\text{Li}^+$ isotope eluted using HCl and H₂SO₄ (1M = 86 and 84.42%, 3M = 89.63 and 84.42%, 5M = 97.88 and 84.66%, respectively).

Although there was an increase in the $^7\text{Li}^+$ isotope desorption rate between the 1 and 3M of HCl and H_2SO_4 , respectively, p-values of 0.06 and 0.105 were obtained, thus indicating that the increase was not significant. However, a significant difference in the desorption rate was observed in the comparison between 3 and 5M with p-values of 0.035 and 0.008 for HCl and H_2SO_4 respectively. Overall, by increasing the acid concentrations from 1 to 5M, an increase of ~11.9 and ~0.3% was observed for HCl and H_2SO_4 , respectively. In view of the cost implications for an industrial scale operation, it was decided that, on the basis of the above information, 1M acid solutions of both HCl and H_2SO_4 should suffice for a continuous process.

5.3.3 Packed-bed column desorption process

Figure 5.3 depicts the relationship between the elution volume and the $^7\text{Li}^+$ isotope concentration in the effluent using 1M solution of HCl and H_2SO_4 , respectively, in an ion-exchange process that was run continuously. HCl was found to have a slightly higher desorption rate when compared to H_2SO_4 at 1M acid concentration during the initial stage of the experiment. However, after 6BV the desorpt $^7\text{Li}^+$ concentration was similar for both the HCl and the H_2SO_4 eluents. These results correlate with other studies in terms of which antimony and copper desorption from an ion-exchange resin was achieved with an 80% antimony desorption (Motoba & Narita, 1998; Fernando, Laing & Kim, 2002).

Additionally, Figure 5.4 illustrates the $^7\text{Li}^+$ desorption rates using 1M HCl and H_2SO_4 respectively, which were achieved during 18BV. An overall elution efficiency >90% was achieved after passing 18BV of HCl and H_2SO_4 acid solutions, respectively. Most of the $^7\text{Li}^+$ isotope (>60%) was eluted during the initial desorption stage of 2BV. The desorption profile confirmed the total removal of $^7\text{Li}^+$ isotope from the Amberlite IRN 217 lithiated resin under the conditions evaluated. This indicated that the stoichiometry quantities of HCl and H_2SO_4 were available to exchange with $^7\text{Li}^+$ on the resin as was illustrated by Fernando *et al.* (2002)

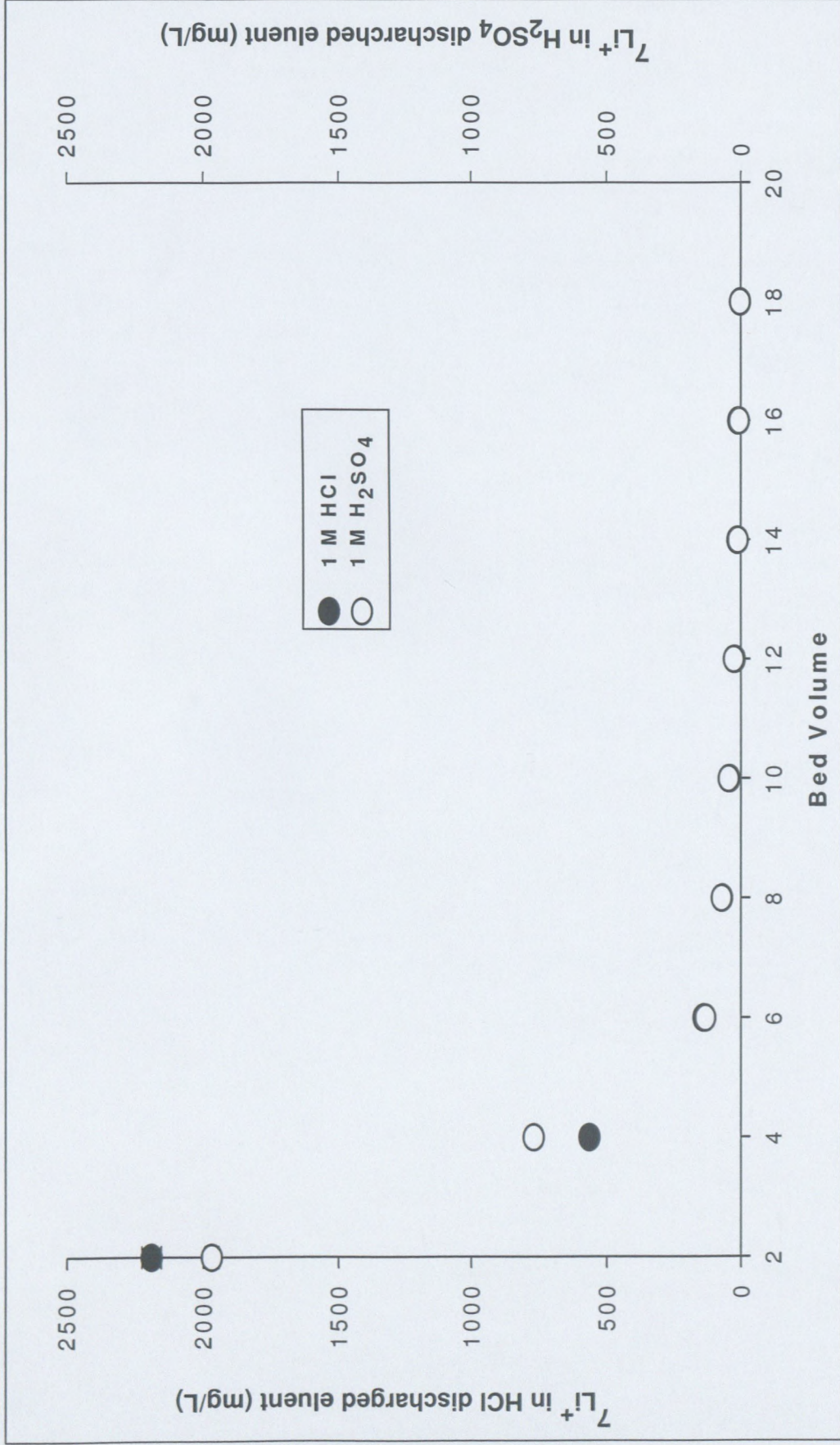


Figure 5.3: Relationship between the eluting volume and the lithium isotope (${}^7\text{Li}^+$) concentration eluted from Amberlite IRN 217 lithiated mixed-bed resin using 1M HCl and H_2SO_4 , respectively

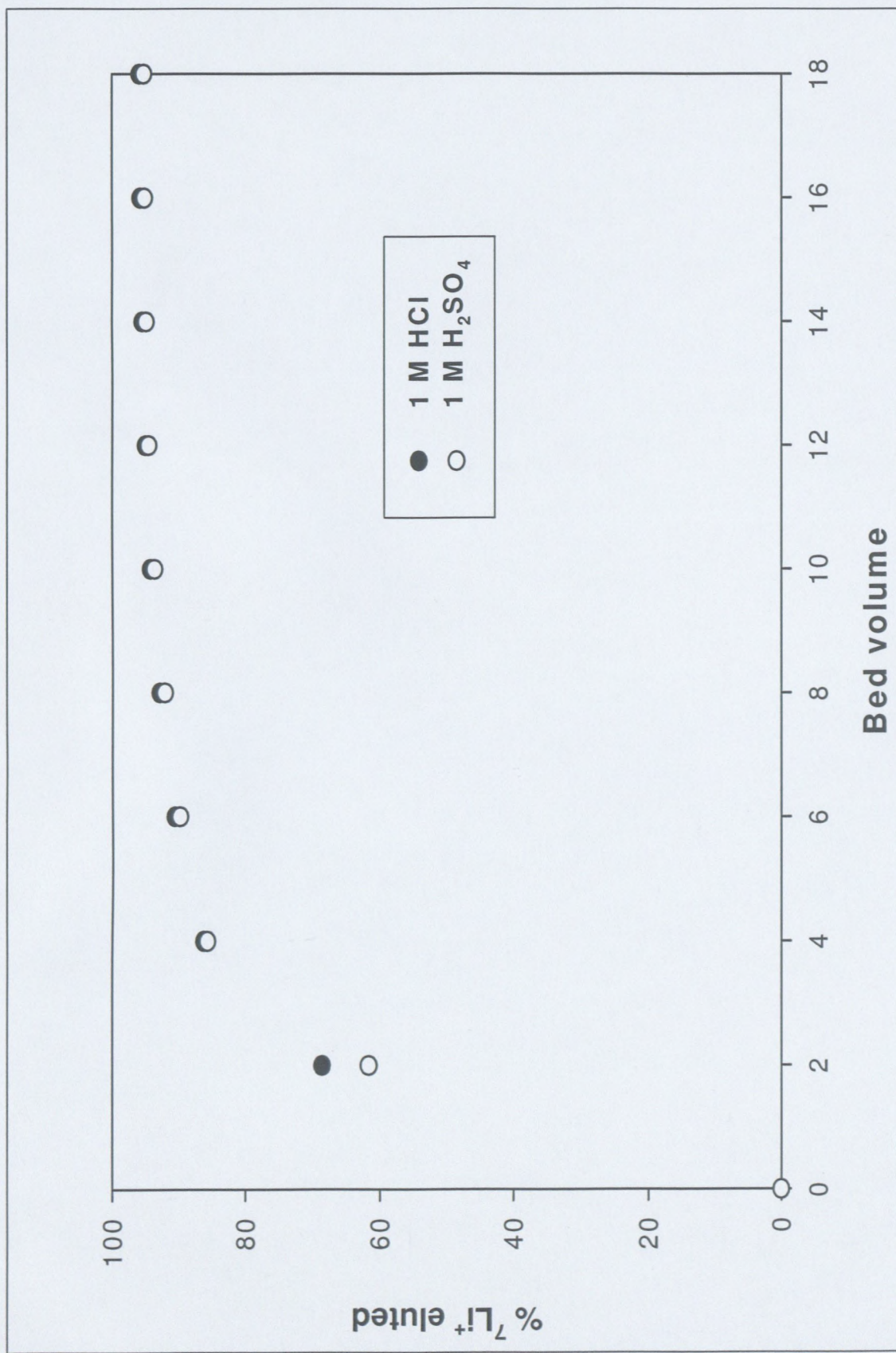


Figure 5.4: Percentage elution of lithium isotope ($^7\text{Li}^+$) from Amberlite IRN 217 lithiated mixed-bed resin in a continuous ion-exchange column

Both the HCl and H₂SO₄ eluent showed the capability of eluting ⁷Li⁺ isotope continuously. However, for cost reduction purposes, it would be beneficial to use H₂SO₄ for elution in place of HCl as H₂SO₄ is less expensive (Bruening, 1994). The experimental and calculated desorption kinetics for 1M HCl and H₂SO₄ are compared in Figure 5.5. The comparison between the simulated and the experimental data was sufficient with correlation coefficients (R²) of 0.999 and 0.994 for 1M HCl and H₂SO₄, respectively (see Figure 5.5). Furthermore, the desorption rate (\bar{k}) was determined by minimising the sum of absolute error between the experimental and calculated data for both HCl and H₂SO₄. The (\bar{k}) was 0.1315 and 0.1211 min⁻¹ for HCl and H₂SO₄ respectively. The sum of the minimum absolute error for both HCl and H₂SO₄ were 647.8 and 434.02, respectively. The higher sum of minimum absolute error was observed at the initial desorption stage 9 to 18 minutes, where a high amount of ⁷Li⁺ isotope was desorbed and this contributed to the higher sum of absolute error (see Appendix G). This indicated that the samples should have been taken between 9 to 18 min as the higher desorption rate occurred at this point. The resin bed-porosity (ϵ) fraction was determined as ~0.44, which was determined using the quantified density of the resin (1.2 g/ml).

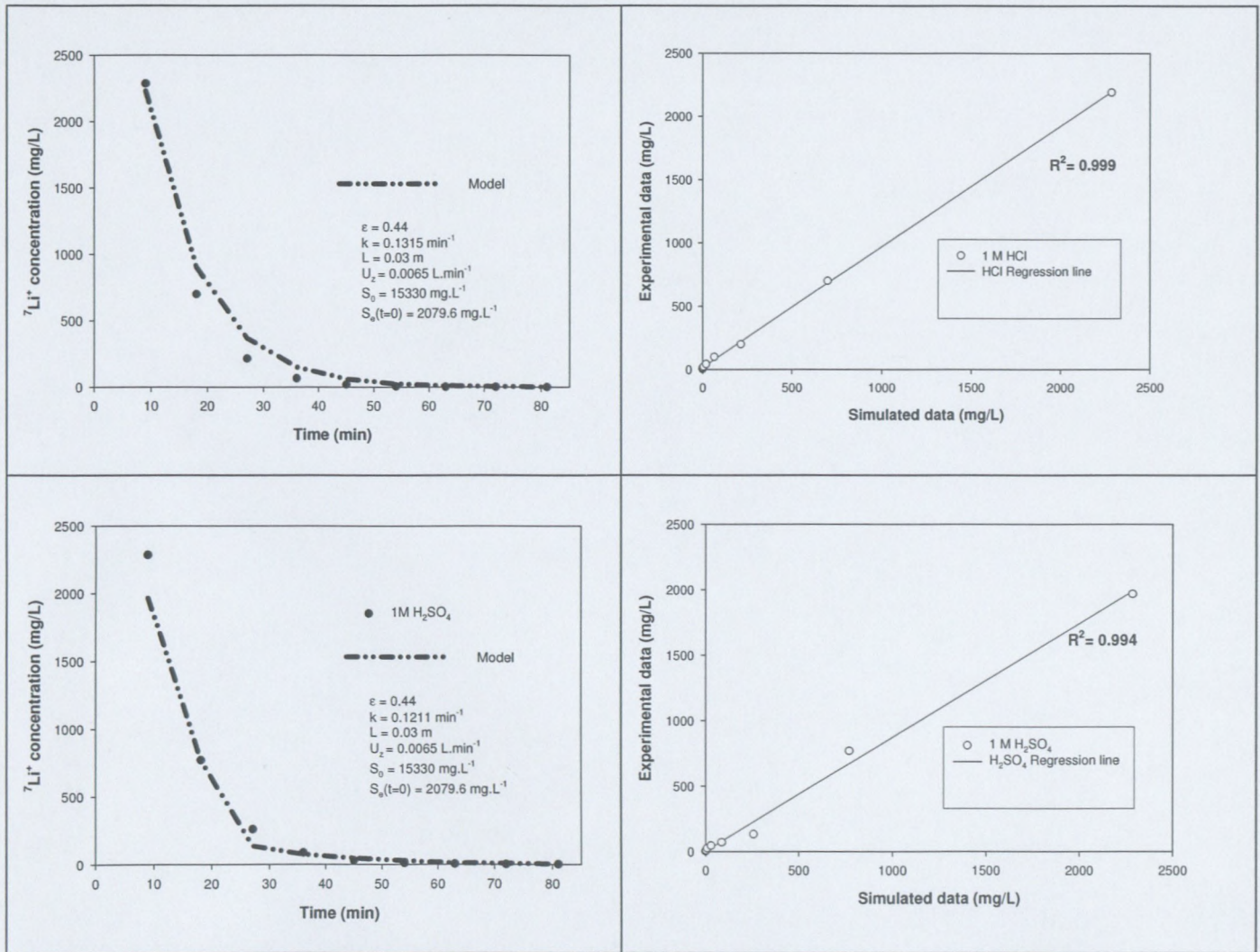


Figure 5.5: Simulated and experimental desorption curve for lithium isotope at 1M HCl and H_2SO_4 and the correlation between experimental and simulated data

A reduction in the overall anion leachates was observed when the recovered effluent from the desorption process was passed through the Amberlite IRN 78 resin. The Amberlite IRN 78 proved to be capable of reducing the anions in the $^7\text{Li}^+$ isotope effluent. The presence of chlorides and sulphates in the $^7\text{Li}^+$ isotope effluent was attributed to the use of the HCl and H_2SO_4 eluent solutions. Furthermore, another possible source of chlorides in the recovered effluent was attributed to the anion degradation as was indicated by the high presence of chlorides in the effluent which had been recovered when H_2SO_4 was used. The specification of sulphates and chlorides in the reactor coolant water is <50 ppb ($\mu\text{g/L}$). In view of the danger of corrosion posed by these anions it is essential that the $^7\text{Li}^+$ isotope solution which was recovered meets the reactor coolant water specification in respect of the level of chlorides and sulphates before being used in the PWR. However, it is hypothesised, that the use of sufficient quantities of Amberlite IRN 78 should be enough to pre-treat the effluent recovered to suitable levels. Figure 5.6 depicts the level of cation leachates which were found on the lithium isotope effluent.

The level of cation leachates was <200 mg/L for all the trace elements analysed. The $^7\text{Li}^+$ isotope recovered from a degraded resin may be adsorbed on new cation resin and be used in the RCV demineraliser with regard to the water treatment which is employed in the primary coolant of a nuclear PWR reactor. An alternative method would be to crystallise the recovered $^7\text{Li}^+$ in such a way that it would be possible to store and to use the $^7\text{Li}^+$ in powder form as an alkalising additive to the coolant of the primary circuit of a nuclear PWR reactor in order to correct the chemistry of the water.

Table 5.3: Averaged anion removal from the ${}^7\text{Li}^+$ effluent using Amberlite IRN 78 anion resin

Anion species ^a	1M HCl		1M H ₂ SO ₄		Reactor coolant specification ($\mu\text{g/L}$)		
	Concentration ^b (mg/L)	Purification ^c (mg/L)	Reduction ^d (%)	Concentration ^b (mg/L)		Purification ^c (mg/L)	Reduction ^d (%)
Cl ⁻	84165.15	105.73	99.87	36460.99	123.36	99.66	<50
SO ₄ ²⁻	48.45	nd	100	48277.26	464.33	99.038	<50
CO ₃ ²⁻	26.92	nd	100	nd	nd	-	nd
NO ₃ ⁻	26.92	nd	100	27.98	nd	100	nd
F ⁻	nd	nd	-	nd	nd	-	<50
PO ₄ ²⁻	0.24	nd	100	nd	nd	nd	nd

nd- not detected

^aAnion species in the recovered ${}^7\text{Li}^+$ eluent

^bAnion concentration in HCl/H₂SO₄ eluent

^cAnion concentration after passing through Amberlite IRN 78 anion resin

^dPercentage reduction of anion leachates by Amberlite IRN 78 resin

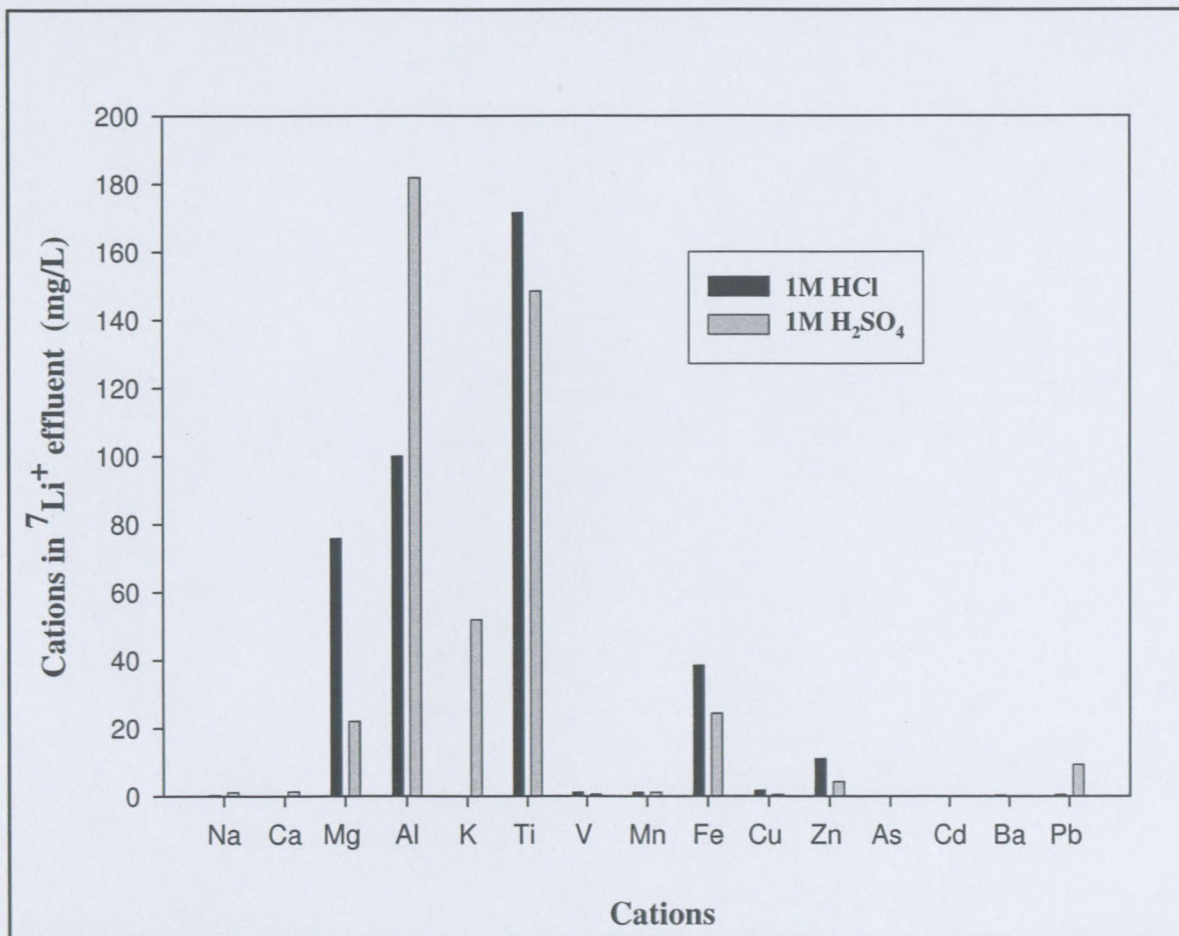


Figure 5.6: Concentration of cation leachates in the recovered effluent

5.4 Conclusion

A comparison between the degraded batch and a new batch of Amberlite IRN 217 lithiated mixed-bed proved that the anion resin in the old batch had lost its capacity. The results presented in this study showed that HCl and H₂SO₄ may be used to recover the ⁷Li⁺ isotope on a degraded ion-exchange resin. It was found that an elution efficiency > 60% was possible to achieve during the initial stages of the desorption process (2 BV) for both HCl and H₂SO₄ eluents. Overall, an elution efficiency of > 90% was achieved after passing 18BV of the eluents. Desorption rates of lithium isotope was ~0.1315 and 0.1211 min⁻¹ for HCl and H₂SO₄ respectively. A higher absolute error was observed at the initial stage (9 to 18 minutes) and this contributed to the higher sum of absolute error of desorption. The bed porosity was determined to be approximately ~0.44. The linear regression fit obtained for the experimental data indicated that the desorption model was appropriate for lithium desorption kinetics from degraded Amberlite IRN 217 lithiated mixed-bed resin using. The Amberlite IRN 78 anion

resin proved to be capable of removing anion leachates in the $^7\text{Li}^+$ isotope effluent. However, a future study will optimize the decontamination of leachates to meet the specification at Eskom Koeberg Power station.

5.5 Summary

In this chapter, diluted HCl and H_2SO_4 commercial grade mineral acids were used to elute the $^7\text{Li}^+$ isotope effectively from degraded Amberlite IRN 217 lithiated mixed-bed resin. The following objectives were realised:

- To elute the $^7\text{Li}^+$ using commonly available reagents such as commercial grade mineral acids.
- To develop a mathematical model for the desorption of the $^7\text{Li}^+$ isotope from degraded Amberlite IRN 217 lithiated resin. This mathematical model was used to predict the desorption rate of the isotope from the resin for the design of a pilot plant.

The next chapter discusses the bio-desorption of the $^7\text{Li}^+$ isotope using biologically produced H_2SO_4 by *A. caldus*. Chapter 6 aims to realise the following objectives:

- To select a suitable micro-organism that is capable of producing acids in an environmentally friendly process. The acid thus produced by the micro-organism identified will be evaluated for its ability to elute the $^7\text{Li}^+$ isotope effectively from the degraded lithiated mixed-bed resin.
- To compare the desorption rate of $^7\text{Li}^+$ using acid produced from a biological process and from freely available mineral acids. A comparison was also made in respect of the level of leachates in the eluent recovered which contained the $^7\text{Li}^+$ isotope using the biologically produced acid and the mineral acids.

The following question will also be discussed:

- Will the mathematical model which was developed be suitable to model the desorption rates of the ${}^7\text{Li}^+$ from the degraded Amberlite IRN 217 lithiated mixed-bed resin for the biologically produced acids?

CHAPTER 6

RESULTS

Bio-desorption of lithium isotope (${}^7\text{Li}^+$) from a degraded lithiated mixed-bed ion-exchange resin using *Acidithiobacillus caldus*

Prepared for the 5th International Symposium on Bio & Hydrometallurgy conference

8-9 November 2010, Cape Town, South Africa

CHAPTER 6: RESULTS

Bio-desorption of lithium isotope (${}^7\text{Li}^+$) from a degraded lithiated mixed-bed ion-exchange resin using *Acidithiobacillus caldus*

6.1 Introduction

The use of micro-organisms for bio-leaching in the bio-hydrometallurgy industry has attracted increasing attention because the process is more environmentally friendly, requires a lower capital cost and is highly efficient compared to conventional methods (Liu *et al.*, 2004). *Acidithiobacillus ferrooxidans* (*A. ferrooxidans*) and *Acidithiobacillus thiooxidans* (*A. thiooxidans*) are considered to be effective in the bacterial bio-dissolution of metal sulphides (bio-leaching). However, another sulphur oxidising bacterium, known as the *Acidithiobacillus caldus* (*A. caldus*), which has an optimum growth in temperatures from 40 to 50°C, has been reported to dominate the sulphur-oxidising bacterial population in both commercial bio-leaching and in bi-oxidation plants (Hallberg *et al.*, 1994; Semenza *et al.*, 2002). *A. caldus* is moderately thermophilic, unable to oxidise iron (II) and its characteristics closely resemble those of the mesophilic bacteria *A. thiooxidans* (Hallberg & Lindstrom, 1994; Hallberg *et al.*, 1996; Rawlings *et al.*, 1997). *A. caldus* is aerobic, gram negative and is a chemoautotrophic micro-organism that grows on elemental sulphur as an energy source to produce H_2SO_4 as the end product. The elemental sulphur is biologically transformed by *A. caldus* in the presence of air, water and essential micro-nutrients to maintain desired cell growth and sulphuric acid production (Cerruti *et al.*, 1998; Young *et al.*, 2004; Liu *et al.*, 2004).

This study focused on the H_2SO_4 production by *A. caldus* using elemental sulphur. This biologically produced H_2SO_4 was used to desorb lithium 7 (${}^7\text{Li}^+$), a high value isotope, from the degraded Amberlite lithiated ion-exchange resin which is used in the nuclear industry. According to Butler (1975), the cell and H_2SO_4 production obtained by a convectional shaking flask using *A. thiooxidans* on elemental sulphur proved to be 0.224g /L with 0.15M of H_2SO_4 being produced in 8 to 11 days. The bioreactor system was optimised by Liu (2003) who used response surface methodology in terms of which cell and H_2SO_4 concentrations of 0.7 g/L and 0.38M were achieved. However, there is limited information on H_2SO_4

production using elemental sulphur by *A. caldus*. The aim of this study was to report on the biological production of H₂SO₄ using elemental sulphur by *A. caldus* in optimised continuous aerated batch bioreactors. In addition, the acid produced was used in the desorption of the ⁷Li⁺ isotope from a degraded lithiated mixed-bed ion-exchange resin. A decontamination process was used to reduce the leachates identified in such a way that it was possible to recover the ⁷Li⁺ containing solution for re-use in the nuclear reactor.

6.2 Materials and methods

6.2.1 Experimental procedure

Experimental procedure for this part of the study was previously explained in Chapter 4, section 4.2.4.1 to 4.2.4.2.

6.2.2 Analytical methods

The analytical method used for this part of the study was previously explained in section 4.2.4.3.

6.3 Results and discussion

6.3.1 Sulphuric acid production

Figures 6.1 (A and B) depict the pH and cumulative production of H₂SO₄ that was obtained in the *A. caldus* aerated batch bioreactor. The H₂SO₄ productivity of culture *A. caldus* on elemental sulphur reached an average cumulative rate of 0.4M over a period of 16 days. As had been reported by Kempner (1996) in respect of H₂SO₄ production using *A. thiooxidans* the rapid drop in pH from an initial value of 2.5 to 0.47 over a period of 16 days proved that the medium had become progressively more acidic as the culture had aged. The H₂SO₄ productivity clearly depends on the type of bioreactor used, the conditions in the bioreactor, the sulphur surface area, the population of cells, the uniform contact between the liquid-solid-gas phase and the availability of dissolved oxygen (Cerruti *et al.*, 1998). The advantage of the continuous aeration in the batch reactor is that the shear forces that break down unstable particles, thus creating finer particles with a higher surface area enable further sulphur

oxidation as a result of the continuous supply of oxygen (Janssen *et al.*, 1994). The H₂SO₄ produced by these batch bioreactors was approximately 2.7 fold more than the H₂SO₄ produced in the experiments carried out by Liu (2003). This increase was in accordance with the findings of Liu (2003), whereby the simulated H₂SO₄ concentration of 0.38M was achieved on the optimal production of H₂SO₄ by *A. thiooxidans* using a response surface methodology. The increase in H₂SO₄ concentration was directly proportional to the sulphur concentration used.

The H₂SO₄ was concentrated using an evaporation technique, which resulted in the acid strength increasing to approximately 1M acid by evaporating 80% (v/v) water. The rate of acid concentration increment was 0.025M H₂SO₄ per percentage moisture loss. The concentrated H₂SO₄ was used to recover the ⁷Li⁺ isotope from the degraded mixed-bed resin. The biologically produced H₂SO₄ was compared to a dilute commercial grade mineral H₂SO₄ solution by desorbing the ⁷Li⁺ isotope from the degraded Amberlite IRN 217 lithiated mixed-bed resin (see section 6.3.2).

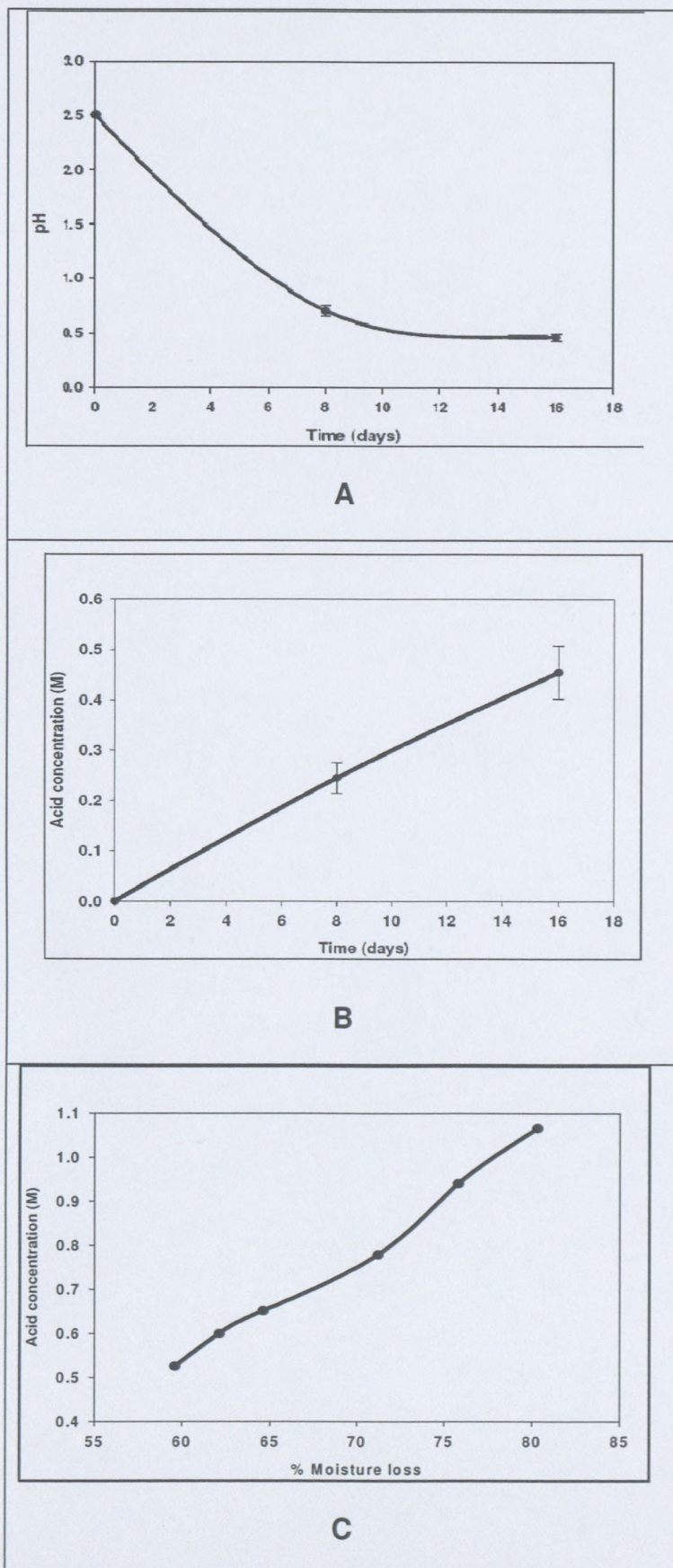


Figure 6.1: [A] pH evolution during oxidation of elemental sulphur, [B] cumulative production of H₂SO₄ in an aerated batch bioreactor with *A. caldus* immobilised on elemental sulphur, [C] graph showing the acid concentration increase with the percentage of moisture loss

6.3.2 Bio-desorption of the $^7\text{Li}^+$ isotope from degraded mixed-bed resin

Figure 6.2 represents the desorption of the $^7\text{Li}^+$ isotope from a degraded Amberlite IRN 217 lithiated mixed-bed resin in a continuous ion-exchange column, using 1M biologically produced H_2SO_4 as compared with 1M commercial grade H_2SO_4 . A desorption rate of >80% was observed using biologically produced H_2SO_4 at the initial stages (2BVs). This was higher than the 61% achieved by commercial grade mineral acid at the same stage. The results showed that the biologically produced H_2SO_4 showed high desorption kinetics in the initial stages of the desorption process as compared with the commercial grade H_2SO_4 . It was hypothesised that the presence of other cations such as sodium (Na^+), magnesium (Mg^{2+}), potassium (K^+) and calcium (Ca^{2+}) in the influent contributed to the observed phenomena. These cations also have an affinity to exchange with the $^7\text{Li}^+$ on the cation part of the mixed-bed resin as compared with the commercial grade acid used (see Figure 6.3). The overall desorption rate was 95% for both the biologically produced H_2SO_4 and the commercial grade mineral H_2SO_4 after passing 18BV. The biologically produced H_2SO_4 proved to be as efficient as the commercial grade mineral H_2SO_4 in desorbing the $^7\text{Li}^+$ isotope from the degraded Amberlite resin. It may, thus, be concluded that biologically produced H_2SO_4 may also be used in the desorption of other metal ions adsorbed on ion-exchange resin using an acid production process, which is more environmentally friendly compared to other conventional methods.

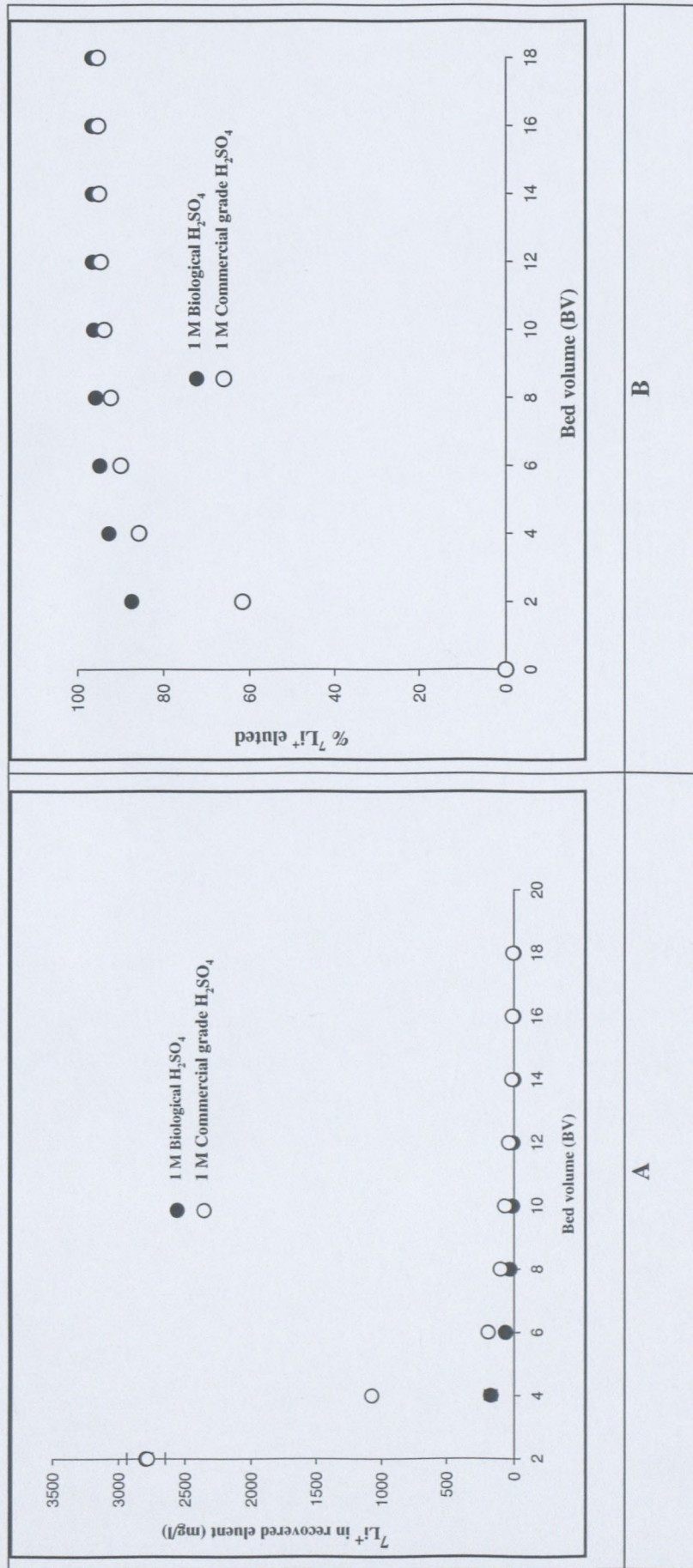


Figure 6.2: (A) Lithium 7 isotope desorption and (B) percent ⁷Li⁺ isotope desorption using biologically produced H₂SO₄ by *A. catidus* cells as compared with mineral sulphuric acid

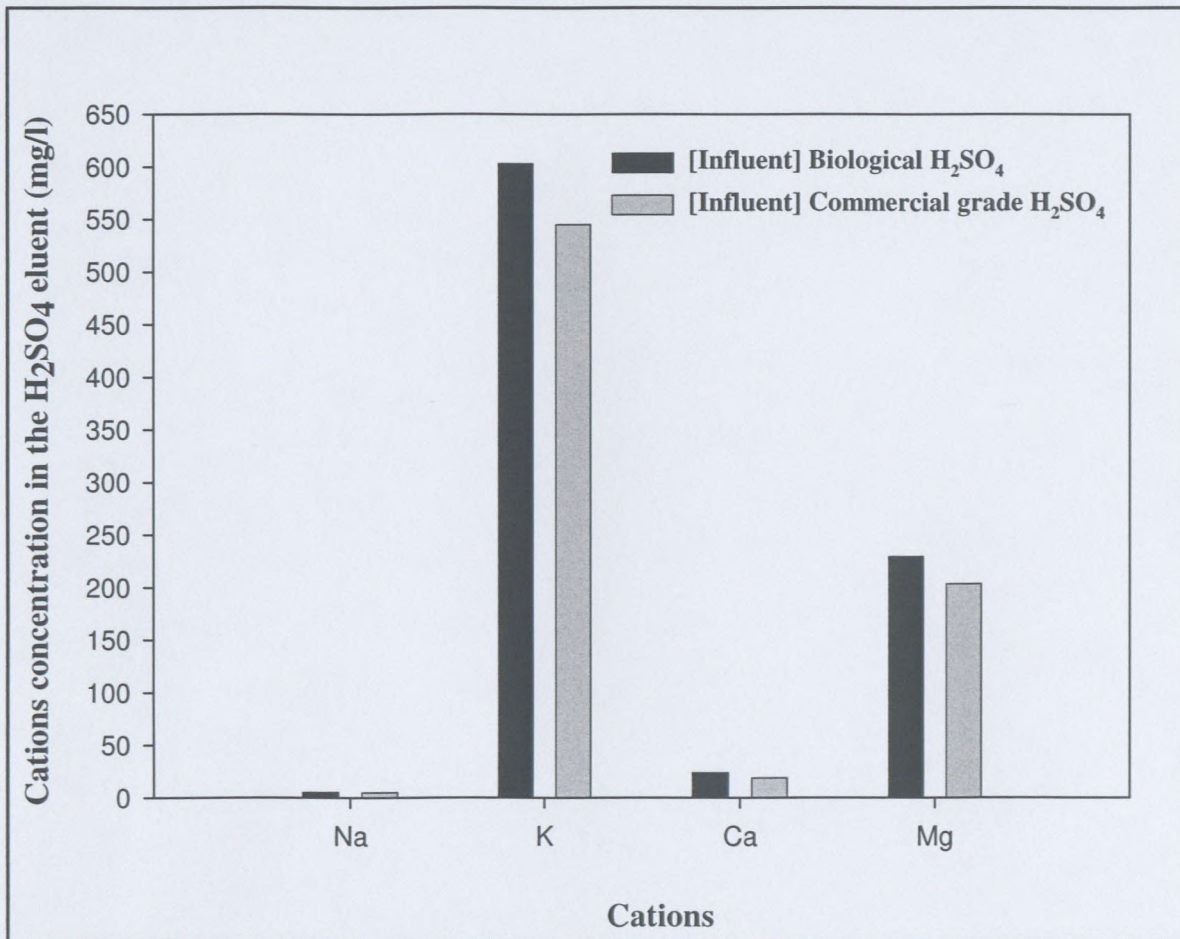


Figure 6.3: Cations in the biological and commercial grade H₂SO₄ influent

Figure 6.3 illustrates the mathematical model fit between experimental and simulated data of the desorbed ⁷Li⁺ isotope using biological H₂SO₄. The comparison between the simulated and the experimental data was sufficient with a correlation coefficient (R^2) of 0.982. The desorption rate (\bar{k}) was determined by minimising the absolute error between the experimental and calculated data and was found to be 0.1829 min⁻¹. The (\bar{k}) value for biological systems was higher as compared to the commercial grade H₂SO₄, showing that there were higher reaction kinetics using biological H₂SO₄ as compared to commercial grade H₂SO₄ which was also observed in Figure 6.2. The sum of the absolute error between the experimental and simulated data was 1297.16. The higher minimum absolute error was again observed to be between 9 to 18 minutes and this was attributed to the higher sum absolute error as observed in both commercial grade HCl and H₂SO₄. Furthermore it was also observed that at between 9 to 18 minutes, biological H₂SO₄ desorption rate was higher as

compared to commercial grade H_2SO_4 . This shows that the sampling procedure should have been adjusted in the initial stage where there is higher desorption rate.

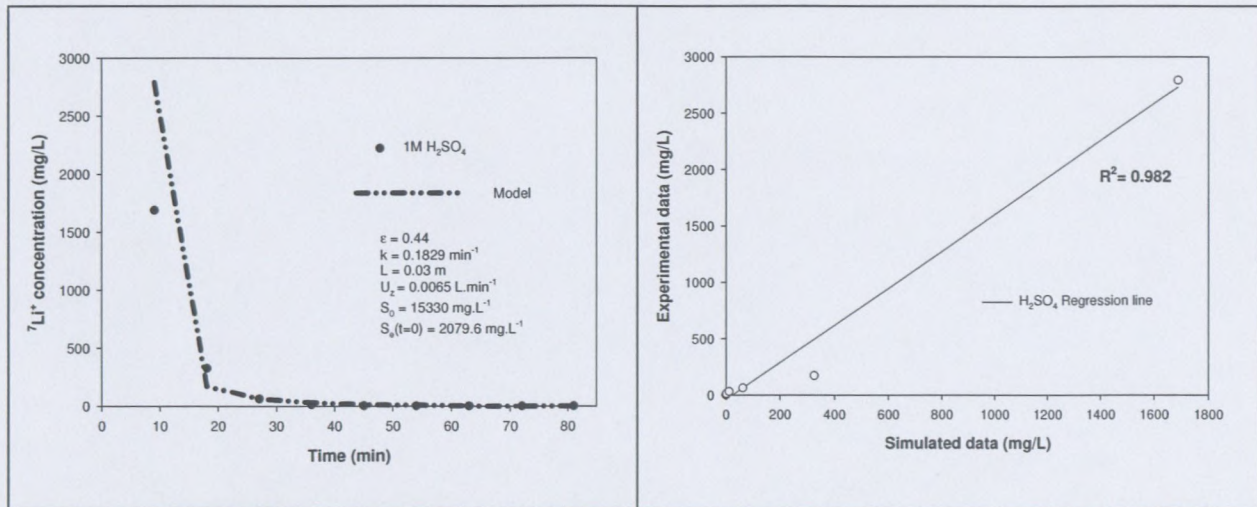


Figure 6.4: Simulated and experimental desorption curve for lithium isotope at 1M biological H_2SO_4 and the correlation between experimental and simulated data.

6.3.3 The amount of leachates in the recovered effluent

Figure 6.5 indicates the level of cations and anions leachates in the $^7\text{Li}^+$ isotope effluent after passing biologically produced H_2SO_4 as compared to passing the commercial grade mineral H_2SO_4 . The level of cations did not exceed 300 mg/L in the effluent, although there were metals such as zinc (Zn^{2+}), calcium (Ca^{2+}) and magnesium (Mg^{2+}) used in the nutrient medium used to produce H_2SO_4 biologically. The presence of these metallic ions was attributed to the trace elements used for cellular growth of *A. caldus*. A large quantity (approximately 50000 mg/L) of anion leachates was found in the effluent. This was, in turn, attributed to the leachates from the eluent solution of both the biological and commercial grade H_2SO_4 used. Furthermore, as the Amberlite IRN 217 mixed-bed resin had been degraded the release of anion leachates further contributed to the higher quantity of anions in the $^7\text{Li}^+$ isotope effluent.

The Amberlite IRN 78 proved to be capable (> 90%) of reducing the anion leachates from the $^7\text{Li}^+$ isotope effluent using both biologically produced H_2SO_4 and commercial grade H_2SO_4 (see Table 6.1).

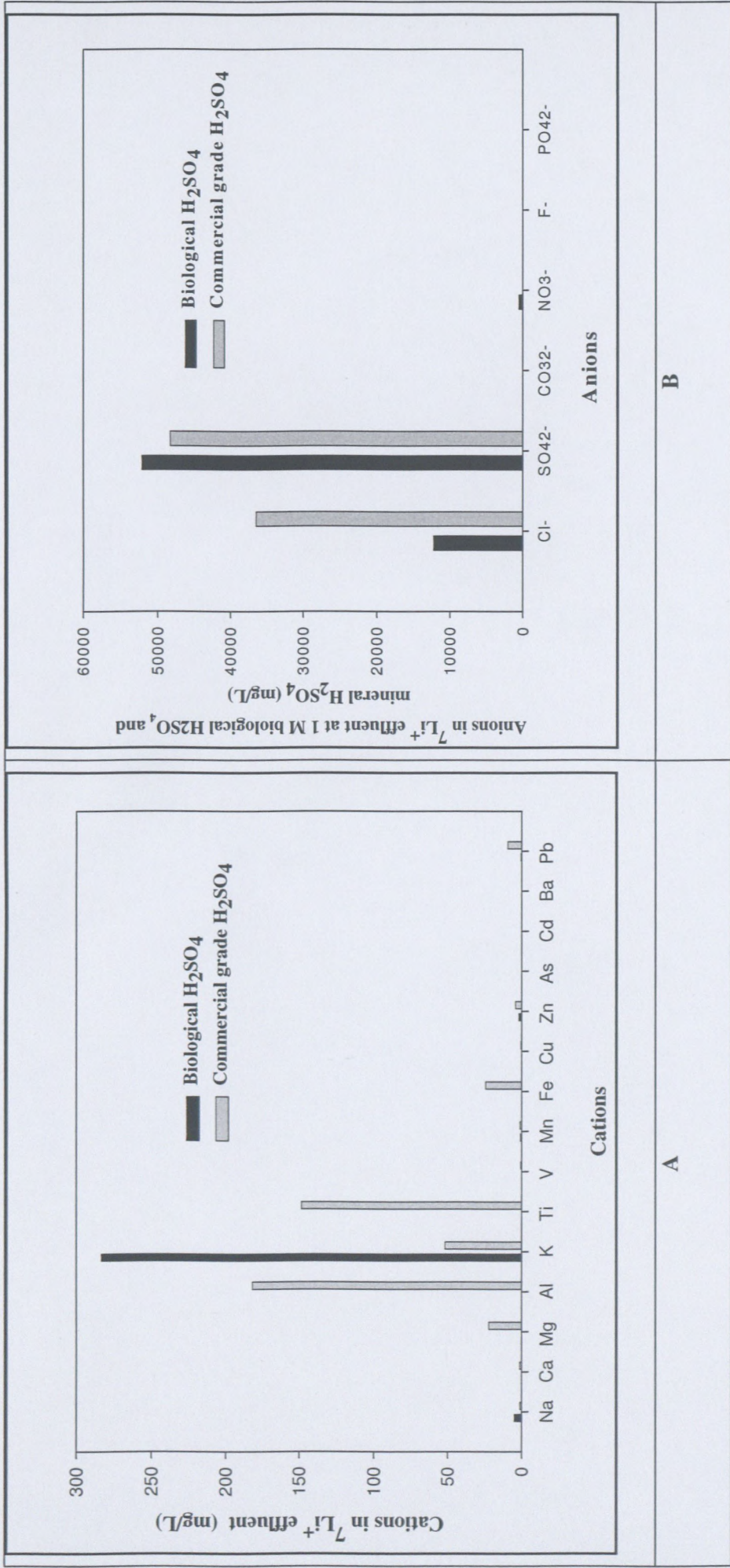


Figure 6.5: [A] Cations and [B] anions leachates in the ⁷Li⁺ isotope effluent from the desorption process

Table 6.1: Averaged anion removal from the ${}^7\text{Li}^+$ effluent using Amberlite IRN 78 anion resin

Anion species ^a	1M biological H_2SO_4		1M commercial grade H_2SO_4			Reactor coolant specification ($\mu\text{g/L}$)	
	Concentration ^b (mg/L)	Purification ^c (mg/L)	Reduction ^d (%)	Concentration ^b (mg/L)	Purification ^c (mg/L)		Reduction ^d (%)
Cl^-	13393.11	88.11	99.	36460.99	123.36	99.66	<50
SO_4^{2-}	51478.18	998.65	98	48277.26	464.33	99.038	<50
CO_3^{2-}	nd	nd	-	nd	nd	-	nd
NO_3^-	0.01	nd	100	27.98	nd	100	nd
F	18.50	0.1	99	nd	nd	-	<50
PO_4^{2-}	557.96	19.55	96	nd	nd	nd	nd

nd – not detected

^aAnion species in the recovered ${}^7\text{Li}^+$ eluent

^bAnion concentration in $\text{HCl}/\text{H}_2\text{SO}_4$ eluent

^cAnion concentration after passing through Amberlite IRN 78 Anion resin

^dPercentage reduction of anion leachates by Amberlite IRN 78 resin



6.4 Conclusion

This study revealed the possibility of producing an acid concentration of 0.4M using *A. caldus* immobilised on elemental sulphur. The application of the biologically produced H_2SO_4 to desorb the $^7\text{Li}^+$ isotope from the degraded Amberlite mixed-bed proved to be efficient. An elution efficiency of $> 80\%$ was achieved at the initial stage of 2BV. This was higher than the 60% efficiency rate of mineral H_2SO_4 at the same stage. The overall elution efficiency of $> 90\%$ was achieved after passing 18BV's – a result similar to that achieved by commercial grade mineral sulphuric acid. The biologically produced H_2SO_4 revealed the same ability to extract the $^7\text{Li}^+$ isotope as compared to the widespread conventional method using commercial grade H_2SO_4 . The decontamination process showed a potential to reduce the leachates level, however the process needs to be optimised to be able to reduce the level of anion and cation leachates required for nuclear reactor specification. The optimisation of the process will be carried on during the course of the next study of the project.

6.5 Summary

In this chapter biological H_2SO_4 was used to desorb the $^7\text{Li}^+$ isotope from degraded Amberlite lithiated mixed-bed resin. The desorption kinetics of the biological sulphuric acid and commercial grade sulphuric acid were compared. The following objectives were met:

- To identify a suitable micro-organism that is capable of producing acidic titres in an environmentally friendly process. The acid produced by the micro-organism selected was evaluated for its ability to elute the $^7\text{Li}^+$ isotope from the degraded lithiated mixed-bed resin in an effective way.
- To compare the desorption kinetics of $^7\text{Li}^+$ from degraded resin using biologically produced acid and commercial grade mineral acids. A comparison was also made between the level of leachates in the recovered eluent containing the $^7\text{Li}^+$ isotope in respect of the biologically produced acid and the commercial grade acids.

CHAPTER 7

OVERALL DISCUSSION AND CONCLUSIONS

7.1 Overall discussion

7.1.1 Capability of eluents in respect of desorpting the $^7\text{Li}^+$ isotope from degraded lithiated mixed-bed resin

During the desorption process in a continuous ion-exchange column both commercial grade (HCl and H_2SO_4) and the biologically produced H_2SO_4 , which had been identified showed a marked capacity to desorpt the $^7\text{Li}^+$ isotope from degraded Amberlite IRN 217 lithiated mixed-bed resin. This was observed in the overall recovery of $> 90\%$ of the $^7\text{Li}^+$ isotope in respect of both the commercial grade and the biologically produced acids.

Higher levels of the anions and cations leachates were observed in the $^7\text{Li}^+$ isotope effluent of both HCl and H_2SO_4 and this was attributed to the degradation of the resin. Both the commercial grade and the biologically produced acid also contributed to the leachates in the $^7\text{Li}^+$ isotope effluent as the resin had lost its capacity to reduce some of the leachates. An overall reduction percentage of 99% of anion leachates was observed after passing the $^7\text{Li}^+$ isotope effluent in a decontamination process filled with Amberlite IRN 78 anions resin. The amount of resin in these studies was not sufficient for the effluent to meet the South African nuclear power station specification of $<50 \mu\text{g/L}$ of anion in PWR. The use of sufficient Amberlite IRN 78 anion resin should enable the pretreating of the $^7\text{Li}^+$ isotope effluent in order to meet the nuclear power station specification and this will be tested in the subsequent studies.

7.1.2 Suitability of the mathematical model

The desorption of the $^7\text{Li}^+$ isotope from the degraded Amberlite IRN 217 lithiated resin showed first order reaction kinetics (see Appendix G) with the both commercial grade and the biologically produced acid. The correlation coefficient (R^2) between the experimental data and the simulated data for the commercial grade (HCl and H_2SO_4) and the biologically produced H_2SO_4 was 0.999, 0.994, and 0.982, respectively. The desorption rate constant for

each eluent solution was determined by minimising the sum of absolute error between the experimental and simulated data. The sum of minimum absolute error for commercial grade (HCl and H₂SO₄) and biological H₂SO₄ was 6.47E2, 4.34E2 and 1.29E3 respectively. Furthermore, the desorption rate constant that minimised the absolute error was 0.1315, 0.1211 and 0.1829 min⁻¹ respectively. The model developed represents a first order partial differential equation that was used to simulate the desorption kinetics of first order reactions.

7.1.3 Overview of the results achieved

The anion part of the degraded Amberlite IRN 217 lithiated mixed-bed resin was confirmed to be degraded when compared to a new batch of Amberlite IRN 217 lithiated mixed-bed resin which had acted as a control. The amount of anions leachates released on the effluent after passing through the Milli-Q water (rinsing) and the desorption eluent (HCl and H₂SO₄) were higher as compared to the control new batch of Amberlite resin. The degradation of the anion resin had resulted in the loss of capacity of the anion part of the resin and, hence, the release of leachates has the potential to cause corrosion if used in the PWR.

The commercial grade HCl and H₂SO₄ showed a higher desorption rate of the ⁷Li⁺ isotope from the degraded resin with an overall desorption percentage greater than 90% after passing 18BV of the desorption eluent. The results showed that 60% of the ⁷Li⁺ isotope was eluted at the initial stage of 2BV for both commercial grade mineral acids. These findings correlate with the findings of a study by Motoba and Narita (1998) in terms of which most antimony was desorbed at an initial stage.

The study also investigated biologically produced H₂SO₄ using the oxidation of elemental sulphur by *A. caldus* in an aerated batch bioreactor. A sulphuric acid production of 0.4M was achieved after 16 days. The 0.4M was concentrated to 1M by evaporating 80% (v/v) water. The 1M biological sulphuric acid showed a desorption rate of >90% which was similar to the desorption rate achieved by the commercial grade mineral acid. However, the biological sulphuric acid manifested a faster desorption rate (80%) at the initial stage of 2BV as compared to that of the commercial grade mineral acid (60%). This was as a result of the high level of other cations such as sodium, potassium, calcium and magnesium which all have higher affinity to exchange with the ⁷Li⁺ isotope in degraded Amberlite IRN 217 lithiated

resin The biological application in the desorption process is a new approach and it proved to be both economic and efficient in recovering the valuable ${}^7\text{Li}^+$ isotope. This approach may also be considered in bio-hydrometallurgy in respect of recovering valuable metals from ion-exchange resin.

7.2 Overall conclusions

Most of the published literature reviewed on desorption processes in hydrometallurgy use commercially grade mineral acids, HCl or H_2SO_4 , to recover minerals from ion-exchange resin. This also includes the regeneration of a different polystyrene-based resin. This study focused on recovery of ${}^7\text{Li}^+$ isotope from a degraded Amberlite resin, which is used in the nuclear power generation industry. The study used commercial grade mineral acids (HCl and H_2SO_4) and also explored the use of a biologically produced H_2SO_4 to recover the valuable isotope from a degraded unusable resin. The implications of the research findings are that biologically produced H_2SO_4 can be used in mineral recovery from industrial resin and to regenerate such resin as it was proven that the use of biologically produced H_2SO_4 performed similarly to that of commercial grade mineral acids, HCl and H_2SO_4 . The desorption process was also modelled using a mathematical model developed to simulate the desorption kinetics of the ${}^7\text{Li}^+$ isotope. The developed model can be modified to take into consideration the desorption kinetics of the process being modelled. These conclusions are supported by the following findings:

- The commercial grade mineral acids (HCl and H_2SO_4) and the biologically produced H_2SO_4 acid were found to be suitable eluents to recover the ${}^7\text{Li}^+$ isotope from the degraded Amberlite resin, with similar results being achieved during the experiments conducted. The mathematical model used was able to simulate the desorption rate of the ${}^7\text{Li}^+$ isotope from degrade Amberlite resin for both commercial grade mineral and biological acids.
- Additionally, the level of anion leachates found in the ${}^7\text{Li}^+$ isotope effluent, was reduced using suitable anion resin, for which a 99% reduction of the anion leachates in the ${}^7\text{Li}^+$ isotope effluent can be achieved.

Overall, the objectives of the research as highlighted in Chapter 1 were successfully achieved.

7.3 Recommendations: future research CHAPTER 8

The next phase of the study will explore the best method to re-use the ${}^7\text{Li}^+$ isotope recovered from the degraded Amberlite IRN 217 lithiated mixed-bed resin. Furthermore, the reduction of cationic and anionic ions to meet the specifications of the PWR must be explored. Several methods may be explored in respect of the adsorption of the ${}^7\text{Li}^+$ recovered to a new cation resin or else crystallised to be stored in powder form. The investigation of the impact of the ${}^7\text{Li}^+$ recovered in the PWR should be pursued in a future study while the evaluation of the use of sulphurous waste should also be a priority. The following should also be considered:

- To assess acid concentration lower than 1M to determine the optimum acid concentration.
- To adjust the sampling time during the initial desorption stage in order to re-evaluate the desorption rate constant and desorption kinetics.
- To optimise the decontamination process in order to reduce the leachates to meet nuclear power station reactor coolant water specifications.

CHAPTER 8

REFERENCES

- Averil, W.A. and Olson, D.L. 1978. A review of extractive processes for lithium from ores and brines. *Energy*, 3: 305–313.
- Bállester, A., González, F., Blázquez, M.L. and Mier, J.L. 1990. The influence of various ions in the bioleaching of metal sulphides. *Hydrometallurgy*, 23: 221–235.
- Barois, G., Alibaud, J.G. and Dumez, C. 2009. Nuclear reactor primary circuit. *United States Patent, US 2009/0141848 A1*. Areva NP, France.
- Barrett, J., Hughes, M.N., Karavaiko, G.I. and Spencer, P.A. 1993. *Metal extraction by bacteria oxidation of minerals*. New York: Ellis Horwood.
- Bhattacharya, P., Sarkar, P. and Mukherjea, R.N. 1990. Reaction kinetics model for chalcopyrite bioleaching using *Thiobacillus ferrooxidans*. *Enzyme Microbiology Technology*, 12: 873–875.
- Blancarte-Zurita, M.A., Branion, R.M.R. and Lawrence, R.W. 1986. Particle size effects in the microbiological leaching of sulfide concentrates by *Thiobacillus ferrooxidans*. *Biotechnology and Bioengineering*, 28: 751–755.
- Boon, M., Meeder, T.A., Thöne, C. and Ras, C. 1999. The ferrous iron oxidation kinetics of *Thiobacillus ferrooxidans* in continuous cultures. *Applied Microbiology and Biotechnology*, 51: 820–826.
- Bruening, R.L. 1994. Elution of antimony from solid phase using concentrated sulphuric acid containing hydrochloric acid. *United States Patent, 5,316,679*. IBC Advanced Technologies, Salt lake City, Utah.
- Butler, R.G. 1975. Pyruvate inhibition of carbon dioxide fixation of the strict chemolithotroph *Thiobacillus thiooxidans*. *Journal of Microbiological Methods*, 21: 2089-93.

- Caratin, R.L., Araujo, S.G., Landini, L. and Lugao, A.B. 2008. Preparation of polymeric matrices by using microwave energy for immobilisation of radioactive waste. *Proceedings of the Polymer Processing Society 24th Annual Meeting*, Salerno (Italy).
- Cardone, P., Ercole, C., Breccia, S. and Lepidi, A. 1999. Fractal analysis to discriminate between biotic and abiotic attacks on chalcopyrite and pyrolusite. *Journal of Microbiological Methods*, 36: 11–19.
- Cerruti, C., Curutchet, G. and Donati, E. 1998. Bio-dissolution of nickel-cadmium batteries using *Thiobacillus ferrooxidans*. *Journal of Biotechnology*, 62: 209–219.
- Cheremisinoff, P.N. 1995. *Handbook of water and waste water treatment Technology*. New York: Marcel Dekker.
- Clark, D.A. and Norris, P.R. 1996. Oxidation of mineral sulphides by thermophilic microorganisms. *Minerals Engineering*, 9: 1119–1125.
- Corpora, G.J., Miller, E., Thomas, G. and David, R. 1996. Method of decontaminating a PWR primary loop. *United States Patent*, 5,517,539. Westinghouse Electric Corporation, Peffer, Greensburg.
- Cupertino, D.C. and Tasker, P.A. 1994. Chemical process for the recovery of metal from an organic complex. *United States Patent*, 5, 364, 452, United Kingdom.
- Curutchet, G. and Donati, E. 2000. Iron-oxidizing and leaching activities of sulphur grown *Thiobacillus ferrooxidans* cells on other substrates: effect of culture pH. *Journal of Bioscience and Bioengineering*, 90: 57–60.
- Dang, V.D. and Steinberg, M. 1978. Preliminary design and analysis of recovery of lithium from brine with the use of selective extractant. *Energy*, 3: 325–336.
- Dorner, H. and Kleiter, W. 1977. Pressurised water-cooled reactor system. *United States Patent*, 4,038,134. Siemens Aktiengesellschaft, Germany.
- Ebbing, D.D. 1993. *General chemistry*. 4th Ed. Houghton Mifflin, Massachusetts.

Fernando, K., Laing, S. and Kim, M.J. 2002. The use of ion-exchange resins for the treatment of cyanidation tailings part 1: Process development of selective base metal elution. *Minerals Engineering*, 15: 1163–1171.

Fortes, M.C.B., Martins, A.H. and Benedetto, J.S. 2007. Selective separation of indium by iminodiacetic acid chelating resin. *Brazilian Journal of Chemical Engineering*, 24: 287–292.

Fowler, T.A., Holmes, P.R. and Crundwell, F.K. 2001. On the kinetics and mechanism of the dissolution of pyrite in the presence of *Thiobacillus ferrooxidans*. *Hydrometallurgy*, 59: 257–270.

Giaveno, A. and Donati, E. 2001. Bioleaching of heazlewoodite by *Thiobacillus sp.* *Process Biochemistry*, 36: 955–962.

Gómez, C., Blázquez, M.L. and Ballester, A. 1999. Bioleaching of a Spanish complex sulphide ore bulk concentrate. *Minerals Engineering*, 12: 93–106.

Hallberg, K.B. and Lindstrom, E.B. 1994. Characterization of *Thiobacillus Caldus* sp.nov., a moderately thermophilic acidophile. *Microbiology*, 140: 3451–3456.

Hallberg, K.H., Dopson, M. and Lindstrom, E.B. 1996. Reduced sulphur compounds oxidation by *Thiobacillus caldus*. *Journal of Bacteriology*, 178: 6–11.

Han, C.J. and Kelly, R.M. 1998. Biooxidation capacity of the extremely thermoacidophilic archaeon *Metallosphaera sedula* under bioenergetic challenge. *Biotechnology and Bioengineering*, 58: 617–624.

Harland, C.E. 1994. *Ion-exchange: Theory and practice*. The Royal Society of Chemistry: United Kingdom.

Hartly, J.N., Gore, B.F. and Young, J.R. 1978. Potential lithium requirements for fusion power plants. *Energy*, 3: 337–346.

Helfferich, F. 1995. *Ion-exchange*. New York: McGraw-Hill.

Janssen, A., Grotenhuis, J.T.C., Lettinga, G. and Rulkens, W.H. 1994. Possibilities for using biologically-produced sulphur for cultivation of *Thiobacilli* with respect to bioleaching processes. *Bioresource Technology*, 48: 221–227.

Jonglertjunya, W. 2003. Bioleaching of chalcopyrite. *Department of Chemical Engineering School of Engineering*. United Kingdom: The University of Birmingham, 258.

Kataoka, Y. and Matsuda, M. 1988. Method for eluting a metal adsorbed on chelating Agent. *United States Patent, 4,786,481* Sumitomo Chemical Company, Limited, Osaka, Japan, 646.

Kempner, E.S. 1996. Acid production by *Thiobacillus Thiooxidans*. *Journal of Bacteriology*, 92: 1842–1843.

Hallberg, K.B. and Lindstrom, E.B. 1994. Characterization of *Thiobacillus caldus* sp.nov., a moderately thermophilic acidophile. *Microbiology*, 140: 3451–3456.

Kitamura, T. and Wada, H. 1978. Properties of adsorbents composed of hydrous aluminum oxide, and its selective adsorption of lithium from sea water. *Nippon Kaisui Gakkaishi*, 32: 78–81.

Konishi, Y., Kogasaki, K. and Asai, S. 1997. Bioleaching of pyrite by *Acidianus brierleyi* in a continuous-flow stirred-tank reactor. *Chemical Engineering Science*, 52: 4525–4532.

Konishi, Y., Asai, S. and Tokushige, M. 1999. Kinetics of the bioleaching of chalcopyrite concentrate by acidophilic thermophile *Acidianus brierleyi*. *Biotechnology Progress*, 15: 681–688.

Koyanaka, Y. and Yasuda, Y. 1977. Concentration of lithium in sea water by ion-exchange resin. *Suiyo Kaishi*, 18: 523–526.

Liu, H.L., Lan, Y.W. and Cheng, Y.C. 2003. The effect of metabolites from the indigenous *Thiobacillus thiooxidans* and temperature on the bioleaching of cadmium from soil. *Biotechnology and Bioengineering*, 83:638-45.

Liu, H.L., Lan, Y.W. and Cheng, Y.C. 2004. Optimal production of sulphuric acid by *Thiobacillus thiooxidans* using response surface methodology. *Process Biochemistry*, 39: 1953-1961.

Lukey, G.C. and Van Deventer, J.S.J. 2000. Selective elution of copper and iron cyanide complexes from ion-exchange resins using saline solutions. *Hydrometallurgy*, 56: 217-236.

Mamo, M., Ginting, D., Renken, R. and Eghball, B. 2004. Stability of ion-exchange resin under freeze-thaw or dry-wet environment. *Soil Science Society of America*, 68: 677-681.

Meintker, M., Boltz, M., Enkler, W. and Ruhle, E. 2003. Method and device for reducing cationic impurities and for dosing lithium in cooling water of a light water reactor, and a cooling-water system of a light water reactor having such a device. *United States Patent, US 6, 656,338 B2*.

Miers, P. 1992. Effects and properties for storage, lay-up and recommissioning of ion-exchange resin. Rohm and Haas Company (abstract).

Mitsch, W.J., Day, J.W., Zhang, L. and Lane, R.R. 2005. Nitrate-nitrogen retention in wetlands in the Mississippi River Basin. *Ecological Engineering*, 24: 267-278.

Motoba, K. and Narita, K. 1999. Method for eluting antimony adsorbed on a chelating agent. *United States Patent, 5,989,430*. Tokyo, Japan: Nippon Mining and Metals.

Nakazawa, H., Fujisawa, H. and Sato, H. 1998. Effect of activated carbon on the bioleaching of chalcopyrite concentrate. *International Journal of Mineral Processing*, 55: 87-94.

Neale, J. 2006. Bioleaching technology in minerals processing. Mintek, Biotechnology Division, 1-3.

Nemati, M., Harrison, S.T.L., Hansford, G.S. and Webb, C. 1998. Biological oxidation of ferrous sulphate by *Thiobacillus ferrooxidans*: A review on the kinetic aspects. *Biochemical Engineering Journal*, 1: 171–190.

Nordmann, F. 2002. Aspect on chemistry in French nuclear power plants. *International Conference on the Properties of Water and Steam*, 22-26 April, Kyoto, Japan.

Ohashi, K., Furutani, Y., Kashimura, E., Minato, A. and Ohsumi, K. 1989. Method of reducing radioactivity in nuclear plant. *United States Patent*, 4,820,473. Hitachi Ltd, Japan.

Otte, J.A.N. and Liebman, D. 1987. Method of removing Cesium from an aqueous liquid and purifying the reactor coolant in boiling water and pressurised water reactors. *United States Patent*, 4,657,731. The Dow chemical Company, Republic of Germany.

Owens, D.L. 1999. *Practical principles of ion-exchange water treatment*. Tall Oaks Publishing: Littleton CO, United States of America.

Rawlings, D.E., N.J., C. and Gardner, M. N. 1997. *Bio mining: Microbes and industrial processes*. Berlin: Springer-Verlag.

Reynolds, T.D. and Richards, P.A. 1996. *Unit operations and processes in environmental engineering*. Boston, Mass.: PWS.

Rideaux, J. 1999. The role of ion-exchange resins in long-term spent fuel storage. *Westinghouse Savannah River site*. South Carolina, United States of America.

Rohm and Haas. 2003. Amberlite IRN 217 lithiated industrial nuclear grade mixed-bed resin Product Data Sheet.

Rowlands, I.T. 1991. Nuclear Plant. *United States Patent*, 5,006,303, England.

Schlonski, S.J., McGlure, M.F. and Copora, G.J. 1992. System for chemical decontamination of nuclear reactor primary systems. *United States Patent*. Westinghouse Electric Corp., Pittsburg, Pa, United States of America.

Semenza, M., Viera, M., Curutchet, G. and Donati, E. 2002. The role of *Acidithiobacillus caldus* in the bioleaching of metal sulphides. *Latin American Applied Science Research*, 32: 303–306.

Shiao, S.J. and Tsai, C.M. 1990. Stability of anion resin. *Nuclear Science Journal*, 6: 523–536.

Silva, D.L. and Brunner, G. 2006. Desorption of heavy metals from ion-exchange resin with water and carbon dioxide. *Brazilian Journal of Chemical Engineering*, 23: 213–218.

Song, C.Q., Greer, A.H. and Halpern, M.E. 1996. Process for preparing ion-exchange resins by chloromethylation of cross-linked styrene copolymer in the presence of saturate hydrocarbon swelling agents. *United States Patent*, 5523327. Sybron Chemical Holdings Inc, Welmington, DE.

Song, M.C. and Lee, K.J. 2003. The evaluation of radioactive corrosion product at PWR as change of primary coolant chemistry for long-term fuel cycle. *Annals of Nuclear Energy*, 30: 1231–1246.

Suzuki, I. 2001. Microbial leaching of metals from sulphide minerals. *Biotechnology Advances*, 19: 119–132.

Tan, C.S. and Liou, D.C. 1988. Desorption of ethyl acetate from activated carbon by supercritical carbon dioxide. *Industrial Engineering Chemistry*, 27: 988–991.

Tang, T.F. and Gordon, G. 1980. Quantitative determination of chlorides, chlorite, and chlorate ions in a mixture by successive potentiometric titration. *Analytical Chemistry*, 52: 1430–1433.

Tichýa, R., Janssen, A., Grotenhuisb, J.T.C., Lettingab, G. and Rulkens B.W.H. 1994. Possibilities for using biologically-produced sulphur for cultivation of *Thiobacilli* with respect to bioleaching processes. *Bioresource Technology*, 48: 221–227.

Tokalioglu, S., Sahin, U. and Kartal, S. 2001. Determination of fluoride and some metal ion levels in the drinking water in Kayseri Province. *Turkish Journal of Chemistry*, 25: 113–121.



Treybal, R.E. 1995. *Mass-transfer operations* (3rd edition). Singapore: McGraw-Hill.

Tsuruta, T. 2005. Removal and recovery of lithium using various microorganism. *Journal of Bioscience and Bioengineering*, 100: 562–566.

Valdes, J., Quatrini, R., Hallberg, K., Dopson, M., Valenzuela, P.D.T. and Holmes, D.S. 2009. Draft genome sequence of the extremely acidophilic bacterium *Acidithiobacillus Calvus* ATCC 51756 reveals metabolic versatility in the genus *Acidithiobacillus*. *Journal of Bacteriology*, 191: 5877–5878.

Veglió, F., Beolchini, F., Nardini, A., and Toro, L. 2000. Bioleaching of a pyrothite ore by a sulfooxidans strain: kinetic analysis. *Chemical Engineering Science*, 55: 783–795.

Young, T.L., Green, M.G., Rice, D.R., Karlage, K.L., Premeau, S.P. and Cassells, J.M. 2004. Materials and method for the biological production of sulphuric acid. *United States Patent, US 6,790,418 B2*. Phillips Petroleum Company.

**APPENDIX A: DATA SHEET FOR AMBERLITE IRN 217 LITHIATED
MIXED-BED RESIN AND AMBERLITE IRN 78 ANION RESIN**



For the Nuclear Industry

APPLICATIONS

AMBERLITE IRN77	AMBERJET type resin. Removal of cationic species and cationic radioisotopes. Control of Li ⁷ content of the reactor coolant.
AMBERLITE IRN97H	AMBERJET type resin with high capacity. Purification of steam generator blowdown conditioned with ammonia. Removal of cationic species and cationic radioisotopes. Control of Li ⁷ content of the reactor coolant.
AMBERLITE IRN9652	Macroreticular resin. Removal of cationic species and cationic radioisotopes. High selectivity for caesium 137. High affinity for Na in steam generator blowdown conditioned with morpholine or ethanolamine.
AMBERLITE IRN78	AMBERJET type resin. Very high capacity. Removal of boron and anionic radioisotopes.
AMBERLITE IRN9766	Macroreticular resin. Removal of anionic radioisotopes and colloids 110Ag.
AMBERLITE IRN150	AMBERJET type mixed bed. Demineralisation and decontamination of radioactive material.
AMBERLITE IRN160	AMBERJET type mixed bed composed of high capacity cation and anion exchange resins. Demineralisation and decontamination of radioactive streams.
AMBERLITE IRN9687	Macroreticular mixed bed. Cationic component loaded with lithium 7 at 99.9 % of isotopic purity. Primary water chemistry control in PWR conditioned with LiOH. High selectivity for Caesium 137.
AMBERLITE IRN217	AMBERJET type mixed bed. Cationic component loaded with lithium 7 at 99.9 % of isotopic purity. Primary water chemistry control in PWR conditioned with LiOH.
AMBERLITE IRN9882	Macroreticular mixed bed. Demineralisation and decontamination of radioactive streams. High selectivity for caesium 137. Can be operated at high flow rate.

PROPERTIES

Product Name	Function	Porosity	Matrix	Ionic Form	Regen. % (mini)	Total capacity (eq/L, mini.)	Shipping weight g/L	Temp. °C, maxi
AMBERLITE IRN77	Strong acid	Gel	Styrene-DVB	H ⁺	99	1.90	800	120
AMBERLITE IRN97 H	Strong acid	Gel	Styrene-DVB	H ⁺	99	2.15	800	120
AMBERLITE IRN9652	Strong acid	MR	Styrene-DVB	H ⁺	99	1.95	800	120
AMBERLITE IRN78	Strong base	Gel	Styrene-DVB	OH ⁻	95	1.20	690	60
AMBERLITE IRN9766	Strong base	MR	Styrene-DVB	OH ⁻	95	0.85	700	60
AMBERLITE IRN150	Mixed bed	Gel	Styrene-DVB	H ⁺ /OH ⁻	99/95	1.9/1.2	690	60
AMBERLITE IRN160	Mixed bed	Gel	Styrene-DVB	H ⁺ /OH ⁻	99/95	2.15/1.2	690	60
AMBERLITE IRN9687	Mixed bed	MR/Gel	Styrene-DVB	7Li ⁺ /OH ⁻	99/95	1.9/1.2	730	60
AMBERLITE IRN217	Mixed bed	Gel	Styrene-DVB	7Li ⁺ /OH ⁻	99/95	1.75/1.2	690	60
AMBERLITE IRN9882	Mixed bed	MR	Styrene-DVB	H ⁺ /OH ⁻	99/95	1.8/0.85	730	60

Rohm and Haas/Ion Exchange Resins - Philadelphia, PA - Tel. (800) RH AMBER - Fax: (215) 537-4157
 Rohm and Haas/Ion Exchange Resins - 75579 Paris Cedex 12 - Tel. (33) 1 40 02 50 00 - Fax: 1 43 45 28 19



AMBERLITE is a trademark of Rohm and Haas Company, Philadelphia, U.S.A.

Ion exchange resins and polymeric adsorbents, as produced, contain by-products resulting from the manufacturing process. The user must determine the extent to which organic by-products must be removed for any particular use and establish techniques to assure that the appropriate level of purity is achieved for that use. The user must ensure compliance with all prudent safety standards and regulatory requirements governing the application. Except where specifically otherwise stated, Rohm and Haas Company does not recommend its ion exchange resins or polymeric adsorbents, as supplied, as being suitable or appropriately pure for any particular use. Consult your Rohm and Haas technical representative for further information. Acidic and basic regenerant solutions are corrosive and should be handled in a manner that will prevent eye and skin contact. Nitric acid and other strong oxidising agents can cause explosive type reactions when mixed with Ion Exchange resins. Proper design of process equipment to prevent rapid buildup of pressure is necessary if use of an oxidising agent such as nitric acid is contemplated. Before using strong oxidising agents in contact with Ion Exchange Resins, consult sources knowledgeable in the handling of these materials.

Rohm and Haas Company makes no warranties either expressed or implied as to the accuracy of appropriateness of this data and expressly excludes any liability upon Rohm and Haas arising out of its use. We recommend that the prospective users determine for themselves the suitability of Rohm and Haas materials and suggestions for any use prior to their adoption. Suggestions for uses of our products of the inclusion of descriptive material from patents and the citation of specific patents in this publication should not be understood as recommending the use of our products in violation of any patent or as permission or license to use any patents of the Rohm and Haas Company. Material Safety Data Sheets outlining the hazards and handling methods for our products are available on request.

**APPENDIX B: SUMMARY AND RECOMMENDATION OF
AMBERLITE IRN 217 LITHIATED MIXED-BED STOCK
INVESTIGATION-ESKOM NUCLEAR POWER STATION.**

PL Browne
CHEMISTRY MANAGER

1st August 2003

SP Mellor
☎ +27 21 550 4298
✉ +27 21 550 5117

SUMMARY AND RECOMMENDATION ON IRN 217L RESIN STOCK INVESTIGATION

The current lithiated resin charge in unit 1 RCV demineraliser has been in service for 9 years and for unit 2 the period is 10 years. At this time the demineralisers on both units are still functioning satisfactorily. Current operating practice in the nuclear industry is to replace the RCV resin charge every 1 to 2 fuel cycles. It is not known for how long the RCV resin charges at Koeberg will be in a servicable condition. To ensure uninterrupted purification of the primary circuit it is necessary to have a standby resin charge qualified as acceptable for use.

Koeberg currently has 6700l of Amberlite IRN217 (lithiated) resin that has been in storage for 18 years (the replacement value of this resin is approximately R8.5 million). However the condition of this resin was unknown and the manufacturer, Rohm and Haas, is not in a position to fulfill the original guarantee. The 2003 Chemistry budget caters for R800 000 for the purchase of a new resin charge. Recently there have been several questions raised on the feasibility of using the Amberlite resin stock. If the resin is proved to be in an acceptable condition for use, this would be a huge cost saving in terms of the allocated money on the budget and for the purchase of future resin charges.

A working group was established to address this issue. The brief from the Chemistry Manager was to determine if the resin is in an acceptable condition for use. The testing was to be kept simple, with the main aim to determine if the potential for leachates entering into the RCP system exists.

Testing Process

Samples from the 3 different batches of the Amberlite IRN 217L resin stock were removed for analysis. A bench test was performed on site to analyse these resins for leachates and resin samples were also sent off-site to the Rohm and Haas laboratories in Durban and France.

The on-site testing involved rinsing the resin samples with demineralised water until a low conductivity was reached, simulating the same flow rates as would be experienced on the plant. The rinse water collected was analysed for cations and anions (by ion chromatography) for both pre- and post oxidation analysis. The post oxidation samples would provide information on the possible leachates as a result of resin breakdown and the release of organically bound impurities.

The chemical analyses that were performed at the Rohm and Haas laboratory in Durban included exchange capacity, moisture and strong base capacity. Optical aspects involved the determination of the % perfect, cracked and broken beads. The Rohm and Haas laboratory in France is analysing the resin samples for hardness, total organic carbon and rinsedown tests.

Test Results

Koeberg test results proved to be negative in respect of the potential for leachates. The difference in concentration between the pre- and post oxidation samples was insignificant. This was observed for all 3 batches. The ionic concentrations of the rinse water from the IRN 217L resin samples was compared with rinse water from a new batch of IRN 78 resin (strong base anion resin) and were found to be much lower.

The Rohm and Haas (Durban) results showed that in most cases the resin met the manufacturer's specifications for a new resin charge. The cation resins from samples 1 (batch 86151) and 2 (batch 76238) are in excellent condition, however the anion portion has lost strong base capacity (between 80 – 90 %) and has degraded optical aspects. The cation resin from sample 3 (batch 68260) is in a reasonable condition as compared to samples 1 and 2. The % of perfect beads is lower. However the strong base capacity of the anion portion is much higher than the previous 2 samples (98%). From the photomicrographs taken of the resin samples it is clear that the broken beads are large in size and that small resin fines should not be a concern.

At this time the results from the Rohm and Haas laboratory in France are not available.

Interpretation of results

Based on the Koeberg test results any of the 3 batches would be suitable for use. From the Rohm and Haas test results, sample 3 appears to be the most acceptable charge for use.

The Rohm and Haas test results were compared with a set of specifications that were proposed by Ken Galt several years ago. According to these specifications, the anion resin from samples 1 and 2 failed on 4 out of the 5 criteria. The cation resin met all the required specifications. For sample 3, the anion resin met all the specifications but the cation resin failed on optical aspect. Only 96.2 % of the resin beads are undamaged compared with the proposed specification of 98% for a new resin charge. As mentioned earlier the size of the broken beads are fairly large, so the presence of excessive resin fines is not evident. There is also a 5 µm filter downstream of the RCV demineraliser which should trap any broken resin beads exiting the demineraliser.

All test results were sent to Denis Aspden and Ken Galt to solicit their opinions on the condition of the IRN 217L resin stock and if it is acceptable for use in the RCV system. Positive feedback was received from both parties. D Aspden confirmed that sample 3 was acceptable for use. K Galt initially had concerns with the % of cracked beads on the cation portion of sample 3. However after viewing the photomicrographs, K Galt is also of the opinion that the slightly higher % cracked/broken beads is not an issue and supports the use of sample 3.

Recommendation

Based on the analysis results from our laboratory and the results from Rohm and Haas, we are recommending that sample 3 (batch 68260) be loaded into the second RCV demineraliser as a back-up to the current demineraliser in service.

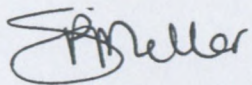
This recommendation is supported by D Aspden and K Galt. Another important factor to take into account is that there is only 1 charge available for batch 86151 and 76238, but for batch 68260, which is the batch that is being recommended, there is a total of 4 charges. This will allow for a spare charge to be available for each unit, and once batch 68260 is placed in service in either unit 1 or 2, monitoring the performance of the resin will confirm the findings as detailed in this letter and attached report.

Conclusion

To conclude, the resin testing has confirmed that the Amberlite IRN 217L resin stock is in a reasonable condition based on test results from Koeberg and the Rohm and Haas Durban laboratories. The expectation is that the Rohm and Haas results from the French laboratory will also support this conclusion. The availability of these results is eminent.

From the three batches of resin available in the Koeberg stores, batch 68260 meets all but one of the specifications, that being the optical aspects on the cation resin. Batch 68260 is recommended as being the most acceptable resin charge to be loaded into the RCV demineraliser for purification of the primary coolant.

Finally Technical Support would like to recognise and thank those individuals from the Plant and Analytical Chemistry Sections for their involvement in resolving this issue.



SP Mellor
CHEMIST
TECHNICAL SUPPORT

CC: NB Caris, AW Fortuin, N v Eeden

Attachments

- 1) Koeberg's test results, report prepared by S Pitsi
- 2) Test results from Rohm and Haas laboratory in Durban
- 3) KJ Galt's comments and proposed resin specifications

**APPENDIX C: ROHM AND HAAS REPORT ON THE AMBERLITE
DEGRADED RESIN**

PL Browne
CHEMISTRY MANAGER

19th August 2003

SP Mellor
☎ +27 21 550 4298
📠 +27 21 550 5117

FINAL FEEDBACK ON CONDITION OF IRN 217L RESIN STOCK

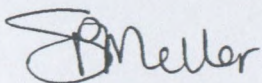
With reference to a letter dated 1st August 2003 (document no. 860703R), it was stated that the analysis results performed by Rohm and Haas in France had not yet been received.

These results have now been made available and the Rohm and Haas report is attached for your record.

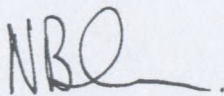
The outcome of the report is that the resins do not conform to normal nuclear grade specifications, however this was not an expectation. Rohm and Haas has confirmed that the anion resin of the batch that was previously recommended (batch no. 68260) is in the best condition with respect to the three different batches available. The report indicates that the cation resin has lost some of its lithium, the indication being that conditioning of this resin bed will take longer than normal. However this was not the case, conditioning the resin charge did not take any longer than expected, the lithium concentration upstream and downstream reached equilibrium values within 15 minutes.

As an added precaution, once the resin charge is placed in service, the lithium concentration will be closely monitored for any impact and if necessary lithium hydroxide will be injected to maintain the desired pH.

It is still the recommendation of Technical Support that this resin batch (batch no. 68260) is acceptable for use in the RCV demineraliser.



SP Mellor
CHEMIST
TECHNICAL SUPPORT

Supported: 
22/08/03

CC: NB Caris, AW Fortuin, N v Eeden

Attachments

- 1) Test results from Rohm and Haas laboratory in France



ION EXCHANGE RESINS

ROHM AND HAAS FRANCE S.A.S.

Usine de Chauny, laboratoires
rue des Grands Navoirs prolongée
BP48, 02301 Chauny Cedex
Tel : +33 (0)3 23 38 34 56

ANALYSIS REPORT

Work done by D VALENTIN

REPORT N°: SA03160

Date : 06/08/2003

Resins received from

References : Primary Plant Purification

Contact name : Ms S MELLOR

End user : ESKOM KOEBERG

1) PURPOSE OF THE WORK / RECEIVED SAMPLES :

Evaluation of the old and unused stock of Amberlite IRN217L in order to use by ESKOM KOEBERG Nuclear Power Station.

2) CONCLUSIONS & RECOMMENDATIONS :

The age of received samples are very old (> 15 years).

The low % of OH form on anionic components and the loss of Lithium on the cationic components after their "rinse down tests" show that the status of these resins do not correspond to our nuclear grade resin specifications.

On the other hand, the resin "non rinsed" release a lot (amine odour particularly).

It looks hazardous to use these old resins.

IDENTIFICATION :

Resin name	AMBERLITE IRN217L
Manufacturing date	1988
Type of resin	Li/OH mixed bed
Reference	N°1 – lot 86151
Comment	RINSED

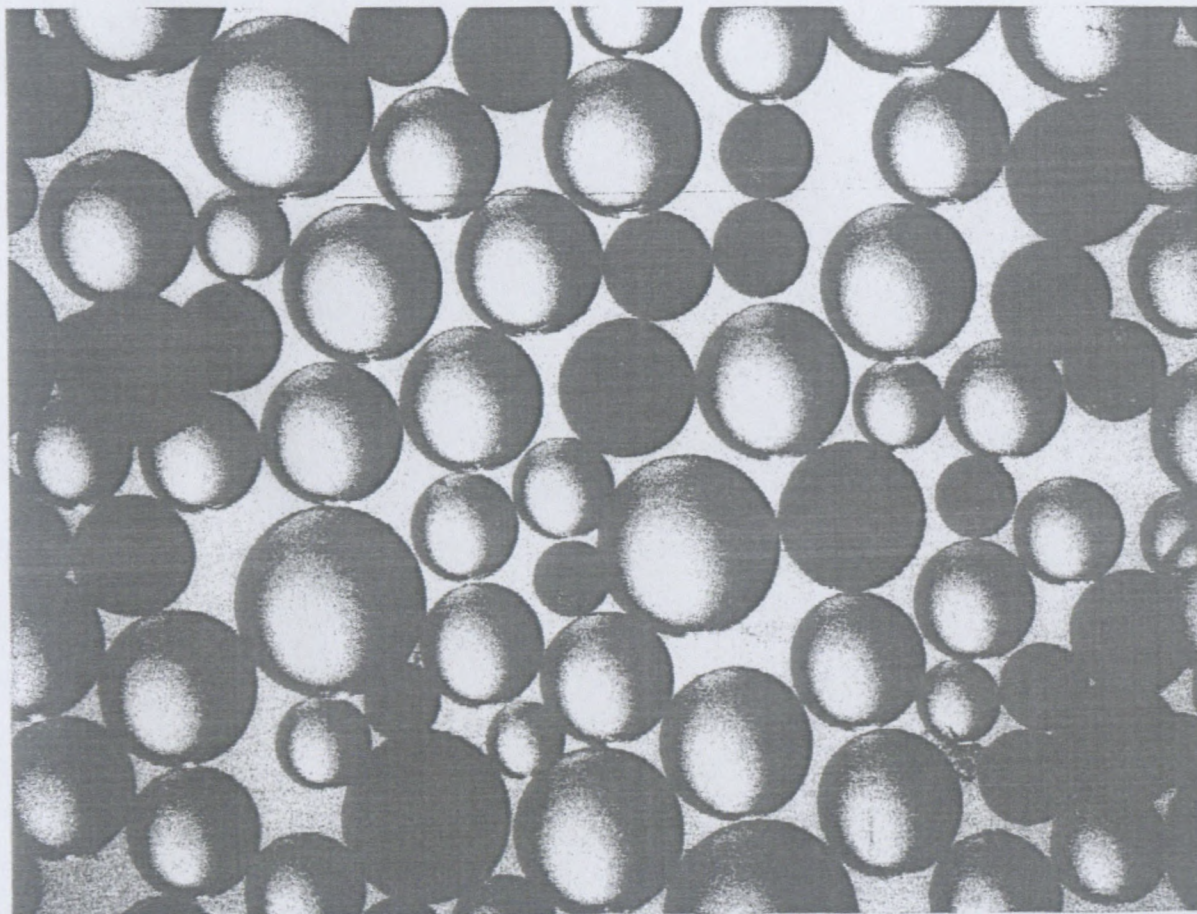
SPECIAL ANALYSIS :

COMPONENTS	CATION RESIN		ANION RESIN	
	Gel solvent type		Gel, IRA402 type	
Type	results	Reference value	results	Reference value
Regeneration %			62% OH	> 95% OH
Carbonates			38 % CO3	< 5% CO3
VOLUMIC RATIO %	46.1	40%	53.9	60%

LiOH RINSE PERFORMANCES :

SAMPLE	MIXED BED	
	results	Reference value
Li rinse (bv)	13	10bv max, 1bv typical

LiOH RINSE : EDF parameter, rinse with LiOH solution at 2.2mgLi/l until Li outlet = inlet
 If Cation resin does not contain enough Li, Li from the solution is consumed.



IDENTIFICATION :

Resin name	AMBERLITE IRN217L
Manufacturing date	1987
Type of resin	Li/OH mixed bed
Reference	N°3 – lot 76238
Comment	RINSED

SPECIAL ANALYSIS :

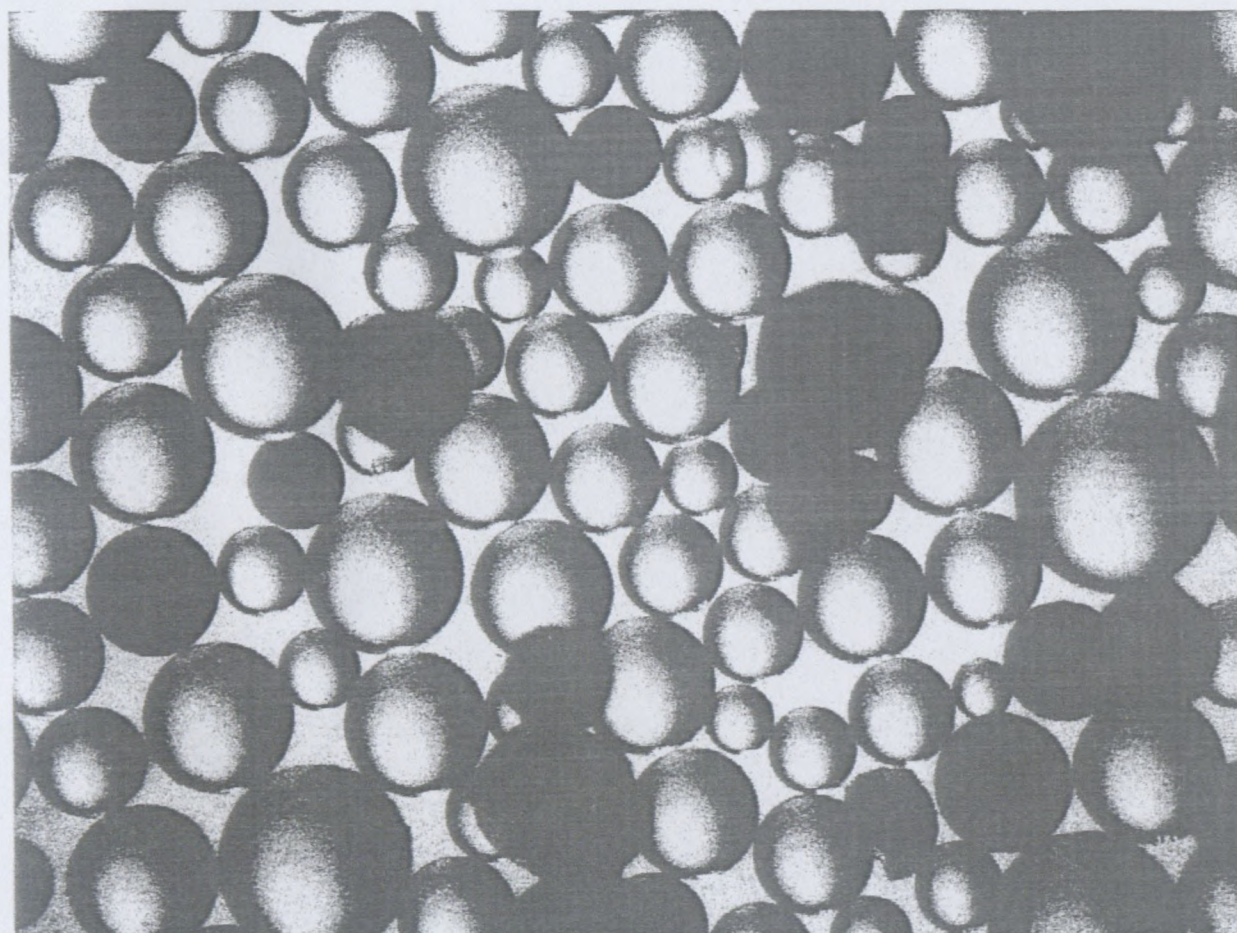
COMPONENTS	CATION RESIN		ANION RESIN	
	Gel solvent type		Gel, IRA402 type	
Type	results	Reference value	results	Reference value
Regeneration %			78 % OH	> 95% OH
Carbonates			22 % CO3	< 5% CO3
VOLUMIC RATIO %	48.3	40%	51.7	60%

LiOH RINSE PERFORMANCES :

SAMPLE	MIXED BED	
Measured parameters	results	Reference value
Li rinse (bv)	12	10bv max, 1bv typical

Comments on rinse : rinsing up, from low Li to outlet=inlet : Li consumption

LiOH RINSE : EDF parameter, rinse with LiOH solution at 2.2mgLi/l until Li outlet = inlet
 If Cation resin does not contain enough Li, Li from the solution is consumed.



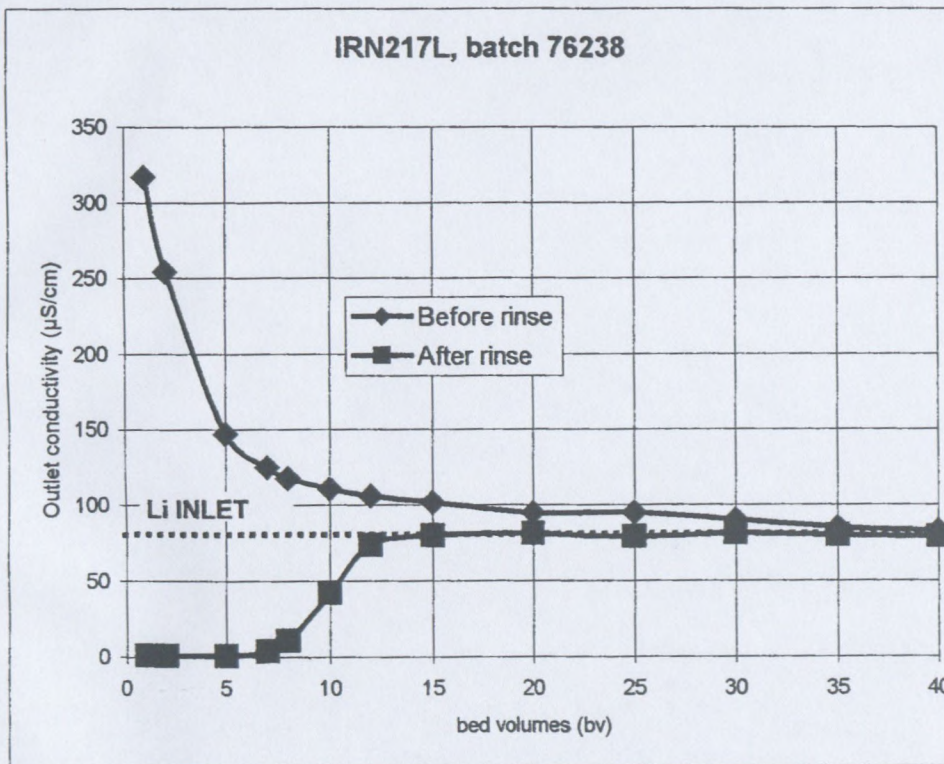
IDENTIFICATION :

Resin name	AMBERLITE IRN217L
Manufacturing date	1987
Type of resin	Li/OH mixed bed
Reference	N°4 – lot 76238
Comment	BEFORE RINSE

LiOH RINSE PERFORMANCES :

SAMPLE	MIXED BED	
Measured parameters	results	Reference value
Li rinse (bv)	32	10bv max, 1bv typical
Comments on rinse : rinsing down, from high Li+amines to outlet=inlet : Amines elution		

LiOH RINSE : EDF parameter, rinse with LiOH solution at 2.2mgLi/l until Li outlet = inlet
 If Cation resin does not contain enough Li, Li from the solution is consumed.



IDENTIFICATION :

Resin name	AMBERLITE IRN217L
Manufacturing date	1986
Type of resin	Li/OH mixed bed
Reference	N°5 – lot 68260
Comment	RINSED

SPECIAL ANALYSIS :

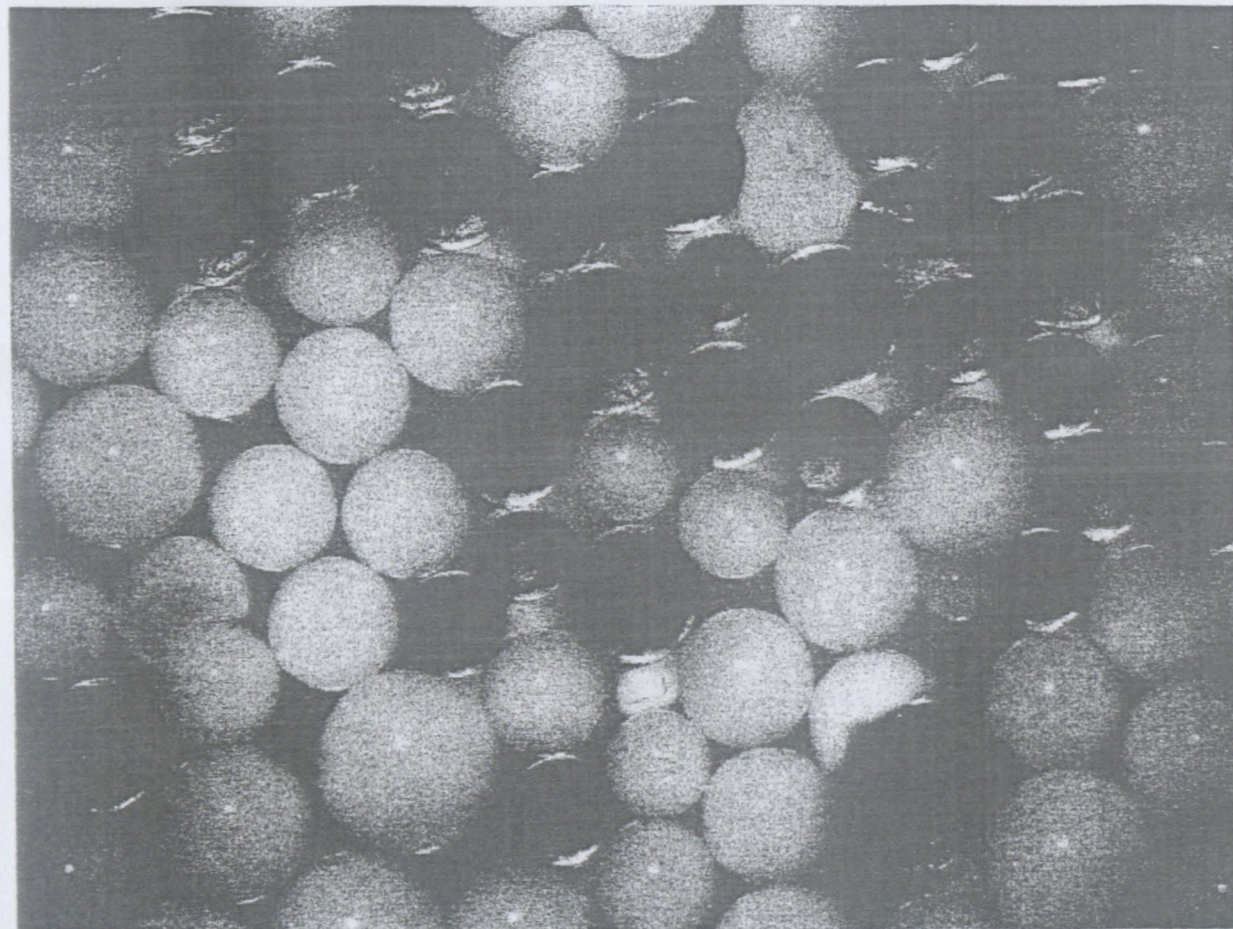
COMPONENTS	CATION RESIN		ANION RESIN	
	Gel non-solvent type		Gel opaque, A101 type	
	results	Reference value	results	Reference value
Regeneration %			89 % OH	> 95% OH
Carbonates			11 % CO3	< 5% CO3
VOLUMIC RATIO %	29.5	40%	70.5	60%

LiOH RINSE PERFORMANCES :

SAMPLE	MIXED BED	
	results	Reference value
Measured parameters		
Li rinse (bv)	21	10bv max, 1bv typical

Comments on rinse : rinsing up, from low Li to outlet=inlet : Li consumption

LiOH RINSE : EDF parameter, rinse with LiOH solution at 2.2mgLi/l until Li outlet = inlet
 If Cation resin does not contain enough Li, Li from the solution is consumed.



APPENDIX D: PREPARATION OF THE NUTRIENTS MEDIUM FOR *ACIDITHIOBACILLUS CALDUS*

Medium:

$(\text{NH}_4)_2\text{SO}_4$	3.00 g
$\text{K}_2\text{HPO}_4 \cdot 3\text{H}_2\text{O}$	0.50 g
$\text{MgSO}_4 \cdot 7\text{H}_2\text{O}$	0.50 g
KCl	0.10 g
$\text{Ca}(\text{NO}_3)_2$	0.01 g
Yeast extract	0.20 g
Sulfur (flowers)	10.00 g
Distilled water	1000.00 ml

Adjust pH with 6 N H_2SO_4 to 1.5 - 2.5.

Trace element solution:

$\text{FeCl}_3 \cdot 6\text{H}_2\text{O}$	11.0 mg
$\text{CuSO}_4 \cdot 5\text{H}_2\text{O}$	0.5 mg
H_3BO_3	2.0 mg
$\text{MnSO}_4 \cdot \text{H}_2\text{O}$	2.0 mg
$\text{Na}_2\text{MoO}_4 \cdot 2\text{H}_2\text{O}$	0.8 mg
$\text{CoCl}_2 \cdot 6\text{H}_2\text{O}$	0.6 mg
$\text{ZnSO}_4 \cdot 7\text{H}_2\text{O}$	0.9 mg
Distilled water	10.0 ml

APPENDIX E: EXPERIMENTAL RESULTS AND SIMULATED RESULTS

Table G1: Averaged experimental data for 1M HCl, simulated data and absolute error (SSD).

Time (min)	Se		SSD
	(experimental)	Se (model)	
9	2190.6	1828.8	361.85
18	700	560.0	140.03
27	200	171.5	28.53
36	100	52.5	47.50
45	42.3	16.1	26.22
54	22.8	4.9	17.88
63	13.8	1.5	12.29
72	10.8	0.5	10.34
81	3.1	0.1	2.96
		Sum	647.60

Table G2: Averaged experimental data for 1M H₂SO₄, simulated data and absolute error (SSD).

Time (min)	Se		SSD
	(experimental)	Se (model)1	
9	1968.5	1825.5	142.97
18	768.7	613.8	154.86
27	134.9	206.4	71.50
36	72.9	69.4	3.50
45	47	23.3	23.66
54	27	7.8	19.15
63	11.3	2.6	8.66
72	7.3	0.9	6.41
81	3.6	0.3	3.30
		Sum	434.02

Table G3: Averaged experimental data for biological 1M H₂SO₄, simulated data and absolute error (SSD).

Time (min)	Se (experimental)	Se (model)1	SSD
9	2792.84	1688.7	1104.12
18	171.97	325.6	153.62
27	62.74	62.8	0.03
36	30.9	12.1	18.80
45	12.63	2.3	10.30
54	7.84	0.4	7.39
63	1.8	0.1	1.71
72	1.01	0.0	0.99
81	0.2	0.0	0.20
		Sum	1297.16

APPENDIX F: DETERMINATION OF REACTION ORDER KINETICS

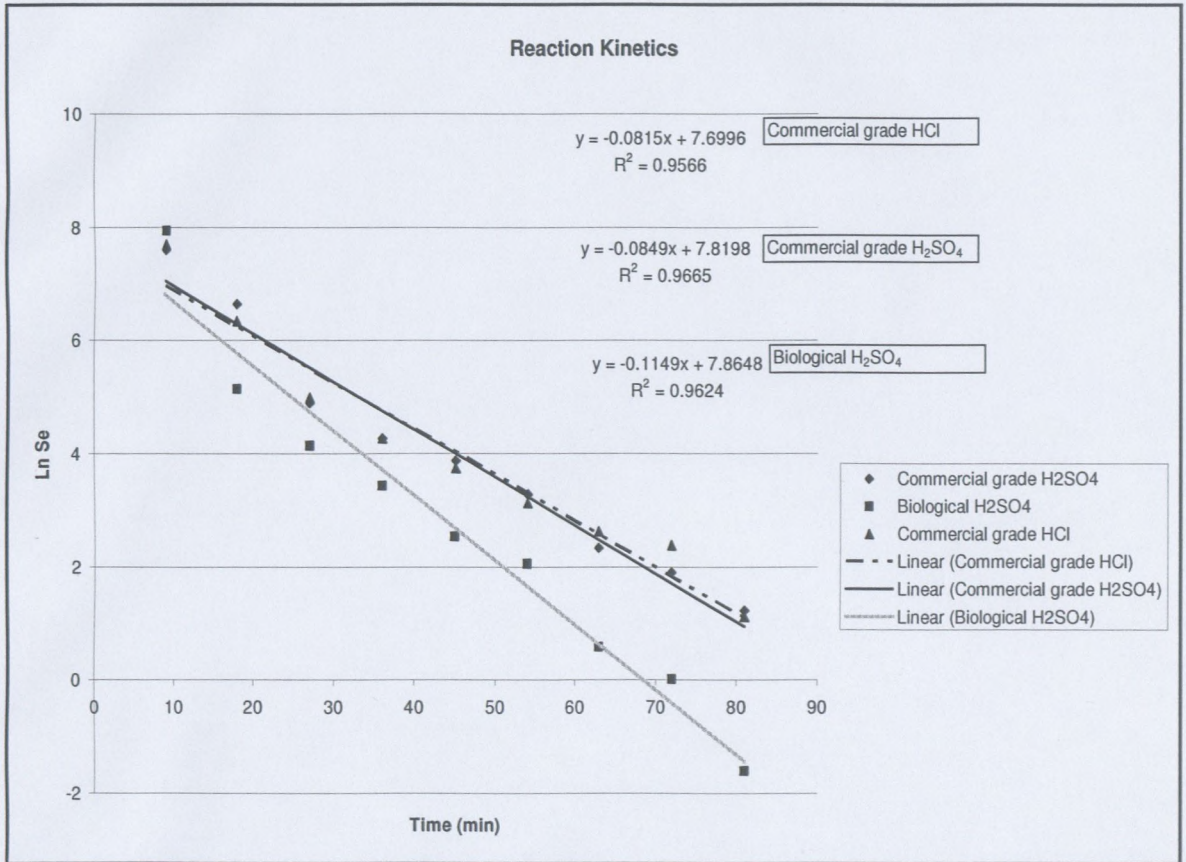


Figure F1: Reaction Oder kinetics

CAPE PENINSULA
UNIVERSITY OF TECHNOLOGY

